

**USP-2**  
**01-25**

DI: 98121

**MERIMON-2000**  
**MERIS for water quality**  
**monitoring in the Belgian-**  
**Dutch-German coastal zone**

**S.W.M. Peters**  
**R.J. Vos**  
**E.J. Hoogenboom**  
**H. Hakvoort**  
**H. van der Woerd**  
**M. Rijkeboer**  
**R. Pasterkamp**

**Rijkswaterstaat**  
Rijksinstituut voor Kust en Zee/RIKZ  
Bibliotheek (Den Haag)

C-4103, 01-25 981



**BELEIDSCOMMISSIE REMOTE SENSING**



**MERIMON-2000**

**MERIS for water quality monitoring in the  
Belgian-Dutch-German coastal zone**

**S.W.M. Peters (IVM-VU)**

**R.J. Vos (WLI Delft Hydraulics)**

**E.J. Hoogenboom (RWS-RIKZ)**

**H. Hakvoort (RWS-MD)**

**H. van der Woerd (IVM-VU)**

**M. Rijkeboer (IVM-VU)**

**R. Pasterkamp (IVM-VU)**

**USP-2 report 01-25**

**USP-2 project 2.1/AP-06**

**ISBN 90 54 11 370 7**

**August 2001**

**This report describes a project carried out in the framework of the User Support Programme  
(USP-2) under responsibility of the Netherlands Remote Sensing Board (BCRS)**

# Contents

Contents	iii
Abstract	vii
Executive Summary	ix
Glossary of Symbols and acronyms	xi
1. Introduction	1
1.1 Historical developments, objectives and scope	1
1.1.1 Scope and main objective	1
1.1.2 History of Ocean colour research in the Netherlands	2
1.2 Problem definition and project actions	4
1.2.1 Gaps in IOP databases	4
1.2.2 Algorithm selection	5
1.2.3 Inventory and testing of validation options / strategies	6
1.3 Approach	8
1.3.1 <i>Action 1</i> : Optical model calibration	8
1.3.2 <i>Action 2</i> : Selection and calibration of algorithms	10
1.3.3 <i>Third action</i> : point and transect validation	11
1.4 How to read this report	13
1.5 Acknowledgements	14
2. Theory of Simulation and measurement of $R(0-)$	15
2.1 Simulation models for $R(0-)$ : Introduction	15
2.2 Simulation models for $R(0-)$	16
2.2.1 Gordon model with pre-factors by Walker	16
2.2.2 Hydrolight	18
2.3 Remote measurement of $R(0-)$	18
2.3.1 Above water radiance measurements	18
2.3.2 Deriving reflectance from radiance measurements	19
2.4 Considerations for the comparison of measured reflectance with simulated reflectance	20
2.4.1 Consequences for algorithms	20
2.5 Some conclusions and Recommendations	22
3. Algorithms for MERIS	23
3.1 Introduction	23
3.1.1 Algorithms and water quality parameters	23
3.1.2 Algorithm type	23
3.1.3 Currently available algorithms for MERIS and the North Sea	25
3.1.4 From MERIS standard algorithms to regional algorithms	26
4. MERIMON field experiments: concentration measurements	29



4.1 Introduction	29
4.2 The Belgica-2000-11 Campaign:	29
4.3 The Mitra-2000 campaign	30
4.4 The Navicula-2000 cruise	31
4.5 Analysis of the concentration data	33
4.6 Some conclusions	35
4.7 MERIS concentration validation and protocols	36
4.7.1 Sampling protocol used	36
4.7.2 Chlorophyll protocol	36
4.7.3 TSM-protocol	36
4.7.4 CDOM-absorption protocol	36
4.7.5 Filter absorption protocol (seston and tripton)	36
4.7.6 MERIS protocols	37
5. Measured reflectance spectra	39
5.1 PR650 reflectance spectra	39
5.1.1 Introduction	39
5.1.2 The PMNS method for R(0-) measurement using the PR650	40
5.1.3 Results from the Gons method for R(0-) measurement	41
5.1.4 L1, L2 and L3 Spectra from the Mitra Campaign.	47
5.1.5 L1, L2 and L3 Spectra from the Navicula Campaign.	48
5.2 EPS-A spectra	50
5.2.1 Measurements synchronous with the Mitra cruise	50
5.2.2 Marsdiep flight	51
5.3 Comparison of Ferry borne Satlantics measurements to EPS-A and PR650	52
5.4 Consequences for MERIS validation	53
6. Evaluation of combinations of algorithms and parameter sets	55
6.1 Introduction	55
6.2 SIOP Variability	55
6.2.1 Variability of the normalized absorption of CDOM	56
6.2.2 Variability in pigment absorption	57
6.2.3 Variability in tripton absorption	58
6.2.4 Variability in seston scattering	58
6.3 Evaluation of algorithms	60
6.3.1 Introduction	60
6.3.2 Semi-empirical algorithms: PMNS-MERIS-TSM algorithm	60
6.3.3 Semi-empirical algorithms: PMNS-MERIS-CHL algorithms	61
6.3.4 Semi-analytical algorithms: the DUP-POWERS TSM algorithm	63
6.3.5 TSM-Ratio Matrix Inversion	63
6.3.6 TCHL-Ratio Matrix Inversion	65
7. Options for MERIS validation	69
7.1 Introduction	69
7.2 Options for transect validation using the NIOZ Satlantics-TESO set-up	69
7.2.1 Reflectance	69
7.2.2 Algorithms	70



7.2.3 Results	70
7.3 Using EPS-A images for MERIS validation	73
7.3.1 Introduction to the Marsdiep case study	73
7.3.2 Reflectance model and algorithm	74
7.3.3 Image processing results	75
7.3.4 Conclusions for MERIS monitoring	76
7.4 Validation of the MERIS-RMI algorithm using SeaWiFS images	76
7.4.1 Introduction	76
7.4.2 Modelling the missing SeaWiFS band (MERIS 705 nm)	77
7.4.3 SeaWiFS processing sequence	78
7.4.4 Calibration of the algorithm using a selected SIOP data set	79
7.4.5 Some conclusions on the set-up of the RMI-MERIS processor	79
7.4.6 Interpretation of the SeaWiFS image of 6 May 2000	81
7.4.7 Interpretation of the SeaWiFS image of 7 May 2000	83
7.4.8 Interpretation of the SeaWiFS image of 7 May 2000	84
7.4.9 Interpretation of the SeaWiFS image of 12 May 2000	85
7.4.10 Other Images	85
7.5 Comparison of SeaWiFS concentrations (TSM and TCHL) to field measurements	86
8. Conclusions and recommendations	91
9. Reference List	97
Appendix I. Contents of the MERIMON CD-Rom	103
Appendix II. Instrumentation and techniques for close range and remote (above water)	
R(0-) measurements	105
II.1 The GONS PR650 method	105
II.1.1 Description of the system	105
II.1.2 Measurement sequence/protocol	106
II.1.3 The Gons PR650 method: theory	106
II.2 The PMNS PR650/PR640 method	107
II.2.1 Measuring above water Transect R(0-) using the Satlantics instrument on board of the TESO Ferry (adapted from Wernand et al., 2000)	107
II.3 The EPS-A scanner on board of the on board of the RWS/NS airplane	109
II.4 The MERIS instrument (textual information mainly extracted from the MERIS website)	110
Appendix III. Some candidate algorithms for water quality detection using MERIS	115
III.1 Semi-empirical algorithms	115
III.1.1 PMNS (Althuis et al., 1996)	115
III.2 Analytical algorithms	118
III.2.1 Introduction	118
III.2.2 The standard Matrix Inversion Method (MIM) as used for EPS-A processing	119
III.2.3 Ratio Matrix Inversion: Rationale	120
III.2.4 Inversion of radiative transfer models	121



## Abstract

This report describes the results of the MERIMON-2000 study. In this project attention is given to the history and state-of-the-art of water quality remote sensing of the Dutch North Sea. The objective is to prepare for the validation and operational use of regional MERIS products. Options are discussed to use data from various operational systems/methods for MERIS validation: 1) the EPS-A airborne multispectral sensor on the coastguard airplane; 2) transect monitoring of suspended matter in the Marsdiep using above water measurements of subsurface reflectance and 3): point measurements of subsurface reflectance using handheld spectrometers.

MERIS will deliver CHL, TSM and CDOM products from a neural networks processor calibrated with global mean optical properties. For regional applications new algorithms must be selected and calibrated on regional data. Dutch efforts traditionally have been directed towards the understanding and application of quantitative methods. This report lists and evaluates several of these methods and introduces the new concept of Ratio Matrix Inversion. Three field experiments (in the "Marsdiep", at the location "Noordwijk 10" and one experiment in Belgian waters) are described. It is concluded that the tested methods and systems may be used for method development and to validate MERIS products in the near future. Some theoretical and practical issues remain to be resolved. E.g. a sensitivity analysis should be done to select the final algorithm. Especially the "Noordwijk-10" site was found to be representative for mean Dutch coastal waters and is selected for future MERIS validation.



## Executive Summary

The MERIMON project aims to bring together past experience and knowledge on water quality remote sensing of the Dutch North Sea and the current state of remote and close sensing technology in order to define options for MERIS validation.

Recent achievements in ocean/inland water colour monitoring in the Netherlands include

- The operationalisation of the EPS-A airborne multispectral sensor on the coastguard airplane
- The operationalisation of transect monitoring of suspended matter in the Marsdiep by NIOZ using above water measurements of subsurface reflectance
- The operationalisation of point measurements of subsurface reflectance using handheld spectrometers by NIOZ, NIOO-CL and IVM
- Advanced insights in optical modelling and especially in model inversion techniques using e.g. Matrix Inversion Methods

These measurement systems have been demonstrated in several case studies including case studies in this report. It was concluded that each method, at its own scale is able to deliver (depending on a number of circumstances) reasonably accurate water reflectance spectra, suitable for validation of MERIS spectra. An integrated validation of the ensemble measurements using these instruments has not been possible mainly because of logistics (not yet an operational standard processor for MERIS products) and because of data quality problems (sun/glint and aerosol gradients in EPS-A images).

MERIMON has studied existing algorithms to select appropriate formulations for MERIS to produce regional correct estimations of TSM and CHL. In this the viewpoint of monitoring was taken. Comparative algorithm evaluation was done to study the applicability and theoretical weaknesses of various types of algorithms for water quality parameters retrieval.

It was noted that comparison of various algorithms requires a rigid treatment of the Q and f factors and the B factor as well which has implications for the standardization of ground truth R(0-) measurements as well as satellite R(0-) observations.

MERIS standard algorithms could not be studied by this project because the definitive parameterisation of the MERIS processor still had to be decided upon in October 2000.

In view of the preparation to the use of MERIS products, this project has tested (and developed) other state of the art algorithms. Based on the outcome of this study and further sensitivity studies, in the next step, the best regional (algorithms calibrated on regional datasets) alternative for MERIS standard algorithms will be selected and calibrated.



The MERIMON results show that concentration ranges in spring 2001 are not consistent with the ranges in the PMNS-data set, therefore it was concluded that the variability of concentrations on the North Sea is still not well understood. It remains therefore important to keep monitoring concentration ranges during remote sensing studies.

In the Netherlands quite some progress has been achieved in the understanding and facilitation of above water measurements of  $R(0-)$ . MERIMON found that various methods can produce good results, especially if the reflected sky radiance term is taken into account.

Algorithms were tested on PR650 observations with the outcomes: that the standard PMNS TSM algorithm for MERIS tends to overestimate TSM in the Marsdiep and to underestimate TSM in the Belgian waters. The PMNS study has proposed 2 CHL algorithms for MERIS. When both are applied to PR650-Gons-L1 observations results are good for the simple band ratio algorithm and bad for the MRA-algorithm. The POWERS algorithm seems to underestimate TSM at low concentrations (less than 20 mg/l) and to overestimate at higher concentrations ( $>20\text{mg/l}$ ). RMI is possibly a suitable technique to map TSM but the scaling differences between simulated spectra (using RMI retrieved concentrations) and measured spectra remains an issue of concern. The MERIS band settings are suitable for TCHL retrieval using RMI in the North Sea coastal waters.

From comparative SIOP analysis it was found that the Marsdiep is very atypical for North Sea waters. Furthermore, there are distinct differences between Belgian coastal water and Dutch coastal waters, which has probably to do with the absorption of the organic fraction of TSM and the differences in absorption of CDOM. The Mitra transect is ideal to monitor a relatively representative mean North Sea Water composition.

From a test case for satellite image processing it was concluded that the results are hopeful in the sense that independent TSM, TCHL and CDOM products seem to be feasible from satellite observations such as from MERIS. The results should however be seen as a rough approximation of MERIS results because of the coarse and sparse band settings of SeaWiFS.

The test case allowed to do a preliminary transect validation of the products. It was found that TCHL is in good agreement with the values obtained along the Mitra transect and that TSM is in disagreement (SeaWiFS 6 May, Mitra 8-9 May) therefore it is recommended that the performance of the RMI method for TSM should be further evaluated.



## Glossary of Symbols and acronyms

Symbol	Description	Units
<i>TCHL</i>	Concentration of Chlorophyll-a and phaeopigments	mg m <sup>-3</sup>
<i>TSM</i>	Concentration of total suspended matter	g m <sup>-3</sup>
<i>CDOM</i>	Concentration of Coloured Dissolved Organic Matter (expressed as absorption at 440nm)	m <sup>-1</sup>
<i>CHL</i>	Concentration of chlorophyll a	mg m <sup>-3</sup>
<i>IOP</i>	Inherent Optical Properties	
<i>SIOP</i>	Specific Inherent Optical properties	
<i>A</i>	Total absorption coefficient	m <sup>-1</sup>
<i>a<sub>CDOM</sub></i>	Absorption coefficient of CDOM	m <sup>-1</sup>
<i>a<sub>w</sub></i>	Absorption coefficient of pure water	m <sup>-1</sup>
<i><math>\bar{a}_{CDOM}</math></i>	Absorption coefficient of CDOM, normalised at 440nm	-
<i>a<sub>CHL</sub></i>	Specific absorption coefficient of CHL	m <sup>2</sup> mg <sup>-1</sup>
<i>a<sub>TSM</sub></i>	Specific absorption coefficient of TSM	m <sup>2</sup> g <sup>-1</sup>
<i>G<sub>440</sub></i>	Absorption by CDOM at 440 nm	m <sup>-1</sup>
<i>B</i>	Total scattering coefficient	m <sup>-1</sup>
<i>b<sub>b</sub></i>	Total back scattering coefficient (scattering for angles > 90° with respect to direction of incoming light)	m <sup>-1</sup>
<i>b<sub>w</sub></i>	scattering coefficient of pure water	m <sup>-1</sup>
<i>b<sub>b,TSM</sub></i>	specific back scattering coefficient of TSM	m <sup>2</sup> g <sup>-1</sup>
<i>B</i>	Backscatter to scatter ratio	-
$\lambda$	Wavelength	Nm
$\theta_0$	Angle of downwelling sun light under water	-
$\mu_{u,d}$	average cosine of upwelling (u) or downwelling (d) light	-
$\theta_z$	Sun zenith angle	-
<i>E<sub>wd</sub></i>	subsurface downward irradiance	W m <sup>-2</sup> nm <sup>-1</sup>
<i>E<sub>wu</sub></i>	subsurface upward irradiance	W m <sup>-2</sup> nm <sup>-1</sup>
<i>F</i>	prefactor in Gordon formulae	-
<i>F</i>	fraction diffuse light of downward irradiance	-
<i>L<sub>wd</sub></i>	subsurface downward radiance	W m <sup>-2</sup> sr <sup>-1</sup> nm <sup>-1</sup>
<i>L<sub>wu</sub></i>	subsurface upward radiance	W m <sup>-2</sup> sr <sup>-1</sup> nm <sup>-1</sup>
<i>Q</i>	conversion coefficient for <i>L<sub>wu</sub></i> to <i>E<sub>wu</sub></i>	-



$R(0^-)$	subsurface irradiance reflectance	
$R(0^-, \lambda)$	subsurface irradiance reflectance at wavelength $\lambda$	-
$R(0^+, \lambda)$	above surface radiance reflectance at wavelength $\lambda$	-
<i>EPS-A</i>	Europe Probe Scanner: hyperspectral imaging spectrometer installed on board of the Dutch coast guard aircraft	
<i>MOS</i>	Modular Optoelectronic Scanner	
<i>MERIS</i>	Medium Resolution Imager	
<i>PR650</i>	Photo Research 650 spectroradiometer	
<i>Satlantics</i>	Portable multi-channel spectroradiometer	
<i>SeaWiFS</i>	Sea-viewing Wide Field-of-View Sensor	
<i>Hydrolight</i>	Computer simulation code for underwater light modelling	
<i>DOC</i>	Demonstration Ocean Colour Project	
<i>ENVISAT-AO</i>	Announcenment of Opportunities for Research for calibration/validation of ENVISAT products	
<i>ESA-DUP</i>	Data User Programme of ESA	
<i>MERIMON</i>	MERIS for water quality MONitoring in the Belgian-Dutch-German coastal zone: this study	
<i>PMNS</i>	Particulate Matter North Sea	
<i>POWERS</i>	Pre-Operational Water and Environment Regional Service Project	
<i>ESA</i>	European Space Agency	
<i>IVM</i>	Institute for Environmental Studies Instituut Voor Milieuvraagstukken	
<i>NIOZ</i>	National Institute for Sea Research	
<i>RWS/MD</i>	Rijkswaterstaat Meetkundige Dienst Department of Waterworks, Survey Department	
<i>RIKZ</i>	Rijks Instituut Kust en Zee Department of Waterworks, National Institute for Coastal and Marine Management	
<i>Belgica</i>	Belgian Monitoring vessel	
<i>Mitra</i>	Monitoring vessel of Rijkswaterstaat	
<i>Navicula</i>	Research Vessel of NIOZ	
<i>MAVT</i>	Meris aand AATSR Validation Team	

---



<i>MIM</i>	Matrix Inversion Method
<i>MRA</i>	Multiple Regression Analysis
<i>NN</i>	Neural Networks
<i>RMI</i>	Ratio Matrix Inversion Method
<i>RS</i>	Remote Sensing

---



# 1. Introduction

## 1.1 Historical developments, objectives and scope

### 1.1.1 Scope and main objective

#### *ESA, MERSOPS and MERIMON*

MERIMON-2000 constitutes the Dutch contribution to the ENVISAT-AO proposal "MERIS region-specific optical properties calibration for water quality monitoring in the Belgian-Dutch-German coastal zone (MERSOPS)". This proposal was submitted to ESA by MUMM on behalf of the contributing parties MUMM, IVM and GKSS. The MERIMON-2000 project addresses a part of the proposed activities in MERSOPS, namely those that can be performed before the end of 2000.

During the MERIMON-2000 project contacts with ESA and the German and Belgian partners have been firmly established. Meetings of the MERIS and AATSR Validation Team (MAVT) have been attended, which has led to contributions to the MERIS validation protocol. Logistical reasons have caused to formally subdivide the ESA-AO project MERSOPS into separate Belgian and a Dutch activities. MERIMON is now known as AO-9096 and has official cal/val status. A statement of work has been submitted to ESA. MERIMON has participated in the first rehearsal exercise with ESA software to test and familiarise with database products ("NILU" database) and Internet software for access to MERIS products.

#### *Objectives*

The *main objective* of the MERSOPS project is to optimise the calibration of the standard MERIS bio-optical model by assimilating region specific information relating inherent optical properties to chlorophyll and suspended matter concentrations. MERIMON-2000 contributes to this objective through a concentrated effort to collect data for calibration and validation of MERIS algorithms and MERIS-type sensor products for Dutch coastal waters.

The MERIMON-2000 project has as *additional end-goal* the operational use of validated MERIS products (with special emphasis on TSM and TCHL) because of the user requirements as expressed in the ESA-DUP POWERS project document (Van der Woerd et al., 1999), which presents the state-of-affairs of summer 1998. *It states that validated (i.e. of known accuracy) series of chlorophyll concentration maps and suspended matter maps are regarded as being the most important end products desired from remote sensing.* Until the availability of MOS and SeaWiFS data there was never any scope for regular delivery of validated products of known accuracy. Only recently (in the Demo Ocean Colour project (DOC: Hoogenboom et al., 2000) and in the POWERS project (Van der Woerd et al., 2000), and in similar projects in Belgium and Germany, steps have been taken to develop and demonstrate such products. In the advent of MERIS there remain some *technical issues to be solved*. Up till now there is no proven technique for TCHL mapping using MERIS. Furthermore there is insufficient insight in



IOP variability. And also important is the fact the validation of satellite water quality products is difficult and remains to be done. This report addresses these issues.

#### *End user involvement*

MERIMON-2000 intended to contribute to operational use by involving the end user in the validation of remote sensing products. This would provide the end-user with hands-on experience anticipating the operational use of MERIS products. MERIS products were however not available during this project phase. Through other projects (funded by 'Rijkswaterstaat' RIKZ), in which TSM atlases based on SeaWiFS observations for the Dutch part of the North Sea were and are being produced, a major end user has expressed his commitment to earth observation products of the kind that MERIS will deliver. This commitment is underlined by the contributions of RIKZ and RWS/MD to this study and the continuous support of RIKZ and RWS/MD in MERIS validation activities.

#### *An outlook to the near future*

The first actual available MERIS data in the near future will be experimental data. In the commissioning phase of the sensor, first the sensor performance in terms of water leaving radiance will have to be validated, after which the validation of the actual thematic level 2 products has to be done. Therefore it is foreseen that validation activities should continue after the MERIMON-2000 project until the sensor and its products have been accepted.

### 1.1.2 History of Ocean colour research in the Netherlands

#### *A Dutch history of ocean colour remote sensing research*

The study of North Sea Waters using remote sensing techniques has been ongoing since the 80s. One of the earliest publications is The North Sea satellite colour atlas by Holligan et al., (1989). The results of Dutch efforts, stimulated by subsequent National Remote Sensing Programs, were published from the early nineties onward. First, the attention was directed at the NOAA satellite with the intention to produce operational products for research and monitoring purposes (Harkink, 1991, Roozkrans and Prangma, 1992). Marees and Wernand (1992) broadened the view towards available multispectral scanners such as the CZCS and CAESAR. They also tested algorithms for SeaWiFS. At that time it was realized that remote sensing studies would benefit greatly from in-situ measurements of reflectance spectra, optical properties and standardized concentration measurements. Therefore the Particulate Matter North Sea (PMNS) studies were initiated which resulted in the publications by Althuis et al., 1995, Althuis and Shimwell, 1995, Kromkamp and Wouts, 1998 and Althuis, 1998. PMNS measurements of North Sea concentrations, spectra and inherent optical properties were re-evaluated by this project (Vos et al., to be published). Because of the unavailability of a suitable ocean colour sensor (in the time between CZCS and SeaWiFS) the images from the suite of NOAA satellites were studied intensively to obtain time series of suspended matter in the North Sea. The NOAA-AVHRR series was designed specifically for land applications: the sensitivity for water studies proved to be low and there were difficulties to obtain calibrated atmospherically corrected image products. This was seen as an opportunity to initiate studies into the integrated synergistic use of NOAA satellite images and field measurements and model simulations of TSM (the RESTWAG studies: Vos &



Schuttelaar, 1995; Vos et al, 1998). These studies demonstrated the possibility to overcome NOAA image calibration problems by using model simulation result and in-situ measurements. With the advent of dedicated new ocean colour sensors like MOS and SeaWiFS these synergistic approaches were (temporarily) abandoned. Especially SeaWiFS benefits from voluminous ground support efforts. Based on the experiences with CZCS, the SeaWiFS project produces images of calibrated at satellite radiance together with sophisticated software (SEADAS) to correct for atmospheric influences. SeaWiFS images are delivered with complete auxiliary data such as wind fields, barometric pressure etc. required to parameterise the complex atmospheric correction schemes incorporated in SEADAS. In separate projects such as the SIMBIOS project extensive field studies and round robin experiments were done to determine global algorithms for CHL concentrations in mainly case 1 water.

The benefits of this complete approach were demonstrated in several projects in the Netherlands, namely the Demo Ocean Colour project (DOC: Hoogenboom et al., 1999) and the ESA-DUP-POWERS project (Van der Woerd et al., 2000). The first project demonstrated the feasibility to derive calibrated TSM products from MOS and SeaWiFS, while the latter project created an operational automated production line for series of calibrated TSM maps of the Dutch part of the North Sea. Although the commercial scope of these products has proved to be limited yet, they are now produced for each available and suitable SeaWiFS image, collated on a yearly basis in printed atlases and distributed in high numbers amongst the user community.

This operationalisation was made possible after a breakthrough in atmospheric correction over case 2 waters (Ruddick et al., 2000). At this point in time the remote sensing community prepares to use the images of the new MERIS sensor onboard of the European satellite ENVISAT (to be launched in October 2001). The spectral band passes and sensitivity of this instrument are specifically designed for turbid coastal waters. ESA develops its own atmospheric correction processor also specifically designed to operate in areas with turbid waters. This MERIMON study builds on previous mentioned studies and anticipates on the use of MERIS data in quantitative determinations of TSM and TCHL in the coastal waters of the Dutch part of the North Sea.

#### *Evolution of ocean colour algorithms in Dutch studies*

Ocean colour algorithms are used for the retrieval of water quality parameters (concentrations of optical active constituents) from satellite data. These water quality parameters are:

- The concentrations of Total Suspended Matter (TSM);
- Part of the (green) algal pigment concentration: measurable is either Chlorophyll-a (CHL) or Total Chlorophyll (TCHL, the sum of Chlorophyll-a and Phaeopigments; sometimes also Chlorophyll-b and Chlorophyll-c are included);
- A measure for the concentration of Coloured Dissolved Organic Matter (CDOM).

The above-mentioned studies by Roozkrans and Vos based on NOAA-AVHRR images used combinations of hydraulic model simulations and in-situ data to quantify TSM from the satellite images. The first approaches towards semi-analytical algorithms in the Netherlands were developed by Dekker (1993) and applied to satellite images in Dekker and Peters (1993). During the PMNS studies semi-empirical algorithms for TSM, CHL and CDOM were developed for the CZCS and SeaWiFS instruments based on a large multi seasonal collection of North Sea spectra and in-situ measured concentrations. Unfortunately these algorithms were not tested on satellite images. With the advent of



sensitive sensors with high spectral capability (such as the airborne EPS-A sensor, and the MOS and MERIS satellite borne sensors) algorithms were sought for that allowed using the full spectral information. Furthermore such algorithms should be based on analytical optical model inversion and henceforth on the optical characteristics of the investigated waters. This has lead to the development of methods such as the Matrix Inversion Method (MIM: Hoogenboom et al., 1998a), Ratio Matrix Inversion (this report) and simplified analytical algorithms based e.g. on one band inversions of the optical model (Van der Woerd et al., 2000). There are very little examples on international developments on TSM algorithms since the international ocean colour efforts are directed at CHL in case 1 waters predominantly. The best and most actual example is the MERIS processor (Doerffer et al., 1997) that will use neural networks to obtain the concentrations of TSM CHL and CDOM. In chapter 3 of this report, a state of the art summary is made of algorithms for retrieval of concentrations from satellite data. In subsequent chapters suitable algorithms for use with MERIS in the Dutch part of the North Sea coastal waters will be discussed.

## 1.2 Problem definition and project actions

From experiences gained within the DOC and POWERS projects, it was learned that there are 3 technical/conceptual problems related to the calibration and validation and operational use of MERIS algorithms and products, namely

- There are gaps in IOP databases
- The final algorithms must still be selected
- Validation options / strategies have to be inventoried and tested

### 1.2.1 Gaps in IOP databases

One of the main unknowns and probable error sources (from an optical modelling point of view) in regional RS-information products is the spatial and temporal variability of inherent optical properties and the influence of this variability on the inverse retrieval of concentrations from RS-images. Knowledge of this variability within the North Sea will enhance the quality of RS-information products (derived from sensors such as MERIS). Therefore the information in existing databases must be combined with specific additional field studies to learn if there exists one general set of SIOP for the North Sea or if, alternatively, SIOP sets per region or per season should be used to parameterise optical models and algorithms.

This report describes the collection of relevant historical data and additional field data (during the spring season of 2000: algal bloom period) to study the variability of SIOP and to assess the effect of this variability on algorithm performance. Recommendations are made on standard data sets and additional field sampling. Literature research and comparative analysis have been initiated to study the quality and representativity of the IOP measurements. This research, complemented with sensitivity analysis (bio-optical model performance with various IOP sets) is essential to the understanding of the quality of MERIS products. Summarizing, the aim of this study is to find the recipe and ingredients for successful assessment of the quality and representativity of the IOP measurements and the influence of spatial and temporal variations on concentration retrieval accuracy.



### 1.2.2 Algorithm selection

Presently, there is a suite of algorithms available for North Sea studies, including the standard algorithms for MERIS. An overview is given in Table 1.1.

Both the EPS-A and Satlantics instrument feature spectral band settings similar to the MERIS band passes (with some exceptions; see ch9.II.4). The PR650 instrument is a handheld spectrometer with a spectral resolution of 8 nm (going from 380-780 nm). PR650 measurements were interpolated to spectra with 1 nm resolution and, for the purpose of this study, convoluted to MERIS, SeaWiFS or EPS-A band pass settings.

Algorithm	Reference	Scanner	Calibration Area + Year
MERIS-CHL	Doerffer et al., 1997	MOS/?	European waters
MERIS-TSM	Doerffer et al., 1997	MOS/?	European Waters
PMNS-TSM	Althuis et al., 1996	CASI/PR650/Satl antics	Dutch North Sea
PMNS-CHL	Althuis et al., 1996	CASI/PR650	Dutch North Sea
EPSA-MIM-TSM	Hakvoort et al., 2000	EPS-A/PR650	Marsdiep & Noordwijk 2000
EPSA-MIM-CHL	Hakvoort et al., 2000	EPS-A/PR650	Marsdiep & Noordwijk 2000
RMI-TSM	This report	SeaWiFS/EPS-A/PR650	Marsdiep, Noordwijk Dutch and Belgian waters, 2000
RMI-CHL	This report	SeaWiFS/EPS-A/PR650	Marsdiep, Noordwijk Dutch and Belgian waters, 2000
EPS-A Wide- band TSM	This report	EPS-A	Marsdiep, 2000
POWERS-TSM	Van der Woerd et al., 2000	SeaWiFS/PR650	Belgian waters, 1998
Hoogenboom TSM	Hoogenboom et al., 2000	Satlantics	Marsdiep, 2000

*Table 1.1: Overview of candidate North Sea algorithms*

There are several reasons for the treatment of this multitude of algorithms by this project:

- 1) The MERIS standard algorithms were calibrated for average European case II water properties but not specifically for North Sea waters
- 2) The definitive parameterisation of the standard algorithms had still to be decided upon during the last attended MAVT meeting (October 2000), it is expected that the final parameterisation will be presented at the MAVT meeting of July 2001.



- 3) A number of alternative algorithms has been tested for North Sea applications only on very small scale
- 4) A CHL-algorithm for North Sea applications using satellite data has not yet been established

Initially MERIMON also aimed to use a prototype of the MERIS processor to test the standard neural networks algorithms for Dutch North Sea applications. This has not been possible since the definitive parameterisations of the NN-model were not decided upon in time. Therefore this study has concentrated on making a first selection of other relevant algorithms for both TSM and CHL retrieval from MERIS. The study addresses the problem of input parameter selection and the possible effects of spatial and temporal variability of IOPs on the performance of selected algorithms (in terms of retrieved concentrations). Ultimately this leads to the validation of the algorithm and the concentration products.

### 1.2.3 Inventory and testing of validation options / strategies

ESA recommends isolated point samples (under perfect conditions) as preferred method for MERIS validation. This will lead, in the case of the North Sea, to very limited opportunities. Moreover, such an approach can only be used if a number of conditions are fulfilled, namely:

- 1) The algorithm parameterisation set (SIOP) is not subject to discussion
- 2) The algorithm itself is fixed
- 3) A tested and approved turbid water atmospheric correction is implemented

Which means that, in the ideal case, validation will only lead to fine tuning of the reflectance and concentration products. However, for MERIS, the following situation is occurring:

1. There is a **restriction** in the validity of the MERIS algorithms for TCHL, TSM and CDOM because the standard MERIS set of SIOP will reflect mean global values for coastal waters, it will not be specific for North Sea waters. Moreover, the algorithm parameterisation set (SIOP) still was not fixed until the last MAVT meeting (October 2000).
2. There are experimental **restrictions** because of the type of processor used for MERIS. The algorithm is a neural networks algorithm, of which, only very recently examples of products have been released. The MERIS neural network will not be made available for experimentation. Neural networks provide robust solutions to the bio-optical inversion problem, however their performance on 'real world' spectra is subject to questioning. Experiments in the Netherlands (Nieuwenhuis, 1999, Rosa, 2000) show that significant errors in the concentrations can occur, with causes as overtraining etc. that have little to do with the optical model. One of the major drawbacks of NN is the fact that algorithm performance not only depends on the parameter set but also on configuration parameters such as: number of hidden layers, number of nodes, transfer function type, and, quite important, on the type of spectral normalization



procedure. Because of these considerations, alternative algorithms must be investigated for regional applications.

3. MERIS will provide a unique *opportunity* to obtain atmospherically corrected images over turbid waters because a complete turbid water approach to atmospheric correction will be implemented. This approach is however new and not yet tested for the North Sea situation (which is quite unique in the sense that TSM concentrations are extremely high at some locations). Therefore, much attention in the validation phase should be given to validation of the MERIS observed Sea surface reflectance spectra.
4. Dutch efforts to set up a multi-level remote sensing facility for coastal waters (in-situ observed spectra, transect measurements of spectra, operational airborne facilities and operational satellite image processing facilities) provide unique *opportunities* for MERIS validation. Since a number of years it has been possible to validate both satellite and airborne remote sensing observations by taking simultaneous point measurements of reflectance spectra using e.g. the PR650 method and by taking point samples for concentration validation. Recently, the possibility of using future Ferry-borne radiometers and observations by the airborne EPS-A (in the coastal zone) for MERIS reflectance and concentration validation has arisen. These observations would allow transect validation instead of point validation. In order to be able to use these measurements for validation of MERIS products, trial cases for the cross validation along transects of in-situ measurements and RS-measurements were established by this project. Because the Ferry borne Satlantics set-up is experimental, this project had access to limited observations only. Hoogenboom et al., (2000) and Wernand et al. (2000) have published preliminary results.

In order to overcome these restrictions and make use of the identified opportunities, the process of validation of MERIS products in the Dutch/Belgian coastal zone, will involve the following project actions:

**Action 1) Optical model calibration:** select sets of SIOP that are typical for the area under consideration: calibrate a selected optical model with these SIOP sets (elaborated in section 1.3.1).

**Action 2) Algorithm development, selection and testing:** algorithms that are suitable for the optical properties and range of concentrations found in the area (elaborated in section 1.3.2).

**Action 3) Develop and test state-of-the-art validation strategies:** sampling along lines (transects) or by using high-resolution airborne imagery and products should complement the tradition point validation methods (elaborated in section 1.3.3).



### 1.3 Approach

#### 1.3.1 Action 1: Optical model calibration

The approach for MERIS validation can be described as a process with 3 actions. In the first action optical models are calibrated and optical parameter sets are standardized and validated, as illustrated in Figure 1.1. This figure shows the process flow in the first action of MERIS validation. Essentially  $R(0-)$  is simulated using a bio-optical model, parameter sets and in-situ measured concentrations. The resulting  $R(0-)$  spectrum is compared to in-situ measured  $R(0-)$  in order to adjust parameter settings. In parallel to this process, one parameter is optimised (namely B) by fitting simulated  $R(0-)$  to measured  $R(0-)$  using a subset of measurements.

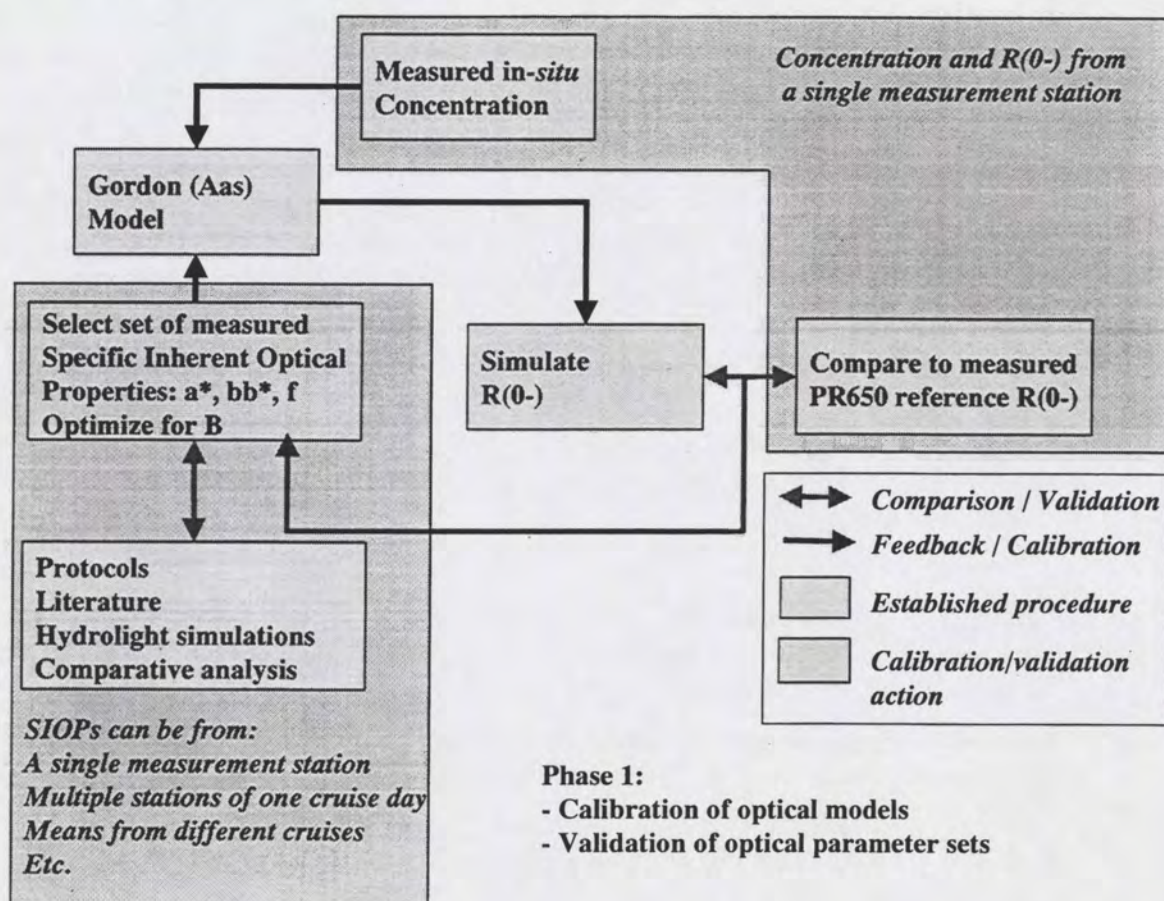


Figure 1.1: First action of MERIS validation.

#### Optical model choice

For reasons of standardization, historic considerations and e.g. to facilitate analytical model inversion, the project team (in an early stage) has chosen to adopt the Gordon model (Gordon, 1975) as the standard bio-optical model for MERIS applications. In



order to be able to describe angular effects correctly, the adaptations of Aas (1987) were included.

### *Protocols and literature analysis*

In the first action protocols are established for the laboratory and field sampling procedures. This project is dependent on MERIS protocols that will be (on some accounts) different from e.g. SeaWiFS protocols. During the MAVT meeting in October 2000, MERIS protocols were presented, but not yet accepted in their final form. Therefore, this project has, for the time being, adopted protocols established in the Netherlands in the "Spectral Library" project (Rijkeboer et al., 1996). These protocols have been used for inland water optical properties determination from 1996 to 2000. Historic and actual data have been compared to ranges found in literature (Hoogenboom, 1999, 2000, Chapter 4 and Appendix II of this report). It is expected that in summer 2001 an international laboratory and field intercomparison/intercalibration experiment will be organised by MAVT in Plymouth to compare and fine tune protocols for the determination of concentrations of CHL, TSM and CDOM, for the determination of inherent optical properties. Also methods for the above water and under water determination of  $R(0-)$  will be compared. After the workshop the definitive protocols for MERIS validation will be published.

### *Hydrolight simulations*

The use of hydrolight simulations to study the effects of various parameter settings on simulated reflectance spectra was reported by Hoogenboom et al., (2000). Results will not be repeated in this report. As chapters 2.3 and 5 will show, there is uncertainty about the exact procedure for reference reflectance measurements using the PR650 method. It is recommended to use hydrolight simulations to study various configurations for reflectance measurements.

### *Comparative analysis*

The issue of comparing various parameter sets will be addressed in chapter 6 of this report.

### *Calibration / validation*

By comparing simulated  $R(0-)$  to measured  $R(0-)$  a final selection of optical model parameters is made. In this study, it turned out that this comparison is quite difficult due to uncertainty in the PR650 procedure and resulting measurements and to remaining uncertainty in optical model parameters. E.g. backscattering is not measured directly, but is derived from light attenuation and absorption measurements. Therefore, this important parameter remains a source of (not completely understood) uncertainty.



### 1.3.2 Action 2: Selection and calibration of algorithms

In the second action algorithms are selected and calibrated. The feasibility of using an analytical models and the availability of sufficiently large in-situ data-sets determine which type of algorithms can be used (semi-analytical or semi-empirical algorithms).

By comparing simulated concentrations to in-situ measured concentrations, algorithms can be selected and calibrated, and sensor configurations can be tested (Figure 1.2).

In action 2 the bio-optical model and parameter sets are inputs from action 1. By using field reference data on spectral reflectances and concentrations, the performance of various algorithms for various sensor band pass settings can be analysed and calibrated.

This report will elaborate experiments with various algorithms, using field reference data from 3 in-situ experiments during 2000 (see chapters 4, 5 and 6).

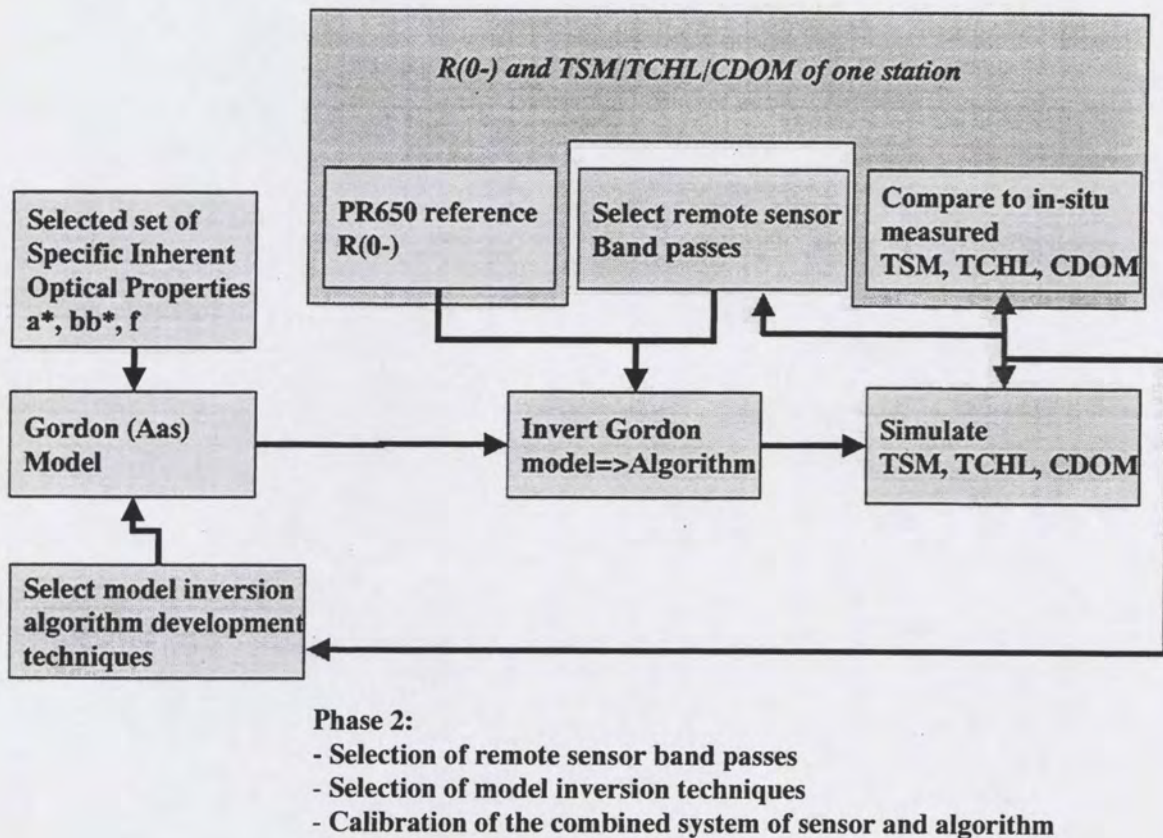


Figure 1.2: Action 2 in MERIS validation (analytical model selection and calibration)



### 1.3.3 *Third action*: point and transect validation

Validation of remote sensing (reflectance and concentration) products on the scale of the Dutch North Sea is a very difficult exercise. This is due to the fact that the comparison of point scale observations with satellite observations (pixel sizes > 300 m x 300 m) is poorly understood. Furthermore, general weather conditions, accessibility of the area, low density regular monitoring etc. allow only to collect very limited numbers of field samples. This is in contradiction to validation data demands caused by the dynamics and spatial variations of the North Sea that can be quite intensive. Such variations impose demands on validation activities such as a close synchronization between field and satellite observations and a network density suitable to validate mean and extreme values of concentrations. Validation of North Sea remote sensing products has been done on limited datasets. Some validation has been attempted in EC-projects such as COLORS and COAST-LOOC. The results of these studies were not available at this time. Van der Woerd et al., 2000, documented the validation of TSM observations based on SeaWiFS images.

An important part of this study addresses the measurement of (hyper)spectral  $R(0-)$  by close sensing (PR-650; Ocean Optics) and from an aircraft (EPS-A) because both close range and EPS-A observations can be used to simulate MERIS observations and validate proxy MERIS products. Close range, above water optical measurements will allow measuring the subsurface reflectance along transects. In combination with a small series of IOP determinations along the transect (for algorithm calibration purposes) these measurements allow to do detailed line mappings across concentration gradients. These line mappings will be used to set up and test a validation framework for the comparison of point samples along the transects with RS-measurements.

The last action in the process to obtain validated products (suitable for operational use) is the actual validation of MERIS observations and proxy data. Since MERIS will not be operational until October 2001, only proxy data can be used to rehearse for MERIS validation. The options that can be considered in the Netherlands are illustrated in

Once the algorithm(s) have been established in action 2 together with parameter sets (action 1), sensor band pass settings etc., validation of the reflectance and concentration products can be performed in action 3. In figure 1.3 a difference is made between the two main observables to be validated, namely reflectance spectra and concentrations.

#### *Issues related to reflectance validation*

There are two major issues to deal with in reflectance validation, namely:

- 1) Are above water measurements suitable for validation purposes?
- 2) Can the frequency of field observations be increased at low costs, to allow sufficiently large group of observations?

Both issues will be discussed in this report. The reliability of above water measurements will be discussed using PR650 measurements (5.1). Low cost high frequency measurements will be discussed using the example of the Satlantics set-up (5.3).



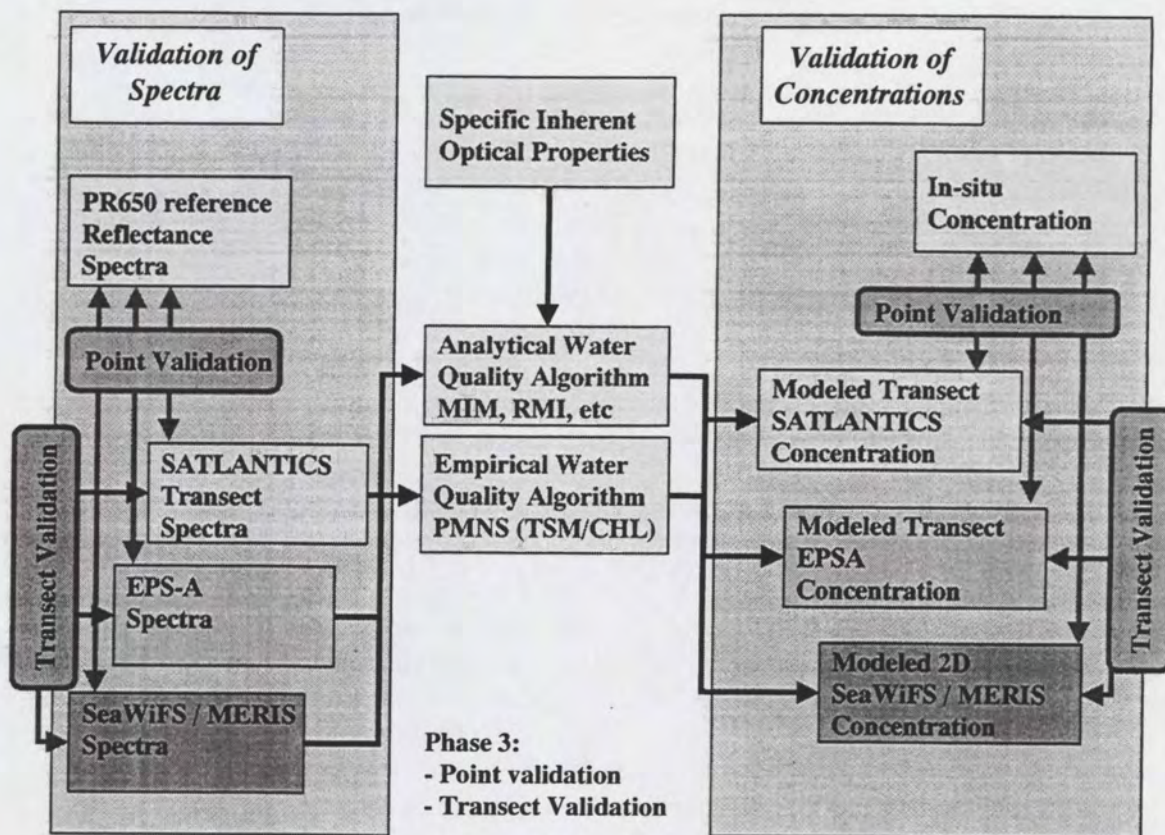


Figure 1.3: Action 3 in MERIS validation.

#### Issues related to concentration validation

The final step in MERIS validation is the validation of MERIS (or proxy sensor) concentration products. Both by means of point and transect validation. In this action still procedures may be identified that require recalibration or adaptation or modification of parameterisations and algorithms to improve concentration measurements in Dutch coastal waters.

Concentration validation should answer the following additional questions:

- 3) Are the selected SIOP parameter sets representative for the area and time period under consideration?
- 4) Is the algorithm suitable to deal with natural variability of SIOP etc.?
- 5) Is there a need for fine-tuning of additional settings such as choices in band (sub-) selection etc.?



## 1.4 How to read this report

Although three separate activities were identified in the previous sections the report is not formatted accordingly. This is because of the complexity of the issues and because of interrelationships and common methods between the 3 activities. Therefore a stepwise structure was chosen for this report. Two decisions are important for the reader:

- 1) Summaries of algorithm theory and instrumentation were placed in appendices. As a consequence some new theory, such as the description of the new Ratio Matrix Inversion, is also placed in the appendices. The benefit for the reader is that he can consult theory whenever necessary while it does not interrupt the main flow of the text.
- 2) An important by-product of this project, namely a literature study and an analysis of historical SIOP data based on PMNS observations together with a comparison with MERIMON-2000 observations will be published in a separate report (Vos et al., to be published).

The structure of the report is as follows:

*Chapters 2 and 3 discuss optical models and inversion options*

- Chapter 2 describes the preferred optical model to simulate R(0-) and briefly the theory for spectral measurements. Conclusions are drawn about some possible causes for disagreement between simulated and measured reflectance spectra.
- Chapter 3 discusses advantages and disadvantages of general types of algorithms. The possibilities to do analytical inversion of the preferred optical model are briefly discussed. The necessity to develop dedicated regional algorithms for MERIS is presented.

*Chapters 4, 5 and 6 present results from measurements*

- Chapter 4 presents the results of the MERIMON field measurements of concentrations. Comparisons are made to the historic PMNS dataset.
- Chapter 5 shows the results of spectral measurements from various sensors
- Chapter 6 summarises results from Vos et al., (to be published) on SIOP measurements

*Chapters 6 and 7 discuss algorithm selection and validation options*

- Chapter 6 also presents the results of studies where several algorithms were calibrated using various SIOP datasets and applied to reflectance spectra of various locations. It also presents the results of the application of algorithms that were calibrated on historical datasets. Thus a first analysis on algorithm performance is done.
- Chapter 7 presents options for MERIS validation. Cases are presented based on Ferry observations in the 'Marsdiep', an EPS-A overflight also over the 'Marsdiep' and SeaWiFS images. Some initial attempts to transect validation are discussed. Future options for MERIS validation are discussed.



### 1.5 Acknowledgements

We are above all grateful to RIKZ as a major partner in this project for contributing substantial amounts of time and resources. Their continuous efforts to bring Earth Observation under the attention of operational services in 'Rijkswaterstaat' are greatly appreciated.

We are very grateful for the access to ship borne facilities. For this and for their support we thank the Captains and crews of the research Vessel the "Mitra" and the "Navicula". In addition, organization of cruises by RIKZ, RWS/North Sea and NIOZ is also gratefully acknowledged. The aid and support of Marcel Wernand with the organisation of the "Navicula" campaign, his assistance with field sampling and spectral measurements and his valuable efforts to make the Satlantics measurements accessible to this project are acknowledged and greatly appreciated. We thank NIOZ for the opportunity to study Satlantics observations.

We also thank RWS/MD for the use of the data collected during the spring cruise of the research vessel the "Belgica". RWS/MD is also gratefully acknowledged for the contribution of EPS-A images and infrastructure to this project. The help of the airplane and sensor operators and the image processing team at RWS/MD is acknowledged.

Dr. Ruddick of MUMM owes our thanks for arranging ship time and cruise logistics. The Captain and crew of the "Belgica" are gratefully acknowledged.

We are grateful to the receiving station of Dundee University, the SeaWiFS project team, The Ocean Color Data Support Team, The Distributed Active Archive Center at Goddard Space Flight Centre and the SeaDAS development team for acquiring, providing, distributing and supporting the use of SeaWiFS data. The use of MUMM's atmospheric correction routines and continuous support are also gratefully acknowledged.



## 2. Theory of Simulation and measurement of $R(0^-)$

### 2.1 Simulation models for $R(0^-)$ : Introduction

#### *$R(0^-)$ : why*

MERIMON requires comparison of simulated and measured  $R(0^-)$  in phase 1 (see chapter 1: Figure 1.1):

1. To determine optimal parameterization sets
2. To determine B by optical closure
3. To validate the reference (PR650)  $R(0^-)$  measurements

In phase 2 reference (PR650)  $R(0^-)$  measurements are used to establish the optimal algorithm simultaneous with optimal remote sensor band pass settings (see Figure 1.2)

In phase 3 reference (PR650)  $R(0^-)$  measurements are used to validate remote sensing measurements of  $R(0^-)$  (EPS-A, Satlantics, SeaWiFS and future MERIS: see Figure 1.3).

The common factor in parameterisation and validation is the subsurface irradiance reflectance ( $R(0^-)$ ). This choice is historically determined (see e.g. Hoogenboom 1999, Dekker 1993) and is, amongst others, based on the consideration that  $R(0^-)$  is a neutral parameter in which variations in viewing geometry, atmospheric conditions and air-water interface conditions have been eliminated as far as is possible.

#### *Problems with $R(0^-)$*

One of the most important terms in  $R(0^-)$  is the upwelling irradiance just below the water surface. Simulation of  $R(0^-)$  requires an adequate formulation of the conversion of simulated upwelling radiance into simulated upwelling irradiance. This requires insight in the angular distribution of the upwelling light field. A formulation of this conversion should be simple enough to allow inversion of the underwater light model to derive algorithms. Simulation models will be treated in chapter 2.1.

Measured  $R(0^-)$  features similar problems. Remote sensors usually measure above water. The quantity that is observed is the water leaving radiance. In this case not only the conversion to upwelling irradiance has to take place, but also the transport of upwelling irradiance through the air-water interface must be taken into account. The remote measurement of  $R(0^-)$  will be treated in chapter 2.3.



### *Simulation models for R(0-)*

Light transport in water can be described by a number of models. A selected simple formulation will be discussed here, mainly because of the proven adequacy to describe the underwater light field and because the feasibility of model inversion. The model simulates the subsurface irradiance reflectance as a function of inherent and apparent optical properties. In general, bio-optical simulation models are used to understand the physical relationship between  $R(0-)$  and concentrations.

## **2.2 Simulation models for R(0-)**

An overview of bio-optical models is given in e.g. Dekker, 1993, Krijgsman, 1994 and (Hoogenboom, 1999). There are several candidate models ((Gordon et al., 1988); (Walker, 1994); (Aas, 1987)) of which the Walker formulation was found to be most relevant to this project.

### **2.2.1 Gordon model with pre-factors by Walker**

#### *Introduction*

The original Gordon model is from 1975 (Gordon et al., 1975)). It relates for each wavelength  $\lambda$ ,  $R(0-, \lambda)$  to the total backscatter ' $b_b$ ' and total absorption ' $a$ '. The model assumes an optically deep medium so that bottom effects can be ignored. Also stratification in the water column and inelastic scattering effects, such as Raman scattering and fluorescence are ignored. Pre-factors are related to the Q-factor (which is a ratio between water leaving radiance and water leaving irradiance) and the formulation includes a quadratic power term. Q can, more precisely, be described as the transformation factor for radiance to irradiance over the upper hemisphere. For isotropic radiance distributions over the hemisphere this factor is  $\pi$ .

#### *The Walker model*

Walker (1994) avoids using the second power term, and does not explicitly need the Q-factor as input. As input for the pre-factor 'f' it uses the average cosines for upwelling and downwelling irradiance ( $\mu_u, \mu_d$ ):

$$R(0-, \lambda) = f(\mu_u, \mu_d) \frac{b_b(\lambda)}{a(\lambda) + b_b(\lambda)} \quad (2.1)$$

$$f(\mu_u, \mu_d) = \frac{1}{1 + \frac{\mu_d}{\mu_u}} \quad (2.2)$$



With:

$R(0, \lambda)$  = subsurface irradiance reflectance (-)

$b_b$  = total backscatter ( $m^{-1}$ ), also a function of  $\lambda$ ;

$a$  = total absorption ( $m^{-1}$ ), also a function of  $\lambda$

$\mu_{u,d}$  = average cosine of upwelling (u) or downwelling (d) light;

### *Concentrations, absorption and backscattering*

The Gordon and the Walker model both assume that the total backscatter and total absorption spectra are respectively the sum of the absorption and backscattering of pure water, and of some optically active water constituents like TCHL, TSM and CDOM:

$$a = a_w + a_{TCHL}^* \cdot TCHL + a_{TSM}^* \cdot TSM + a_{CDOM}^* \cdot CDOM \quad (2.3)$$

$$b_b = b_{b,w} + Bb_{TSM}^* \cdot TSM \quad (2.4)$$

The total absorption or scattering per constituent is determined by the product of specific (per unit concentration: indicated by the \*) absorption or scattering and the concentration of the constituent. No scattering for CDOM and chlorophyll-*a* is assumed.

### *Elaboration of f*

For relatively clear skies ( $\mu_d \approx \cos(\theta_0)$   $\mu_d = 0.5$ ) and optically deep waters 'f' can in good approximation be related to the sun-angle with zenith ( $\theta_z$ ):

$$f = \frac{1}{\left(1 + \frac{\mu_d}{\mu_u}\right)} \quad (2.5)$$

$$\mu_d = 0.7F + (1 - F)\cos(\bar{\theta}_0) \quad (2.6)$$

$$\mu_u = 0.5 \quad (2.7)$$

$$\bar{\theta}_0 = a \sin(\sin(\bar{\theta}_z) / n) \quad (2.8)$$

With:

$F$  = fraction of diffuse downwelling light;

$\theta_0$  = angle of downwelling skylight under water;

$\theta_z$  = angle of downwelling skylight above water (or sun zenith angle);

$n$  = refractive index of water (1.33).



This model was applied to Lake IJssel by (Hakvoort et al., 2000). The Hydrolight model (Mobley, 1994) can be used to generate look-up tables for  $(\mu_u, \mu_d)$ .

In practice the Q factor is still needed to convert radiance measured at a sensor to irradiance. This problem is addressed in the section 3.2.

### 2.2.2 Hydrolight

Hydrolight (Mobley, 1994) solves the radiative transfer equations (RTE) using the invariant imbedding method. In this method standard operators are derived for an infinitesimally thin layer. These standard operators can be used to compute the radiances for the complete water column (in a number of layers) via the *imbedded rules* and the *invariant imbedding relations*. In this way, no explicit integration of the RTE is required. As input the method requires the SIOP for the water column.

Presently, Hydrolight is used by RIKZ to simulate experimental field conditions and to generate Look-up Tables for  $(\mu_u, \mu_d)$  (Hoogenboom, 2000).

## 2.3 Remote measurement of R(0-)

### 2.3.1 Above water radiance measurements

Within this study most R(0-) measurements take place above water: the measured quantity at the sensor is  $L_t$ . Depending on the distance of the sensor to the water surface and the viewing geometry, corrections for extra radiance from the atmosphere (path radiance:  $L_a$ ) and for additional radiation due to reflections of incoming light at the water surface directly into the sensor ( $L_r$ ) are required to get the water leaving radiance  $L_u$ :

$$L_t = L_a + L_r + \gamma L_u(0, -) \quad (2.9)$$

$$L_r = \rho_s L_s \quad (2.10)$$

Here  $\gamma$  corrects for refraction of light at the air-sea interface. The factor  $\rho_s$  relates the incident radiance at the surface  $L_s$  to the directly reflected outgoing radiance  $L_r$ . For handheld sensors the path radiance may be neglected; the correction for  $L_r$  is critical.

Factor  $\rho_s$  was recently studied by Mobley. In the past this factor is assumed to be constant for not too large viewing angles of the detector ( $\theta_v < 42^\circ$ , at an azimuth  $\varphi_v$  of  $135^\circ$ ) (Gons, 1999). However, in some cases  $\rho_s$  can be influenced by sun glitter and cloud glitter (Mobley, 1999), especially for *high wind speed*. The ratio further depends on local sky illumination conditions and sun zenith angle. The presence of clouds can lead to so-called 'cloud glitter'. Unfortunately, cloud glitter disturbs also the spectral shape of



radiance spectra (especially in the red part of spectra). Near surface observations using handheld spectro-radiometers can be corrected for most of these effects because the spectrum of downwelling light can be measured additionally. On the EPS-A there is no such facility at present, while the altitude of satellites is too high for such a measurement. Therefore to avoid sun and cloud glitter in remotely sensed images careful mission planning is required or specific algorithms to remove the affects.

### 2.3.2 Deriving reflectance from radiance measurements

In the situation where upwelling and downwelling light fields are measured by a optical sensor, then remote sensing reflectance  $\rho_w$  and subsurface irradiance reflectance  $R(0-)$  are defined respectively by:

$$\rho_w(\theta_0, \theta_v, \varphi_v, \lambda) = \frac{L_u(0-, \theta_0, \theta_v, \varphi_v, \lambda)}{E_d(0-, \lambda)} \quad (2.11)$$

$$R(0-, \lambda) = \frac{E_u(0-, \lambda)}{E_d(0-, \lambda)} = \frac{Q(\theta_0, \theta_v, \varphi_v, \lambda, \dots) L_u(0-, \theta_0, \theta_v, \varphi_v, \lambda)}{E_d(0-, \lambda)} \quad (2.12)$$

With:

- $\theta_v$  = Viewing zenith angle of the sensor with respect to z-axis, in the yz-plane;
- $\varphi_v$  = Azimuth angle between vertical planes from sensor to observation point and the sun to observation point;
- $E_{u,d}$  = Irradiance (upward or downward);
- $L_u$  = Radiance (upward), depending on sun zenith angle and viewing geometry of the sensor;

In the case of measured  $R(0-)$  it is of importance to know  $Q$  because it influences the  $R(0-)$  directly. Morel (Morel and Gentili, 1993b) quotes that 'Q' factors for *turbid Case 2 waters* would be steadily approximately 3.5. In the PMNS project (Althuis et al., 1996) a factor of  $Q=5$  is used. Gons uses a sun zenith angle formulation for  $Q$  (Gons, 1999), whereas Ruddick (Ruddick et al., 2000) simply uses a factor of  $\pi$  in the Seadas-MUMM software for processing of SeaWiFS radiance images to reflectance images. It is apparent that there is no consensus about the  $Q$ -factor.



## 2.4 Considerations for the comparison of measured reflectance with simulated reflectance

As defined in equation 3.9, the remote sensing reflectance is the ratio between upwelling radiance and downwelling irradiance just below the water surface; the use of the transformation factor 'Q' is avoided.

The use of the remote sensing reflectance gives an advantage in the case where simulated and measured reflectances have to be compared (such as in MERIS validation). In this case one may divide the "observed R(0-)" and the simulated R(0-) both by Q:

$$\frac{R(0-, \lambda)}{Q(\theta_0, \theta_v, \varphi_v, \lambda, \eta, \beta, \dots)} = \frac{f(\theta_0, \theta_v, \varphi_v, \lambda, \eta, \beta, \dots)}{Q(\theta_0, \theta_v, \varphi_v, \lambda, \eta, \beta, \dots)} \frac{b_b}{(a + b_b)} \quad (2.13)$$

$$\text{Measured } R(0-)/Q \text{ (eq 3.10)} = \text{Simulated } R(0-)/Q \text{ (eq 3.1)}$$

The rationale behind this transformation is that variations of the pre-factor 'f/Q' are (much) less than that of the factors 'f' and 'Q' alone. (Gordon et al., 1988) (Morel and Gentili, 1991a), (Morel and Gentili, 1993b), (Morel and Gentili, 1996c)). Therefore it is argued that using a constant for the ratio for f/Q will lead to a reduction of errors in comparison with methods that calculate Q and f separately. Gordon (Gordon et al., 1988) uses '(f/Q)' = 0.0949. According to Morel, the mean value of '(f/Q)' is 0.0922.

### 2.4.1 Consequences for algorithms

#### *Consequences of unknown Q (on algorithms based on R(0-))*

In this report a number of algorithms for the North Sea are described (Table 1.1 and chapter 3):

- Semi-empirical algorithms relate directly observed surface reflectance (R(0-) or other form) to concentrations. If R(0-) is used then the results of these algorithms are linearly dependent on Q.
- One band algorithms based on semi-analytical inversion of equation 3.1 are also linearly dependent on Q.
- (Semi-) analytical matrix inversion algorithms based on the linearisation of equation 3.1 retain linear dependency on Q.
- Ratio algorithms assuming a spectrally neutral Q (such as Ratio Matrix Inversion presented in this report) are dependent on the error in this assumption: the larger the spectral variability, the larger the error in the concentration. It is expected



that this type of error is of a magnitude lower than the error in the case of linear dependency on  $Q$ .

### *Consequences for comparing results from various regional studies*

Although  $Q$  and  $f$  factors were approximated, good results have been gained in the past with analytical inversion algorithms for  $R(0-)$  (one band or simple matrix inversion) (Vos et al., 1999), in combination with in-situ measured SIOP (Gons, 1999), (Rijkeboer et al., 1999), (Ruddick et al., 2000). Examples of one-band semi-analytical algorithms can be found in Dekker et al., 1999; Pasterkamp, 1999 and 2000, and Van der Woerd (2000).

It is clear that comparison of various studies requires a rigid treatment of the  $Q$  and  $f$  factors involved. It is also important to consider an important secondary effect, namely that the backscatter ratio, which is unknown, is determined from optical closure. This means that the backscatter ratio used in various studies depends on the assumptions for  $f$  and  $Q$  as well. The determination of the backscatter ratio is usually done on a limited data set, which, in turn, leads to errors due to unaccounted variations

### *Consequences of unknown ' $f/Q$ ' for ratio algorithms*

The MODIS ocean science team (Carder et al., 1999) argues that for ratio-algorithms based on ' $R/Q$ ' the constant factor ' $f/Q$ ' will cancel completely from the equations as long as ' $f/Q$ ' is not dependent on wavelength. Morel has showed that this approximation is accurate for wavelengths between 440nm and 565nm assuming normal viewing conditions: see Morel (Morel and Gentili, 1993b). In that case, both ' $f$ ' and ' $Q$ ' never need to be evaluated since the relative error of a ratio algorithm is only 3.5%. Also Aiken (Aiken et al., 1995) follows this approach for retrieval of pigments from SeaWiFS. The Ratio Matrix Inversion algorithm presented in this report also makes use of this proposed property.

### *Affects on the MERIS standard algorithm*

The most rigorous way to circumvent the problem of having to make assumptions for  $f$  and  $Q$  seems to be by solving the radiative transfer equations for atmosphere and water column simultaneously for given SIOP, sun angles, sensor geometry, atmosphere and volume scattering function. But, in this case the unknown  $Q$  is replaced by an unknown volume scattering function and its spatial and temporal variability! Doerffer and Schiller (Doerffer and Schiller, 1997) did these simulations for the configuration of the MERIS sensor on board of ENVISAT. A number of these simulations were used to train a neural network that, subsequently, will be used to inversely retrieve concentrations from MERIS observed spectra. This approach can be generalized for local regions (using local SIOP instead of global SIOP), but for every region the neural network has to be trained again, which may be time-consuming.

Neural networks have the advantage that output results are always within input ranges. The standard MERIS processor solves simultaneously for the concentrations of CHL,



TSM and CDOM, and for the atmospheric optical depth per wavelength band. Such an approach makes it increasingly difficult to trace irregularities because errors in the atmospheric optical depth are hardly verifiable yet (Pasterkamp et al., 2001).

At the moment there is little experience with the neural networks approach. It is essentially a physically based black box method, in the sense that the solution provided by the neural network may very well be a "local minimum" instead of the optimum solution. Also, neural networks always provide a solution, even when matching of simulated and measured spectrum was not achieved at all. Therefore, and this is incorporated in the MERIS ground segment, it is necessary to provide a quality indicator based on the comparison of reflectances.

## 2.5 Some conclusions and Recommendations

### *Conclusions*

- Since MERIMON especially deals with local variability of inherent optical properties, fast and easy to use inversion models are absolutely required. Therefore, attention has to be paid to the effect of Q and f factors and the volume scattering function on the end-results.
- Ground truth R(0-) data must be determined with procedures that are as close as possible to satellite R(0-) data. At present this is not the case for the Gons PR-650 model for R(0-) and the MUMM-Seadas software for R(0-) for the SeaWiFS sensor.
- Similar problems are reported from the PMNS project in section 3.4.2 and from the PNMS+ project (Kromkamp and Wouts, 1998). The PR-650 spectra measured for PMNS are not reliable, since the correction for skylight was not done during the measurements. Hoogenboom used the original (uncorrected) spectra, (Hoogenboom et al., 1997) when he assessed the quality of the PMNS data set. Also the use of a Q-factor of '5' is questionable for these spectra.
- These *transformation problems* will also arise when converting the MERIS normalised water leaving radiances to level 2 R(0-) end-products. Since 'Q' from a neural-network-Monte-Carlo-photon approach can never be reproduced by any ground truth algorithm, calibration inaccuracies for absolute R(0-) values may occur.

### *Recommendations*

- Standardization of the use of 'f' and 'Q' factors is required to make various data sets on level 2 apparent optical properties consistent. It is advised therefore to generate look-up tables from these Monte-Carlo simulations (or neural networks or from *Hydrolight* (Mobley, 1995) for the 'f' and 'Q' factors. When the Tables are not available it is advised to have some default well defined and well documented settings for the 'f' and 'Q' factor.

It is advised to measure the volume scattering function in-situ. However, new experimental methods must be developed for this in the Netherlands. Experimental equipment for this has been developed by Hobi-Labs (Maffione et al., USA, <http://www.hobilabs.com>).



### 3. Algorithms for MERIS

#### 3.1 Introduction

##### 3.1.1 Algorithms and water quality parameters

Algorithms are either inversions of optical models (such as e.g. the Gordon-Walker model) or semi-empirical relationships between concentrations and observable optical entities such as  $R(0-)$ . Algorithms are used for the retrieval of water quality parameters (concentrations of optical active constituents) from satellite data. These water quality parameters are:

- The concentrations of Total Suspended Matter (TSM);
- Part of the (green) algal pigment concentration: measurable is either Chlorophyll-a (CHL) or Total Chlorophyll (TCHL, the sum of Chlorophyll-a and Phaeopigments; sometimes also Chlorophyll-b and Chlorophyll-c are included);
- A measure for the concentration of Coloured Dissolved Organic Matter (CDOM).

In this chapter, a state of the art summary is made of algorithms for retrieval of concentrations from satellite data.

##### 3.1.2 Algorithm type

There are four general types of algorithms, namely:

- 1) Semi-empirical algorithms and band ratio-algorithms. The configuration (including spectral band selection) of the algorithm is based on physical considerations;
- 2) Analytical algorithms based on complete inversion of physical (bio-optical) models;
- 3) Semi-analytical algorithms based on the inversion of physical models, using a-priori knowledge on concentration of some optical active constituents
- 4) Inversions of numerical radiative transfer models: e.g. neural networks algorithms

All algorithms have as input an apparent optical property such as  $R(0-)$  spectra or remote sensing reflectance spectra (Carder et al., 1999). These spectra are derived from radiance measurements at a sensor. If a satellite or aircraft does the observations, the radiance measurements must be corrected for atmospheric effects, white capping, sun glint and sky glint at the seawater interface. Measurements from handheld spectracolorimeters need to be corrected mainly for sun glint and sky glint at the seawater interface. Analytical algorithms additionally require a set of Specific Inherent Optical Properties (SIOP) as input. SIOP are phenomenological parameters that describe the scattering and absorption characteristics of the water quality parameters. Each type of algorithm has its merits and disadvantages:



### *Semi-empirical algorithms and band ratio-algorithms*

Semi-empirical algorithms (Althuis and Buiteveld, 1996), (Carder et al., 1999) require only superficial knowledge of the optics involved. The algorithms may use subsurface irradiance reflectance (Althuis et al., 1996), the remote sensing reflectance (Carder et al., 1999) or the water leaving radiance. Some of these models are still based on an analytical model and the Specific Inherent Optical Properties (e.g. Gons, 1999). All semi-empirical models use parameters that are fitted with statistical methods using field data and satellite data. An advantage of all semi-empirical models discussed in this report, is that no SIOP are required. They are calibrated for a specific region and period based on calibration data representing the state of the art of the calibration period. Once calibrated, the algorithm is fixed. Adaptations to other circumstances are costly because for each calibration sufficient field observations are necessary. Semi-empirical algorithms are robust, easy to implement and fast. Unfortunately it is difficult to validate semi-empirical algorithms because, besides the calibration dataset also a validation dataset must be acquired, whereby sampling conditions should not be too dissimilar.

### *Analytical algorithms*

Analytical algorithms require insight in simplified bio-optical models such as the Gordon/Walker model. They need to be calibrated using limited datasets of inherent optical properties, concentrations and reflectance spectra. The present state of the art is that almost all parameters can be measured with a reasonable accuracy in the field or in the laboratory. Some parameters, however, remain unknown and must be assessed from optical closure or from literature. Analytical algorithms most often are a form of the Matrix Inversion Method (MIM) (Hoogenboom et al., 1998a) or e.g. the Ratio Matrix Inversion method (this report) or methods based on Principal Component Analysis (PCA) (Krawczyk, 2000). Analytical algorithms have the advantage that the processor can be built independent of the parameterisation dataset. This means that the algorithms can be easily adapted to other conditions and times. Techniques such as Matrix Inversion and Ratio Matrix Inversion are relatively fast and have proved to be robust as well. All analytical algorithms described in this report rely on  $R(0^-)$  observations, which means that atmospheric correction is a critical step in the processing. Analytical algorithms essentially match a simulated reflectance spectrum to a measured reflectance spectrum. This means that there are additional possibilities for validation, namely on the level of concentrations but also on the level of reflectance spectra. This also means that accuracy assessments can be based on both types of validation (see e.g. Vos et al., 2000)

### *Semi-analytical algorithms*

Semi-analytical algorithms are a special case of analytical algorithms. Full inversion of the Gordon/Walker model requires accurate SIOP of all optical active constituents, but also correct spectra that are measured in a sufficient number of relevant spectral bands. If there is incompleteness in any of these conditions, it occurs that one of the concentration variables (usually CDOM) is difficult to obtain with sufficient accuracy. This may influence the retrieval accuracy of other concentrations (CHL and TSM), which leads to algorithms that assume mean concentration values for the critical parameter (e.g. CDOM). If the only parameter of interest is TSM then CHL can be assumed to be constant as well. Values for the constant parameters have to be determined from field samples. Optical simulation modelling experiments have shown that TSM retrieval (depending on the exact formulation of the analytical inversion: 1 band; 2 bands or multi bands and the spectral band positioning) can be relatively insensitive to errors in the CDOM and CHL boundary conditions (Pasterkamp et al., 1999 RESWES, Vos et al., 2000).



### *Analytical inversions of radiative transfer models*

Radiative transfer models use more basic equations for light transfer in the water column. Some of the models solve also light transfer through the atmosphere simultaneously. Forward models either use the invariant embedding method (Mobley, 1994) or Monte Carlo techniques (Doerffer and Schiller, 1994). Neural network inversions of numerical radiative transfer codes (including Monte Carlo simulation models (Doerffer and Schiller, 1997)) require a profound insight in the workings and theory of radiative transfer. They are also a special case of analytical models. The bio-optical model is calibrated using observations of SIOP, and other parameters such as the volume scattering function. The optical model is used to train the neural network that is, subsequently, used as a fast and robust means to derive concentrations from input spectra. Neural networks have the advantage that output results are always within input ranges. An important example of an (future) operational neural network processor is the standard MERIS processor. This processor solves simultaneously for the concentrations of CHL, TSM and CDOM, and for the atmospheric optical depth per wavelength band. Such an approach makes it increasingly difficult to trace irregularities because errors in the atmospheric optical depth are hardly verifiable yet (Pasterkamp et al., 2001). At the moment there is little experience with the neural networks approach. It is essentially a physically based black box method, in the sense that the solution provided by the neural network may very well be a "local minimum" instead of the optimum solution. Also, neural networks always provide a solution, even when matching of simulated and measured spectrum was not achieved at all. Therefore, and this is incorporated in the MERIS ground segment, it is necessary to provide a quality indicator based on the comparison of reflectances.

### 3.1.3 Currently available algorithms for MERIS and the North Sea

A selection of currently available algorithms that might be applicable to North Sea waters is listed in Table 3.1. This table is an adaptation of Table 1.1.

Algorithm	Reference	Algorithm type
MERIS-CHL	Doerffer et al.,	Neural network
MERIS-TSM	Doerffer et al.,	Neural network
PMNS-TSM	Althuis et al.,	Semi-empirical
PMNS-CHL	Althuis et al.,	Semi-empirical
EPSA-MIM-TSM	Hakvoort et al., Earsel	Analytical
EPSA-MIM-CHL	Hakvoort et al., Earsel	Analytical
RMI-TSM	This report	Analytical
RMI-CHL	This report	Analytical
Eps-a Wide-1band TSM	This report	Semi-analytical
POWERS-TSM	Van der Woerd et al., POWERS	Semi-analytical
Hoogenboom TSM	Hoogenboom et al., OO	Semi-analytical

*Table 3.1 An overview of types of algorithms used for North Sea remote sensing*



### 3.1.4 From MERIS standard algorithms to regional algorithms

#### *Standard products*

The standard concentration products that are under development for MERIS (based on the MERIS Algorithm Theoretical Baseline Document (ATBD): Doerffer and Schiller, 1997) are:

1. Phytoplankton pigment index expressed as chlorophyll-a concentration, unit:  $\mu\text{g/l}$
2. Non-absorbing suspended particle concentration (NSP), unit:  $\text{mg/l}$
3. *Gelbstoff* (yellow substance) absorption at 440 nm, unit:  $\text{m}^{-1}$

Note that the chlorophyll-a concentration is the total chlorophyll (TCHL) minus the phaeopigments. NSP is approximately the same as TSM and gelbstoff concentration would equal the CDOM concentration. A true comparison of Dutch TSM, TCHL and CDOM and the MERIS concentration products can be done after publication of the definite measurements protocols. This is because the protocols used to measure the concentrations (that in turn were used to calibrate/validate the standard optical model) define the concentration products. Deviations between MERIS protocols and Dutch protocols have already been noted and will have to be accounted for.

The definition and documentation of standard ESA MERIS algorithms is given in the MERIS Level 2 Algorithms Theoretical Basis Document (ATBD 2.12) (Doerffer and Schiller, 1997). This document describes the theoretical basis for algorithms for data retrieval of water quality parameters from MERIS level 1B, Top of the Atmosphere (TOA), satellite imagery. In the ATBD, also requirements for data collection with respect to calibration and validation of the algorithms are given.

#### *Discussion of the ATBD*

Although the ATBD gives the impression to be a complete document, some issues remain to be discussed:

1. The ATBD document needs comparison with other approaches, like the MODIS ATBD document (Carder et al., 1999) and other algorithms for *regional areas*;
2. The ATBD document considers (at present) only *global scale data products*. Since it is generally expected that these are not accurate for regional applications, adaptations or alternatives have to be considered. Remote sensing experts in the Netherlands and Belgium employ different approaches (*for local or regional applications*) than those followed in ATBD. These experts have methods and facilities to sample the local specific inherent optical properties and therefore their methods may be a good alternative to standard MERIS products for local regions.
3. The ATBD document is still theoretical in the sense that only *computer-simulated* data have been used for validation of the algorithms until now. Since MERIMON is a project that collects true field data for calibration and validation, the field campaigns and used methods must first be compared with the data needs for the employed algorithms. Consequences of inaccuracies in the field data and collected spectra need be analysed;



4. The ATBD does give an overview of in-situ data available on reflectance spectra, concentrations and SIOP for the North Sea.

### *Consequences for MERIMON*

Given these four factors the following questions of importance to MERIMON arise:

- Will standard ESA-MERIS algorithms be suitable for North Sea applications?
- Should the preparation for MERIS validation wait until standard products are available, or should alternative approaches be tested and validated using proxy sensors (for the time being)?

The answer to the first question lies in the fact that the MERIS standard algorithms were calibrated for average European case II water properties. Therefore it is questionable whether this parameterisation is representative for the North Sea waters under consideration. Tests should confirm the (in-)validity of MERIS algorithms, but this proved to be impossible to do in 2000 since the definitive parameterisation of the MERIS processor still had to be decided upon during the last attended MAVT meeting (October 2000). This automatically leads to the answer of the second question. While MERIS standard products remain unavailable, other state of the art algorithms should be tested (and if necessary developed) to select and calibrate the best regional (algorithms calibrated on regional datasets) alternative for MERIS standard algorithms.

### *Regional algorithms*

MERIS algorithms for the North Sea have been developed in the past years, based on technology and insight at the moment, and focus of the research projects involved. The PMNS study e.g. has resulted in robust semi-empirical TSM, CDOM and CHL algorithms for MERIS and SeaWiFS. These algorithms have not yet (to the best knowledge of the present author) been applied to series of SeaWiFS images of the Dutch North Sea. Therefore their performance during other years or alternative circumstances remains to be tested. Analytical algorithms would have the advantage that they can be transposed to other regions and to other sensor configurations. Completely analytical algorithms for TSM and CHL were developed only recently (Matrix Inversion Methods: Hoogenboom et al., 1999; Hakvoort et al., 2000, Neural Networks: Doerffer et al., 1997 and the new Ratio Matrix Inversion algorithm: this report).

### *Why develop new algorithms*

MERIS is expected to have the capability to monitor CHL concentrations in coastal waters because it contains the essential spectral configuration and it features turbid water atmospheric correction. The MERIS instrument will be the first to offer this service. So far, operational and accurate CHL retrieval for case II waters has not yet been demonstrated using other satellite observations (SeaWiFS) because:

- 1) The spectral configuration of SeaWiFS is not sufficient for CHL-mapping in coastal waters (missing band at approximately 700 nm).
- 2) Standard atmospheric correction procedures of SeaWiFS caused, until recently (Ruddick et al., 2000), problems over turbid coastal waters
- 3) North Sea SIOP in periods of algal blooms were missing or inaccessible (COLORS and COASTLOOC projects) which has hampered the development of adequate (semi-) analytical CHL algorithms such as the Gons (1999) formulation.



This report will introduce a solution for the missing spectral band problem for SeaWiFS and demonstrate the performance and robustness of the MUMM atmospheric correction procedures over coastal waters for CHL detection. Additionally, MERIMON gathered information on North Sea SIOP during algal blooms. Based on these innovations a new analytical algorithm was built, tested and applied to SeaWiFS data.



## 4. MERIMON field experiments: concentration measurements

### 4.1 Introduction

In 2000 two small field trips were organized to gather data for various purposes. One additional campaign was organized outside the setting of the project (Belgica-2000 cruise): this campaign was explicitly aimed at gathering field data simultaneous to the first EPS-A overflight of 2000. This flight unfortunately was cancelled due to instrumentation problems.

### 4.2 The Belgica-2000-11 Campaign:

Data were collected during the Belgica cruise 2000-11 and documented in Rijkeboer, 2000a. The cruise was carried out from the morning of April 17, 2000 until the afternoon of April 19, 2000 and was participated by different scientist working in several projects. The cruise was organized by the Multicolour project, having the overall objective to develop theoretical algorithms and practical tools for mapping suspended particulate matter and chlorophyll concentration by optical remote sensors such as SeaWiFS, MODIS, MOS and MERIS. In the framework of this project cruise 2000-11 consisted of three principal activities:

- A. (ULB) Measurements of inherent optical properties for calibration of an ocean colour model.
- B. (MUMM) Measurements of suspended matter concentration for the validation of satellite-derived maps.
- C. (IVM) Measurements of (specific) inherent optical properties and above-water radiance spectra for development and calibration of algorithms for retrieving water quality parameters from the EPS-A airborne spectrometer deployed by the Dutch Meetkundige Dienst (MD).

Here only the results of activity C will be discussed. The coordinates and conditions at the sample locations are given in Table 1.1.

*Table 4.1 Coordinates and conditions at sampling stations in Belgica cruise.*

Date	Time UTC	Station	Latitude deg mins	Longitude deg mins	Depth m	Wind m/s	Temp oC	Salinity 0/00	Clouds %
17.4	09:59	230	51°18.537	2°51.091	15.9	10.6	8.2	31	80
17.4	11:37	MC4	51°20.406	2°50.500	19.6	16.3	8.4	32	80
17.4	11:58	MC5	51°22.244	2°49.789	26.0	12.6	8.4	32	70
17.4	12:52	130	51°16.305	2°54.304	14.0	11.4	8.6	32	50
17.4	14:14	120	51°11.160	2°42.287	13.2	12.4	8.9	33	70
17.4	14:57	115	51°09.346	2°36.229	15.9	10.7	9.0	33	70
18.4	07:04	710	51°26.609	3°08.202	9.0	9.0	8.4	30	5
18.4	07:50	250b	51°30.032	3°12.633	11.6	8.5	8.6	31	5
18.4	09:14	700	51°22.671	3°13.092	11.1	8.4	8.7	29	40
18.4	09:58	150b	51°24.664	3°19.716	13.8	7.7	8.8	28	60
18.4	11:08	MCZ	51°24.658	3°07.291	12.9	7.5?	8.5	31	40



18.4	11:45	MCA	51°29.228	3°08.086	18.5	7.5?	8.7	31	20
18.4	12:20	MCB	51°28.425	3°03.326	25.8	7.5?	8.6	31	80
18.4	12:47	MCC	51°27.678	2°58.501	22.8	7.5?	8.6	32	70
18.4	13:30	MCD	51°26.755	2°53.260	32.1	7.5?	8.6	33	50
19.4	8:37	330	51°26.001	2°48.590	22.8	4.7	8.7	32	0
19.4	9:31	MCE	51°25.265	2°56.369	22.7	4.4	8.7	31	20
19.4	11:01	MCF	51°24.241	3°03.872	18.7	3	8.8	31	90
19.4	11:46	MCG	51°23.343	3°12.531	13.1	3.8	8.9	29	100

### Concentration measurements

The TCHL concentration varied between 6 to 52 mg m<sup>-3</sup> (Table 3.1). The TSM varied between 11 and 98 g m<sup>-3</sup>. At sample locations 230; MC4; MC5; 130; 120; 115; MCC; MCD; MCF; MCG algal colonies were visible by eye.

Table 4.2 Measured concentrations of total chlorophyll (TCHL), Chlorophyll a (Chl-a), total suspended matter (TSM) and organic suspended matter (OSM) and Secchi-depth.

Station Sampling code	TCHL (mg m <sup>-3</sup> )	Chl-a (mg m <sup>-3</sup> )	TSM (g m <sup>-3</sup> )	OSM (g m <sup>-3</sup> )	OSM (%)	Secchi (m <sup>-1</sup> )
230	17.9	12.0	30.0			0.9
MC4	15.8	10.4	21.9			1.5
MC5	23.6	16.6	21.4			
130	51.8	35.5	97.7	37.3	38	0.7
120	49.7	36.3				0.7
115	47.4	35.2				0.9
710	12.1	6.4	50.4	16.7	33	0.5
250b	9.5	5.8	40.2	16.8	42	0.6
700	11.3	6.3				0.3
150b	8.7	5.9	37.8			0.6
MCZ	12.4	8.0	55.7	15.4	28	
MCA	5.6	4.0	16.1	5.0	31	1.2
MCB	6.2	4.1				1.6
MCC	6.7	4.7				2.0
MCD	19.6	14.7	15.9	8.2	52	2.2
330	11.8	8.7	10.5	5.5	52	1.9
MCE	13.4	9.9				1.5
MCF	11.1	8.2	21.1	5.9	28	1.0
MCG	4.5	2.9				0.5

### 4.3 The Mitra-2000 campaign

Members of the MERIMON team participated in one of the regular Mitra cruises, namely the cruise that was organised from the afternoon of May 8, 2000 until the afternoon of May 9, 2000.



Water quality parameters collected during the Mitra cruises on 8 and 9 May 2000.

The coordinates and conditions at the sample locations are given in Table 4.3.

Table 4.3 Coordinates at in-situ sampling stations in Mitra cruise.

Date	Time	Station	Latitude	Longitude
8.5	13:05	SH(1)	52° 05' 51"	4° 15' 33"
8.5	16:35	KW(2)	52° 09' 45.441"	4° 15' 58.945"
8.5	17:23	NW(3)	52° 18' 11.262"	4° 18' 19.839"
9.5	7:30	NW(4)	52° 18' 11.871"	4° 18' 27.090"
9.5	8:00	NW(5)	52° 18' 03"	4° 18' 54"
9.5	9:55	NW(6)	52° 17' 39.875"	4° 18' 24.225"
9.5	10:30	NW(7)	52° 14' 48.735"	4° 18' 02.609"
9.5	10:45	NW(8)	52° 12' 25.945"	4° 17' 39.277"

The TCHL concentration varied between 12 to 31 mg m<sup>-3</sup> (Table 3.1). The TSM varied between 6 and 13 g m<sup>-3</sup>.

Table 4.4 Measured concentrations of total chlorophyll (TCHL), Chlorophyll a (Chl-a), total suspended matter (TSM) and organic suspended matter (OSM) and Secchi-depth (SH = Schevingen Harbour, KW = Katwijk, NW = Noordwijk, NWSCH = Noordwijk-Scheveningen).

Station Sampling code	TCHL (mg m <sup>-3</sup> )	Chl-a (mg m <sup>-3</sup> )	TSM (g m <sup>-3</sup> )	OSM (g m <sup>-3</sup> )	OSM (%)	Secchi (m <sup>-1</sup> )
SH(1)	12.33	8.51	13.10	4.19	32	0.7
KW(2)	17.61	13.54	10.90	5.57	51	1.5
NW(3)	30.56	24.49	5.87	3.52	60	
NW(4)	31.08	25.23	7.26	3.60	50	3.0
NW(5)	27.30	22.57	8.15	4.44	54	2.3
NW(6)	12.95	10.58	5.61	2.41	43	2.5
NW(7)	29.06	25.23	7.10	3.49	49	
NW(8)	29.27	23.09	11.58	6.50	56	

Concentrations collected at 8 stations for this cruise are given in Table 4.4. During the cruise TSM varied from 5-13 mg/l and TCHL varied from 13-31 µg/l. Except for Schevingen harbour (SH), the organic content of TSM is surprisingly high and above 50%. At several sample locations algal colonies were visible by eye.

#### 4.4 The Navicula-2000 cruise

Measurements were also done in the Marsdiep at a fixed location (Lat: 52.58089N, Lon: 4.46577E) opposite of the harbour of Den Helder. The measurements were carried out on board of the Navicula (NIOZ) on 22 and 23 May 2000.

The data was collected within the framework of the MERIMON and RWS/TESO projects. In the framework of these projects several activities took place:



- A. (RIKZ) Measurements on turbidity (LISST) and output of meetvis.
- B. (NIOZ) Measurements on reflectance (PR-650), optical water quality parameters (algal pigments by HPLC and suspended matter concentration), species composition and AC9.
- C. (MD) EPS-A flight (23 May 2000).
- D. (IVM-I) Measurements on reflectance (Ocean Optics 2000) and inherent optical properties (Ocean Optics 2000).
- E. (IVM-II) Measurements on reflectance (PR-650), optical water quality parameters (Chlorophyll-a, suspended matter concentration) and inherent optical properties.

Results from activities C and E will be discussed in this report.

The time and station number of sample locations are given in Table 4.5.

*Table 4.5 Date and time of in-situ sampling at stations in Marsdiep.*

Date	Time	Station
22.5.2000	10:25	MD1
22.5.2000	11:25	MD2
22.5.2000	12:25	MD3
22.5.2000	13:25	MD4
22.5.2000	14:25	MD5
23.5.2000	7:19	MD6
23.5.2000	8:20	MD7
23.5.2000	9:41	MD8
23.5.2000	10:09	MD9
23.5.2000	11:20	MD10
23.5.2000	12:21	MD11
23.5.2000	13:20	MD12

Concentrations collected at 12 stations for this cruise are given in Table 4.6. During the cruise TSM varied from 8-12 g m<sup>-3</sup> and TCHL varied from 7-31 mg m<sup>-3</sup>. The organic content of TSM is surprisingly high and above 50% for the stations where it was determined. At several sample locations algal colonies were visible by eye.

*Table 4.6 Measured concentrations of total chlorophyll (TCHL), Chlorophyll a (Chl-a), total suspended matter (TSM) and organic suspended matter (OSM) and Secchi-depth.*

Station Sampling code	TCHL (mg m <sup>-3</sup> )	Chl-a (mg m <sup>-3</sup> )	TSM (g m <sup>-3</sup> )	OSM (g m <sup>-3</sup> )	OSM (%)	Secchi (m <sup>-1</sup> )
MD1	14.71	8.95				
MD2	17.15	10.66				
MD3	9.89	4.51				
MD4	11.14	4.74				
MD5	7.51	3.11				
MD6	14.35	8.14	10.42	5.39	52	



MD7	15.49	11.84	9.34	6.62	71
MD8	26.00	20.05	8.84	6.01	68
MD9	30.87	22.13	11.02	7.33	66
MD10	28.08	21.16	11.73	7.77	66
MD11	24.24	18.13	10.38	6.97	67
MD12	13.88	8.29			

#### 4.5 Analysis of the concentration data

Figure 4.1, Figure 4.2 and

Figure 4.3 illustrate the ranges of concentrations and correlations between the variables. Apparently there is no correlation at all, which is in agreement with the findings of the PMNS study.

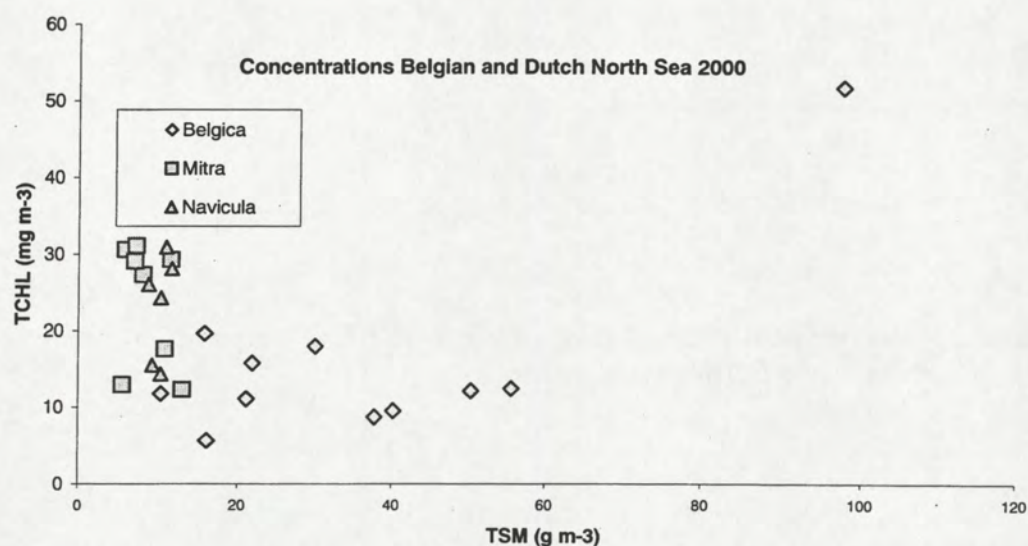


Figure 4.1 Concentrations of TCHL and TSM measured in 2000 in Belgian and Dutch coastal waters

TSM concentrations in the Marsdiep (Navicula data) and at the Mitra locations are significantly lower than TSM values measured in Belgian waters. This has been observed regularly in SeaWiFS based TSM concentration maps (Van der Woerd et al., 2000). TCHL concentrations are highest in the Dutch waters. TCHL variability is high and not related to TSM variability (Figure 4.1).



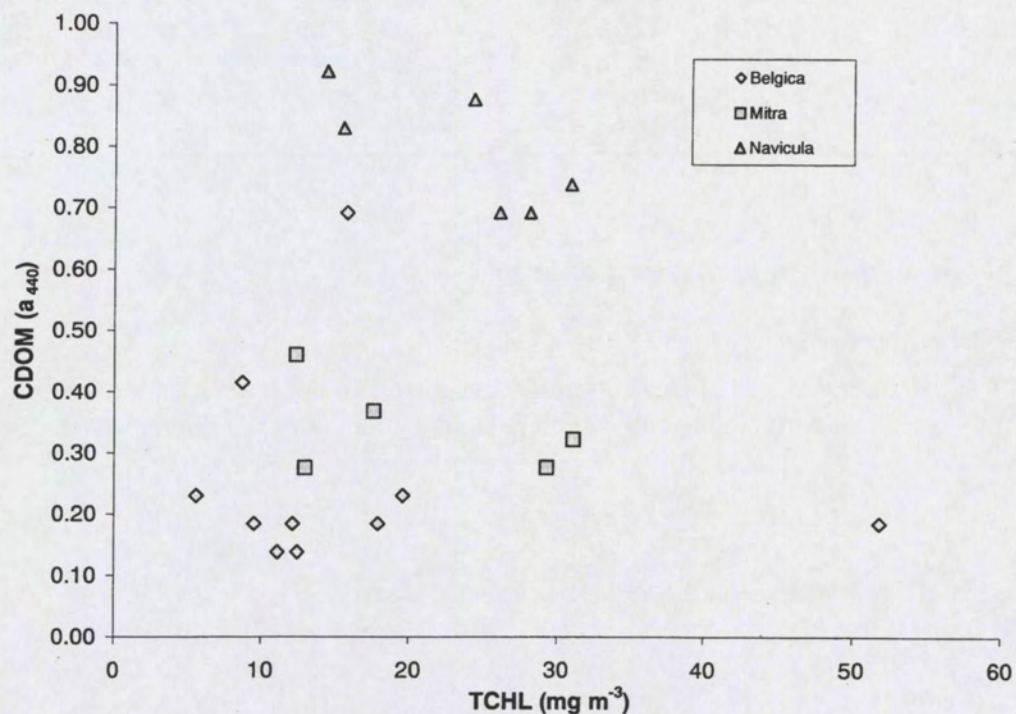


Figure 4.2 Concentrations of CDOM (as  $a_{440}$ ) versus TCHL measured in 2000 in Belgian and Dutch coastal waters

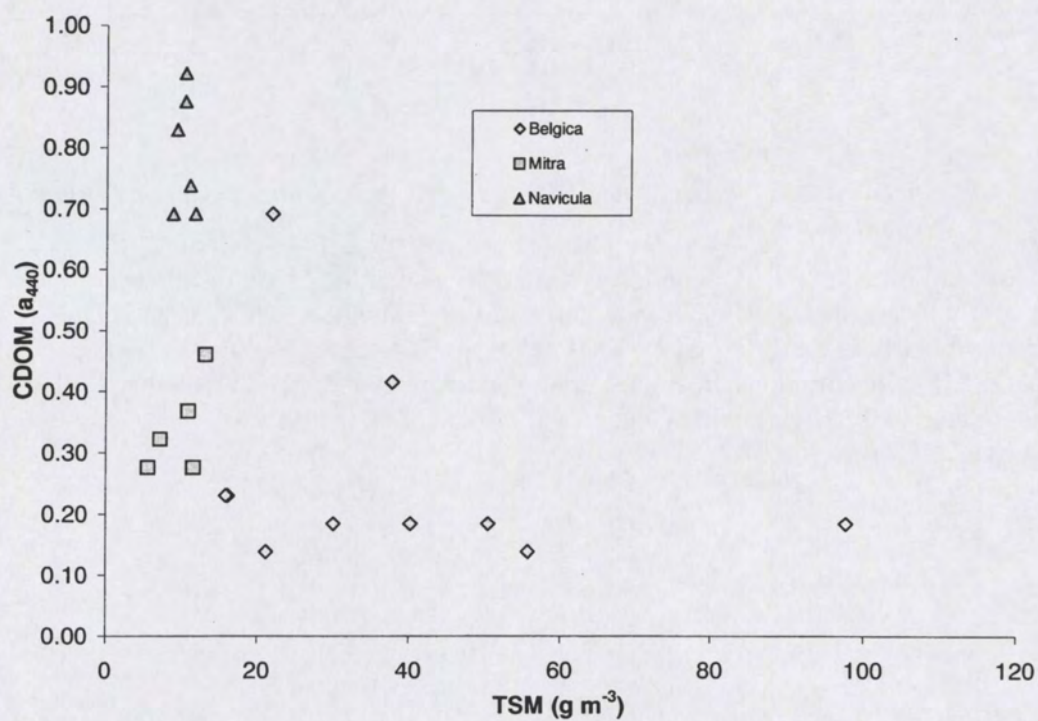




Figure 4.3 Concentrations of CDOM and TSM measured in 2000 in Belgian and Dutch coastal waters

Comparison with historical PMNS data (Figure 4.4) indicates that MERIMON has taken samples at locations (MARSDIEP, BELGIUM) and at time frames where relatively high concentrations of both suspended sediments and chlorophyll occur. Although the same range can be found in the PMNS database, it is obvious that over the year and over larger areas significantly lower concentrations will be found. It is important to realize that PMNS algorithms were calibrated on a dataset with mean TCHL =  $7.4 \text{ g m}^{-3}$  and mean TSM =  $10.8 \text{ g m}^{-3}$ , while MERIMON averages are: TCHL =  $20.6 \text{ g m}^{-3}$  and TSM =  $21.6 \text{ g m}^{-3}$ .

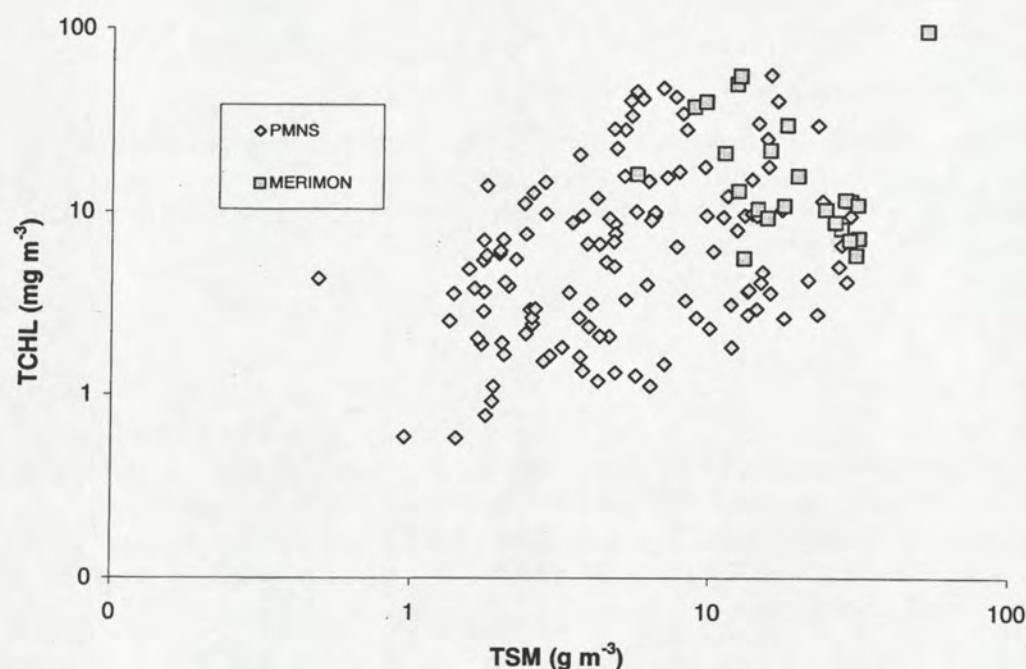


Figure 4.4 Historical (PMNS) and year 2000 data (MERIMON) on TCHL and TSM.

#### 4.6 Some conclusions

MERIMON results show that the variability of concentrations on the North Sea is still not well understood. It remains therefore important to keep monitoring concentration ranges during studies that involve remote sensing, especially when using semi-empirical algorithms. Particularly, because the relationships between  $R(0-)$  and TSM, and between  $R(0-)$  and Chlorophyll are highly non-linear (Van der Woerd et al., 2000; Pasterkamp, 1999). Therefore care must be taken to apply algorithms based on the PMNS dataset (PMNS-TSM, PMNS-CHL and POWERS-TSM) to the MERIMON data. First the validity for the high-range values should be checked.



## 4.7 MERIS concentration validation and protocols

### 4.7.1 Sampling protocol used

Subsurface water samples were taken with a 20 l pps. One litre water was immediately stored in a bottle and placed in the refrigerator waiting for further analysing of the inherent optical properties in the laboratory (NIOO-CL, Nieuwersluis). The samples for Chlorophyll-*a* and phaeopigment were filtered immediately on board and stored deep-frozen. Also a sample for determining CDOM absorption was filtered on board and kept cool in the dark. All fresh samples (transported in bottles on ice, in the dark) were analysed within 48 h after sampling.

### 4.7.2 Chlorophyll protocol

Chlorophyll-*a* and phaeopigment were determined spectrophotometrically according to the Dutch standard method NEN 6520 (1981), by extraction in 80 % ethanol at a temperature of 75°C. The total chlorophyll concentration (TCHL) is defined as the sum of Chlorophyll-*a* and phaeopigment.

### 4.7.3 TSM-protocol

Samples for seston dry weight concentrations were filtered immediately on board over preweighed 0.45  $\mu\text{m}$  Whatman GF/F filters and kept dry (room temperature) and in the dark until further analysis. The total suspended matter or seston dry weight (TSM) concentration was measured after drying the filters at 80°C. Ignition loss was determined by ashing the filters with the TSM at 550°C (NEN 6484, 1982). All analyses were performed in duplicates.

### 4.7.4 CDOM-absorption protocol

Water samples were used for determining spectra of absorption and beam attenuation using a Philips PU8800 UV/VIS double-beam spectrophotometer. The spectra were measured between 350 and 750 nm, at 1-nm intervals. The absorption of the coloured dissolved organic matter (CDOM) was determined from optical density measurements in 5-cm sample cells. The CDOM component of the water sample was obtained after filtration through a 0.45  $\mu\text{m}$  Whatman GF/F filter.

### 4.7.5 Filter absorption protocol (seston and tripton)

Absorption spectra of seston (phytoplankton and tripton) and tripton were determined using the filter pad method (Trüper and Yentsch, 1967) with 0.45  $\mu\text{m}$  Whatman GF/F filters. The absorption was calculated on a basis of a calibrated relationship between the optical density of a suspension in a sample cell and the optical density on a filter, see Weidemann and Cleveland (1993). The volume of water sample filtered was adjusted to obtain an optical density on the filter between 0.4 and 0.5 at 440 nm. The absorption



spectrum of tripton was obtained after extraction of the pigments from the filter (Kishino *et al.*, 1985) using hot ethanol (80 %, 75°C). The extinction at 750 nm was subtracted from the entire spectrum, as a correction for residual scattering. The phytoplankton spectrum was derived by subtracting the tripton spectrum from the seston spectrum.

#### 4.7.6 MERIS protocols

During the last MAVT meeting MERIS protocols were presented. These have been established mainly to guarantee continuity and compatibility with the dataset on which MERIS algorithms are calibrated. It appeared that there remained some uncertainty on issues such as:

- Filter pore size for TSM determination
- Type of water and volume to desalinise the sample
- HPLC or filterpad method for CHL concentration measurement
- Etc.

Future MERIMON research should study the MERIS protocols and compare them with PMNS and MERIMON-2000 protocols in order to determine the best set of measurements to comply with ESA standards and to remain compatible with historic research (PMNS, MERIMON-2000).



## 5. Measured reflectance spectra

### 5.1 PR650 reflectance spectra

#### 5.1.1 Introduction

During the Belgica-2000, Mitra and Navicula campaigns described earlier in this report,  $R(0-)$  spectra were measured using the Gons method (see chapter 9.II.1.3). Experience over the years has proven that this method provides relatively accurate and reproducible spectra. Gons et al., 2000, made recently some additional remarks to the performance of the method. They found that of 90 measured spectra, 10 were negative in NIR values. The article describes an analysis of seawater spectra, comprising also North Sea spectra, obtained in 1998. It was found that, depending on sky and water surface conditions,  $R(0-)$  can be significantly in error, particularly for relatively clear water.

This report will show that spectra measured with this method are quite accurate in shape, which means that the form of the spectrum can be approached quite well by bio-optical modelling using mean site SIOP and in-situ measured concentrations. There is, however, systematic uncertainty about

- 1) The offset of spectra due to the assumption of a constant sky reflectance factor. In reality this factor is dependent on surface conditions, wave height and wave orientation etc.
- 2) The scaling of measured spectra relative to the scaling of modelled spectra. This was already discussed in chapter 2. Measured spectra are converted from remote sensing reflectance to  $R(0-)$  by applying the  $Q$  factor. Modelled spectra (in the Gordon/Walker approach) are converted from single scattering albedo to  $R(0-)$  using the  $f$  factor. Additionally, the scaling of modelled spectra depends on the  $B$  factor. The factors  $f$  and  $Q$  have different meaning so they cannot cancel each other.  $B$  is usually determined from optical closure. This involves the fitting of a modelled spectrum to a measured spectrum (with choices for  $f$  and  $Q$ ). Therefore  $B$  is not an independent parameter.

Follow-up studies on North Sea spectral measurements for e.g. MERIS validations should address this problem and look for methods to reduce the uncertainties between measurements and simulations of spectra. Probably the (' $f/Q$ ') approach is helpful. Attempts should be made to study the meaning and spectral characterization of ' $f/Q$ '. Standardization of this factor will automatically lead to more robust parameterisations for  $B$  as well.



### 5.1.2 The PMNS method for $R(0-)$ measurement using the PR650

Spectra measured with the PMNS method (Althuis, 1996) also suffer from unaccounted offsets due to incomplete compensation of the sky reflectance. A first order approach to compensate for reflected sky radiance is to subtract the value measured at 752 nm from the spectrum. This method is based on two assumptions, namely 1): there is no water leaving radiance at this wavelength and 2): the sky reflectance is spectrally uniform. This method is suitable to standardize  $R(0-)$  or remote sensing reflectance measurements, but simulations show that there can be a  $R(0-)$  value of 1 to 5% in turbid waters in this wavelength (see Figure 5.4) which will lead to substantial errors. Not accounting for the spectral variation in reflected sky radiation can also lead to substantial errors, as shown in Figure 5.1. In this figure the mean normalized (between 1 and 0) sky radiance is shown as measured with a PR650 at a zenith angle of 42 degrees for 10 locations at 3 days.

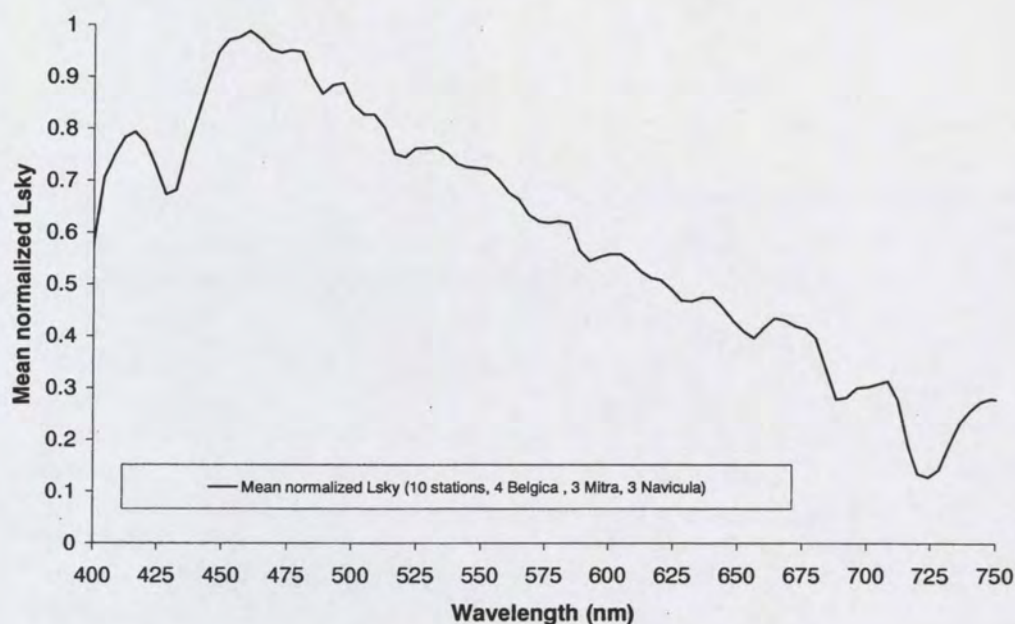


Figure 5.1: Mean normalized sky radiance

Obviously, there is quite a spectral variation (due to Mie and Raleigh scattering and absorption processes in the atmosphere) in the sky radiance received by the surface. The variations from site to site are also quite substantial (not shown in the figure).  $R(0-)$  spectra that are not corrected for sky radiance will feature too high values around 450 nm with linearly declining contribution towards the red/NIR. Local spectral variations both in the blue and NIR region will significantly disturb the spectral shape of the measured  $R(0-)$ . This means that correction by subtraction of 752 nm observations from the entire spectrum is hazardous because the non-linearity involved is not compensated for.



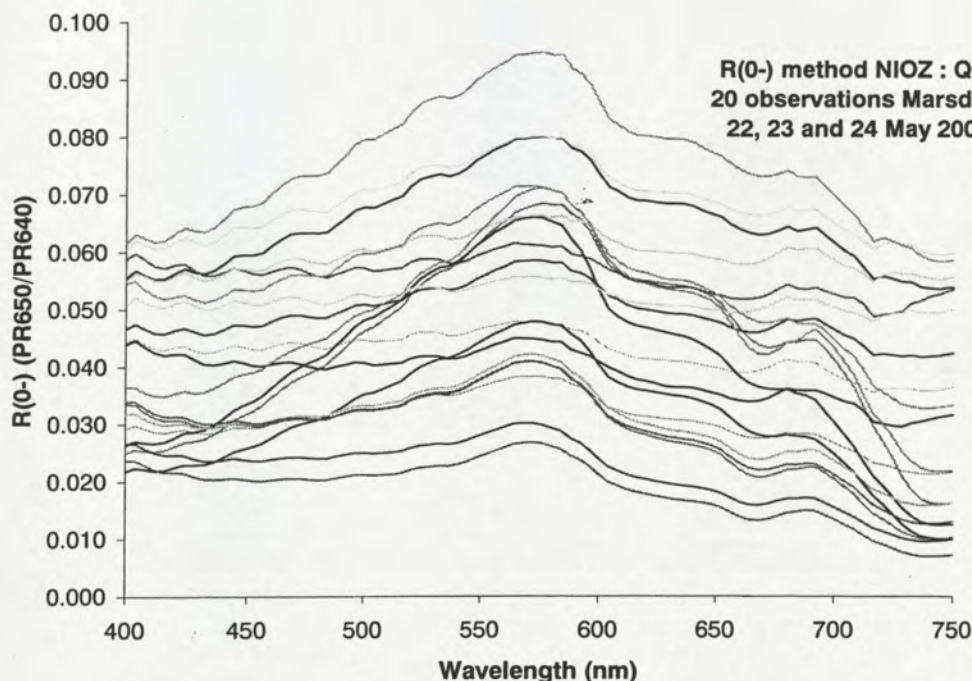


Figure 5.2: Examples of  $R(0-)$  spectra measured using the PMNS method.

In Figure 5.2 20 spectra are shown that were observed in the Marsdiep during the intensive field campaign organized by the MERIMON and TESO projects. These spectra were not corrected for reflected sky radiance, which results in sinusoidal behaviour in the region from 400 to 550 nm. From 450 down to 400 nm a number of spectra show a slight increase, which may be due to sky reflectance. The same is true for the range of 725 to 750 nm. The spectral increase from 725 to 750 nm is small but it will influence the performance of algorithms based on the baseline subtraction method.

### 5.1.3 Results from the Gons method for $R(0-)$ measurement

An alternative method for above water  $R(0-)$  measurement was proposed by Gons, 1998 and 1999. He suggests to subtract the measured sky radiance from measurement of the upwelling radiance using a scaling factor (based on the fresnel reflectance)  $r_{sky}$ . This scaling factor is set to 0.026 in very still waters and to 0.029 in all other situations, thus ignoring the natural variability in surface conditions. The Gons method was used to obtain  $R(0-)$  spectra in all three field campaigns. An overall view of the results is given in Figure 5.3.



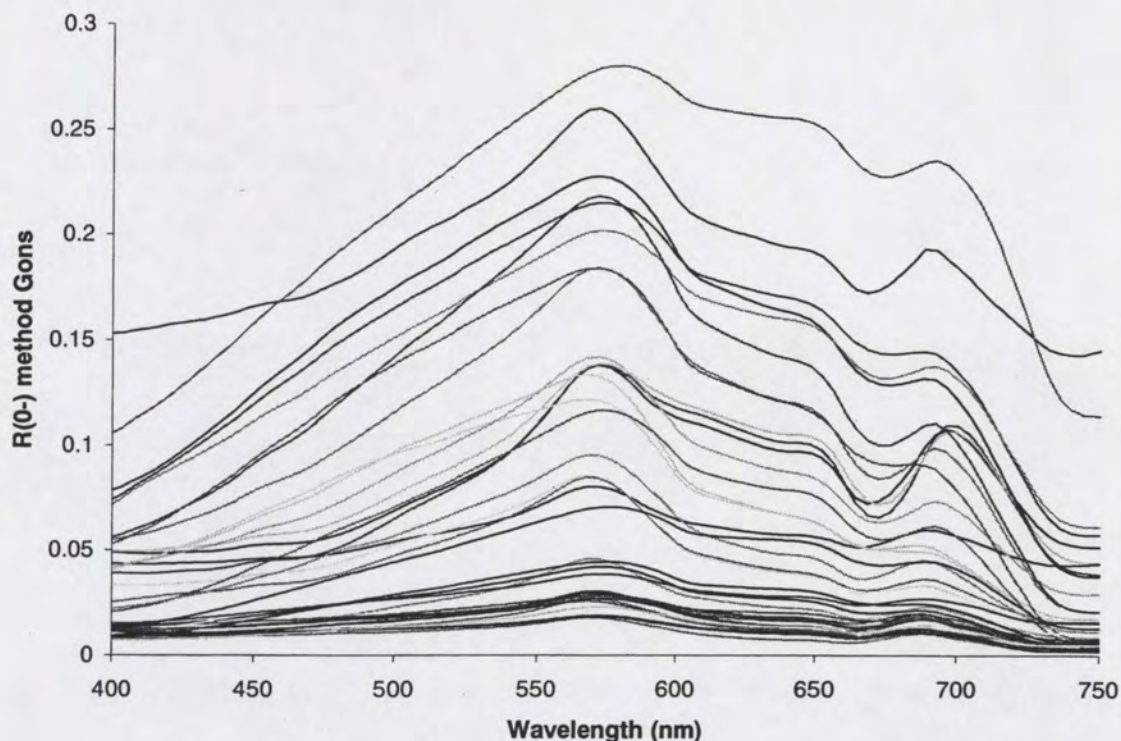


Figure 5.3:  $R(0-)$  measured (means from triplets) during the Belgica-2000, Mitra and Navicula cruises using the Gons method.

Spectra measured with the Gons method do not show sky radiance relicts. There is no sinusoidal behaviour in the range from 400 to 550 nm. Also the spectra show the expected decreasing behaviour towards the 400 nm and towards the 750 nm. Still, a number of spectra are offset which is related to the constant value for the  $r_{sky}$ . Therefore an attempt was made to model the offset from properties within the spectrum. After some experimentation it was found that there is a relationship between the offset at 750 nm and the ratio of 550 nm and 750 nm observations. It was found to have the following form:

$$R(0-)_{750,mod} = a_1 + \left( \ln \left( \frac{R(0-)_{560,mod}}{R(0-)_{750,mod}} \right) \right)^{a_2} \quad (5.1)$$

The coefficients  $a_1$  and  $a_2$  were determined for the 4 sets of mean SIOP that were derived from the field measurements. Before the offset can be calculated settings for  $f$  and  $B$  must be chosen. This inherently limits the applicability of this approach.



	Belgica-I	Belgica-II	Mitra	Navicula
a1	-0.96850	-0.96340	-0.98242	-0.99266
a2	-0.02640	-0.03422	-0.01502	-0.00628
F	0.33	0.33	0.33	0.33
B	0.016	0.016	0.025	0.020

Table 5.1: Results for  $a_1$  and  $a_2$  from bio-optical model simulations.

Table 5.1 shows the settings for  $f$  and  $B$  and the results for  $a_1$  and  $a_2$ . The all-mean value for  $a_1$  is: -0.97675 and  $a_2$ : -0.02048. There are two ways to adjust the spectra to the new offset. The first method is the baseline subtraction method where a constant value is subtracted from the spectrum. A second method is to keep subtracting the measured sky radiance spectrum by adjusting the  $r_{sky}$  factor until the value at 750 nm is the same as the prescribed offset. In this study the second method was explored.

When this method is used to recalculate  $R(0-)$ , the results are quite different from before as illustrated by Figure 5.4.

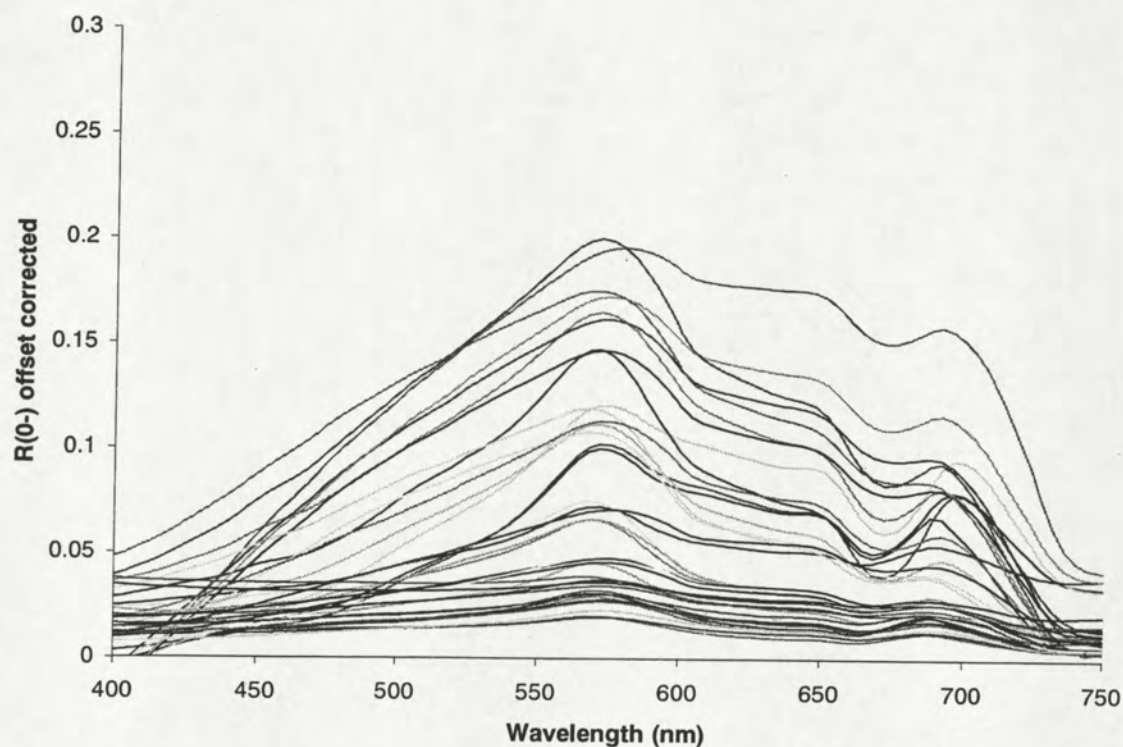


Figure 5.4:  $R(0-)$  spectra calculated by adjusting the  $r_{sky}$  factor

Visual interpretation of Figure 5.4 indicates that probably the offset in the spectrum is corrected quite well, except for some spectra with large amplitudes. Here the correction



in the blue part of the spectrum is too large which results in negative values around 400 nm.

In the following text the original PR650 spectra will be referred to as L1 spectra and offset corrected spectra as: L2 spectra. Also a L3 class of spectra will be distinguished. These are simulated model spectra based on the Gordon model, local mean SIOP and concentrations retrieved from the Ratio Matrix Inversion method (see chapter 9.III.2.3).

### L1, L2 and L3 Spectra from the Belgica-2000 Campaign

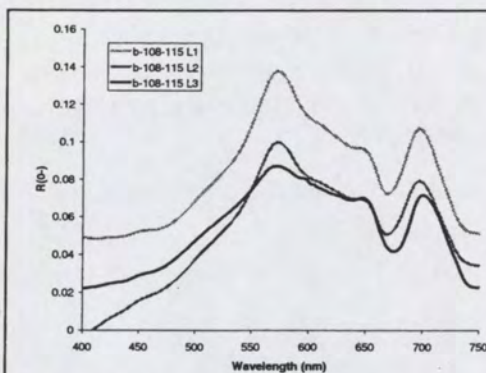


Figure 5.5.1

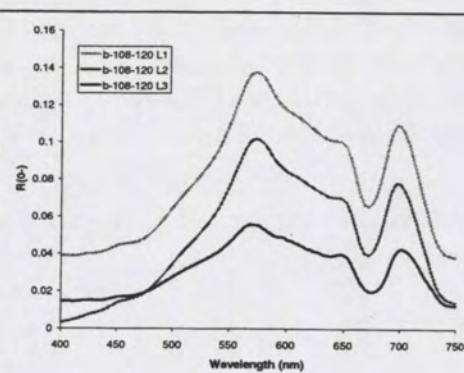


Figure 5.5.2

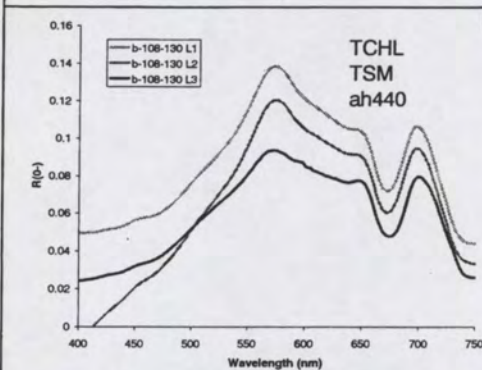


Figure 5.5.3

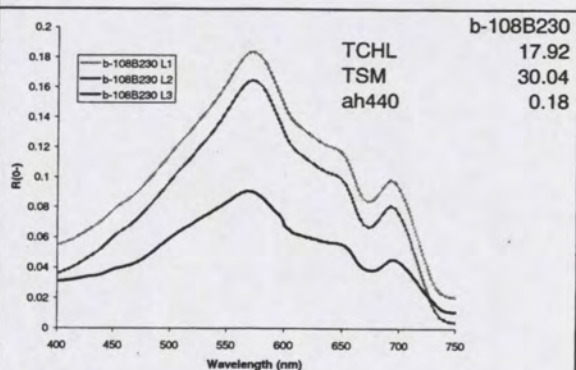


Figure 5.5.4

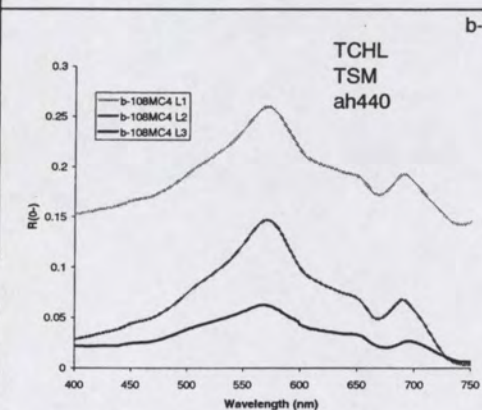


Figure 5.5.5

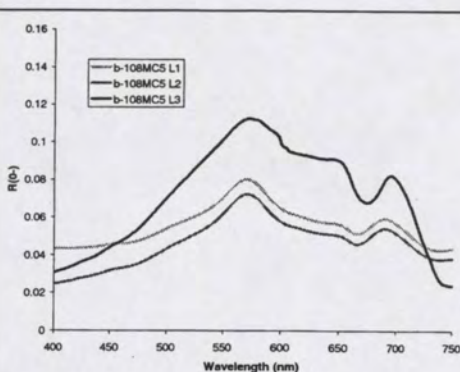


Figure 5.5.6



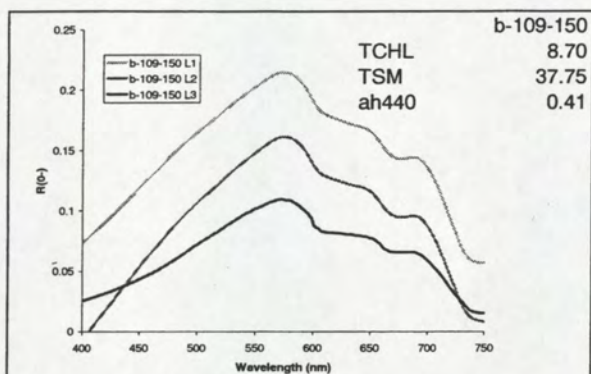


Figure 5.5.7

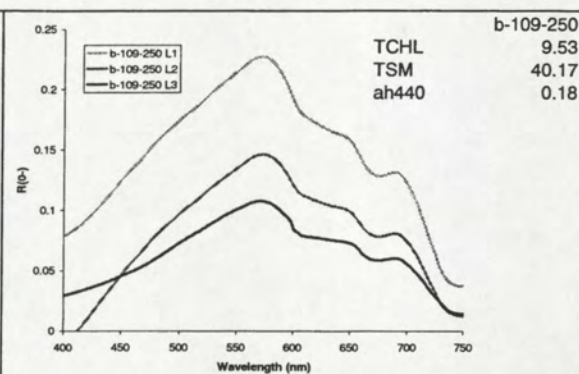


Figure 5.5.8

Figure 5.5 First series of PR650-Gons-L1, L2 and L3 spectra measured during the Belgica-2000 campaign (Note differences in scale!).

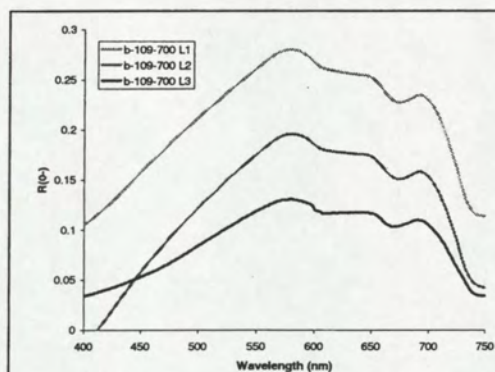


Figure 5.6.1.

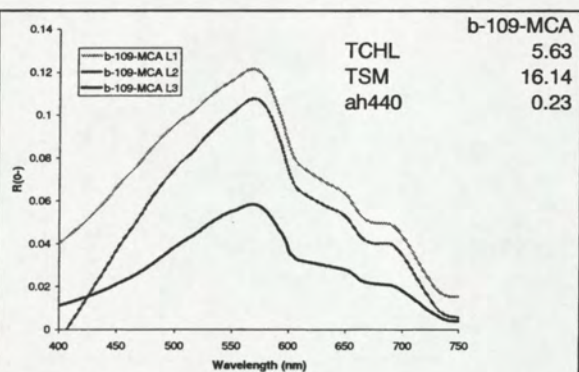


Figure 5.6.2.

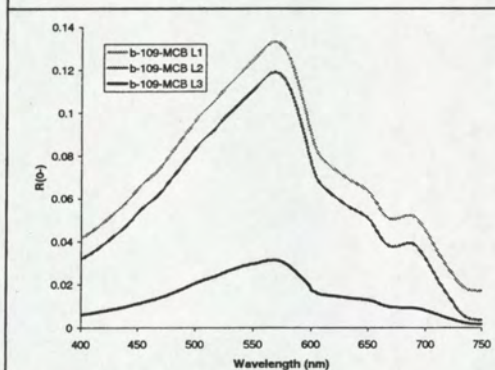


Figure 5.6.3

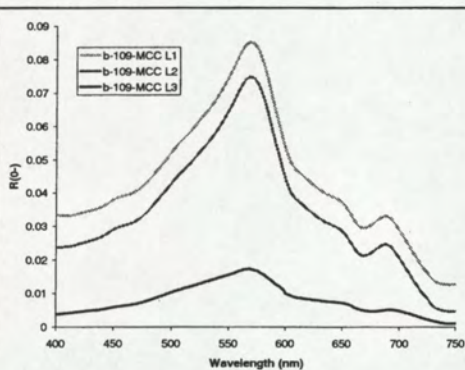


Figure 5.6.4



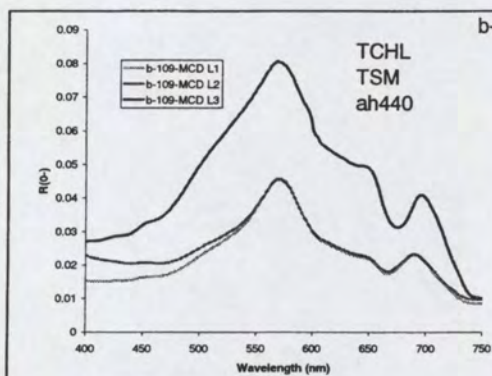


Figure 5.6.5

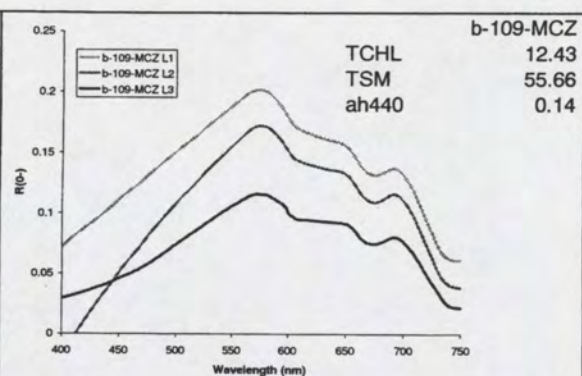


Figure 5.6.6

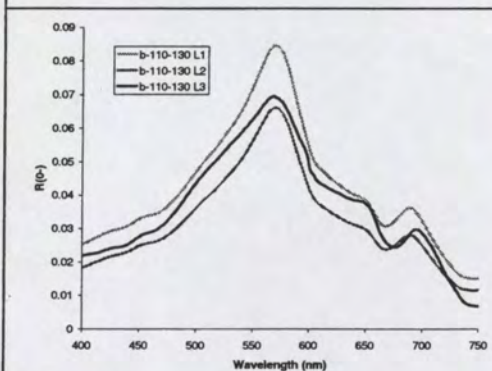


Figure 5.6.7

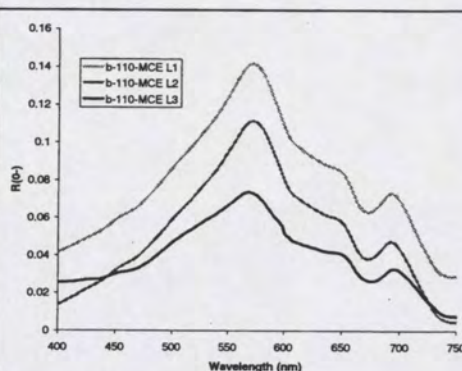


Figure 5.6.8

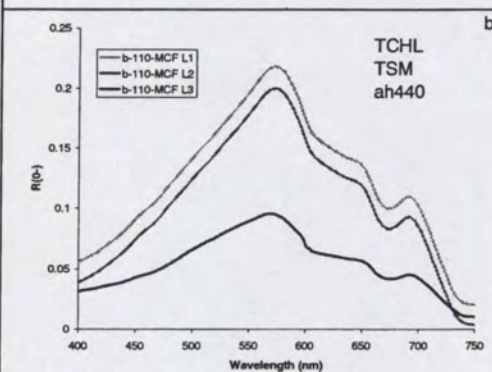


Figure 5.6.9.

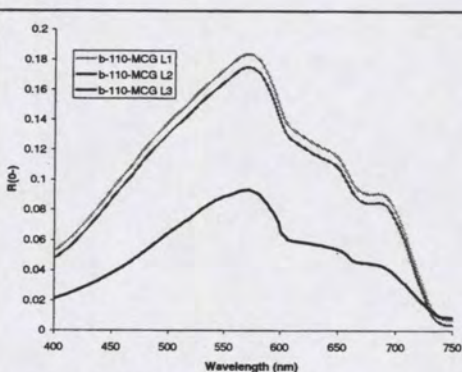


Figure 5.6.10

Figure 5.6 Second series of PR650-Gons-L1, L2 and L3 spectra measured during the Belgica-2000 campaign (Note differences in scale!).

Samples from the Belgica-2000 campaign show TSM values from 5 to 97  $\text{g m}^{-3}$ ; TCHL values from 5 to 51  $\text{mg m}^{-3}$  and CDOM values from 0.14 to 0.61  $\text{m}^{-1}$ . The type of spectrum therefore is widely varying. The b-109-150 and b109-MCZ spectra are typical examples of sediment-dominated spectra. There is little CHL absorption around 667 nm.

A combination of the effects of high TSM and high CHL can be observed in spectrum B108-130. B109-MCD is an example of a TCHL dominated spectrum. Here absorption in the red region around 667 nm and in the blue region between 450 and 550 has strong impact on the shape of the spectrum. A different class of spectra is represented by b109-



MCA. The only component of importance in this spectrum is TSM, but at low concentrations.

Model simulations were done with the Gordon model, using as input the concentrations derived from the Ratio Matrix Inversion method ( $f=0.33$ ; SIOP local means). The model results show that there is a strong similarity in the shape of the spectrum, but a discrepancy in scaling between measured and modelled spectra. In almost all cases, the modelled  $R(0-)$  is much lower than the measured spectrum. This means that  $Q$  was too high, or  $f$  was too low or  $B$  was too low. Probably a combination of these factors has occurred. In future choices have to be made to fix (or determine)  $Q$  and  $f$  and to standardise the conditions in which  $B$  is set. In chapter 7 it will be demonstrated that for this dataset Ratio Matrix Inversion is the only method that derives reasonably accurate concentration values from L1 PR650 spectra. It is expected that the results from other algorithms will improve if the scaling in the  $R(0-)$  measurements relative to the simulation model values is better understood.

#### 5.1.4 L1, L2 and L3 Spectra from the Mitra Campaign.

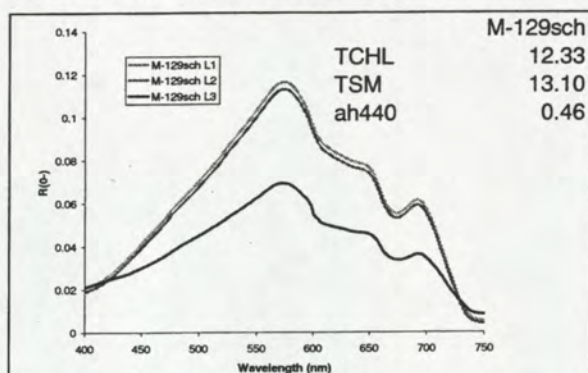


Figure 5.7.1

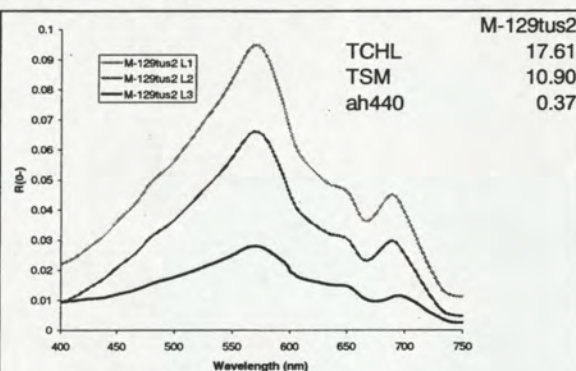


Figure 5.7.2

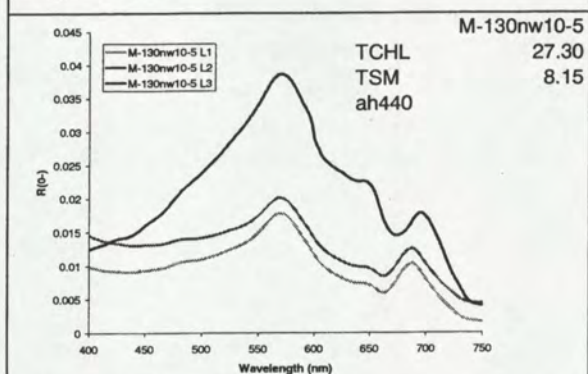


Figure 5.7.3

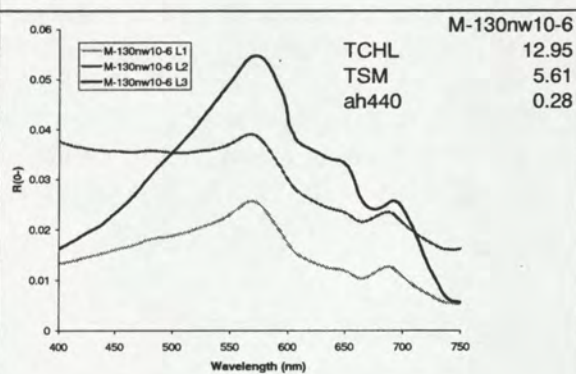


Figure 5.7.4



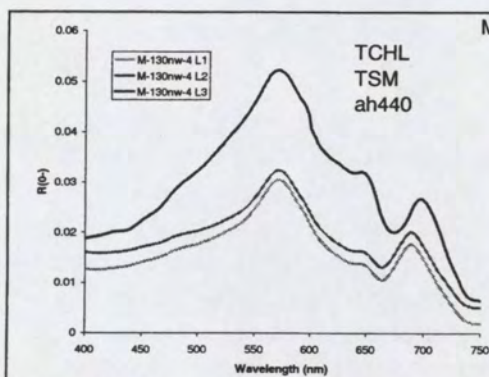


Figure 5.7.5

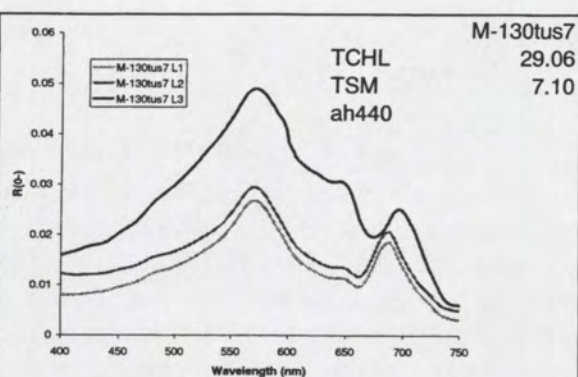


Figure 5.7.6

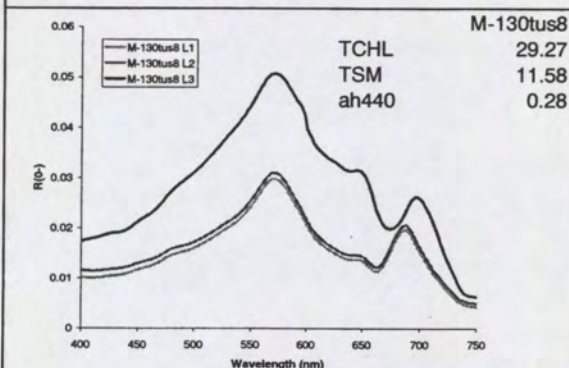


Figure 5.7.7

Figure 5.7 PR650-Gons-L1, L2 and L3 spectra measured during the Mitra campaign

Mitra samples show less variety than the Belgica samples. TSM ranges from 5 to 13  $\mu\text{g m}^{-3}$ ; TCHL ranges from 12 to 31  $\mu\text{g m}^{-3}$  and ah440 ranges from 0.28 to 0.46  $\text{m}^{-1}$ . One feature is very pronounced in the Mitra spectra: the CHL absorption valley around 667 nm and the small peak around 700 nm are both shifted to the left in the measured spectra. This is an indication of a contribution by fluorescence (Hoogenboom, 1999 found the same shift in PMNS spectra). A result of this shift is that TCHL is less accurately determinable by all algorithms.

#### 5.1.5 L1, L2 and L3 Spectra from the Navicula Campaign.

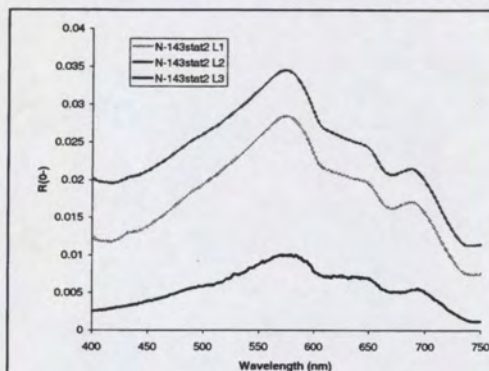


Figure 5.8.1

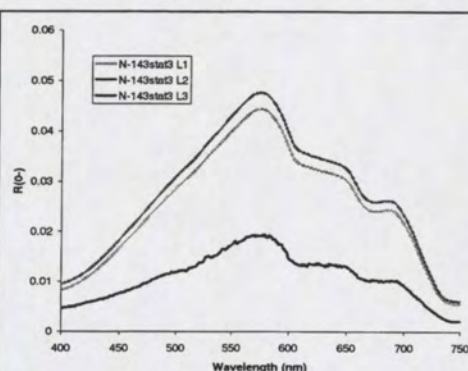


Figure 5.8.2



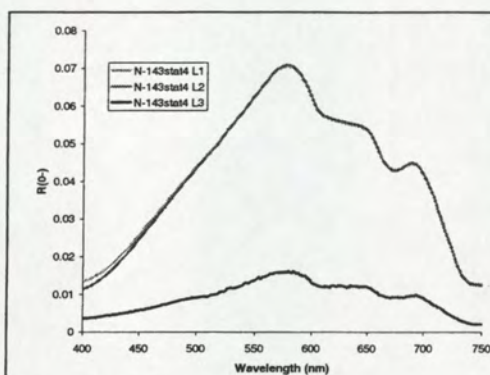


Figure 5.8.3

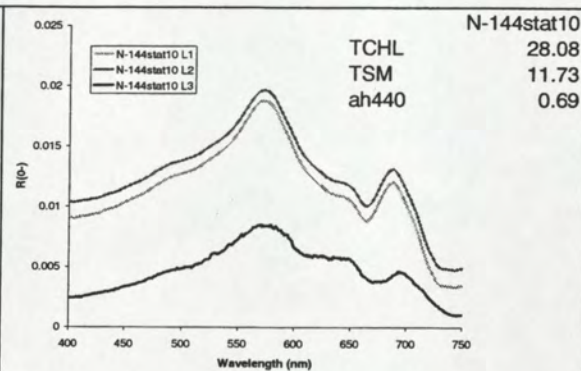


Figure 5.8.4

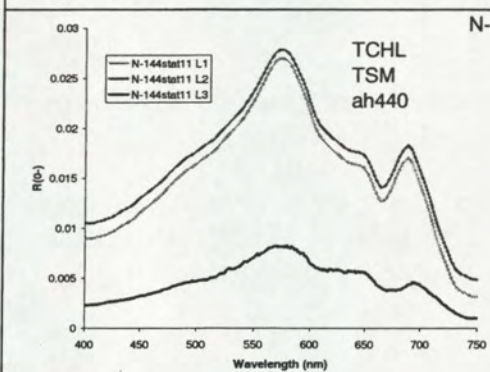


Figure 5.8.5

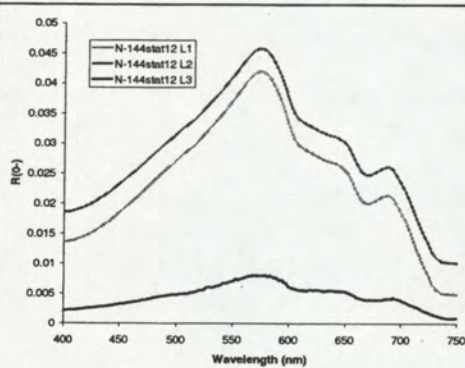


Figure 5.8.6

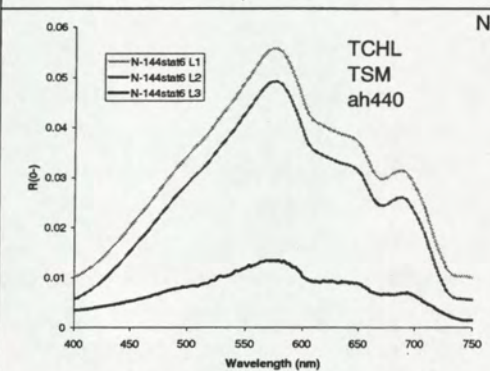


Figure 5.8.7

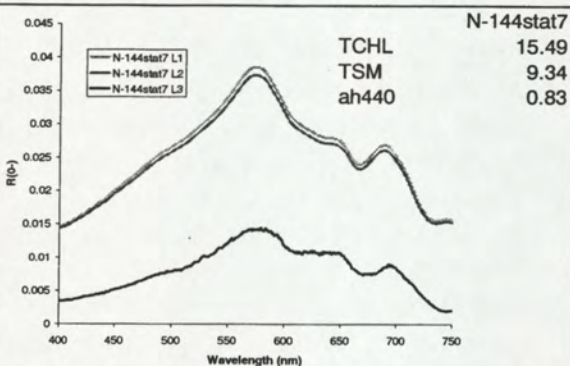


Figure 5.8.8

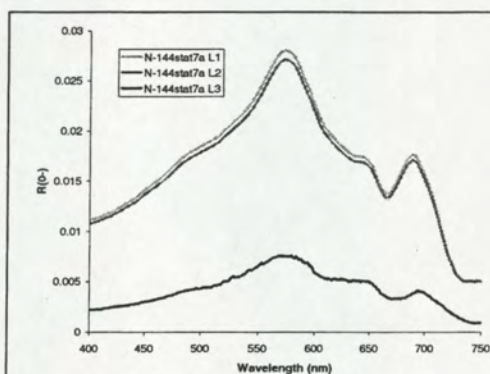


Figure 5.8.9

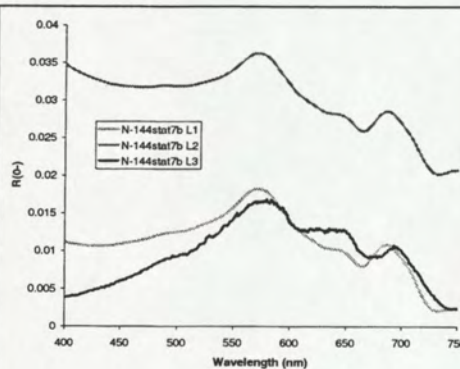


Figure 5.8.10



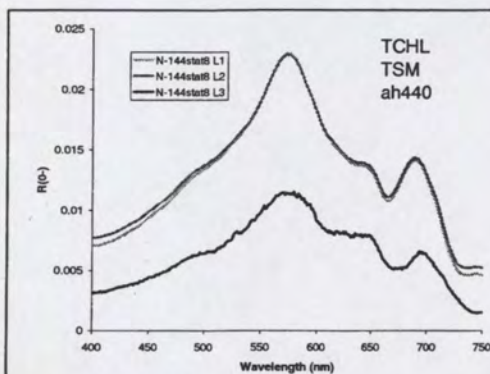


Figure 5.8.11

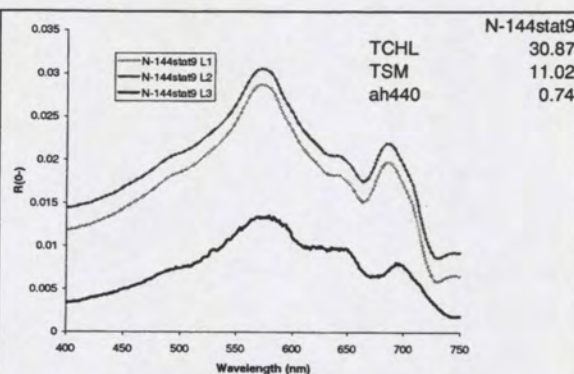


Figure 5.8.12

Figure 5.8 PR650-Gons-L1, L2 and L3 spectra measured during the Mitra campaign

Navicula spectra are quite atypical for North Sea conditions. This is primarily due to the high CDOM content (0.7 – 0.9). Because TSM values are low and TCHL values are also relatively high, Marsdiep spectra have low amplitudes. Modelled reflectances have maximum values of approximately 2%.

## 5.2 EPS-A spectra

### 5.2.1 Measurements synchronous with the Mitra cruise

At 8 and 9 May 2000 at 9:58h and 9:35h (UTC) respectively, data takes were made from the North Sea near Noordwijk with the EPS-A. Coordinates of the flown track were 52 7,8N 04 14,3E to 52 18N 04 18,3E (see Figure 5.9). The following instrumental settings were used; water quality adapter block, 8 scans per second, normal grating. The flight altitude was 10000ft and the flight speed was 120 knots thus obtaining a pixels size of 8,5m in nadir. Weather condition was very hazy at both days. At the second day clouds started appearing in the north. Horizontal visibility was 5km. The raw image was corrected for rolling of the platform, dark current and the pixel sizes were recalculated such that all pixels of the images had the same size as the nadir pixel. Finally the calibrated radiance intensities as detected by the sensor were calculated. To get the subsurface reflectance an atmospheric correction procedure 'TOOLKIT' (De Haan et al., 1996) was applied.



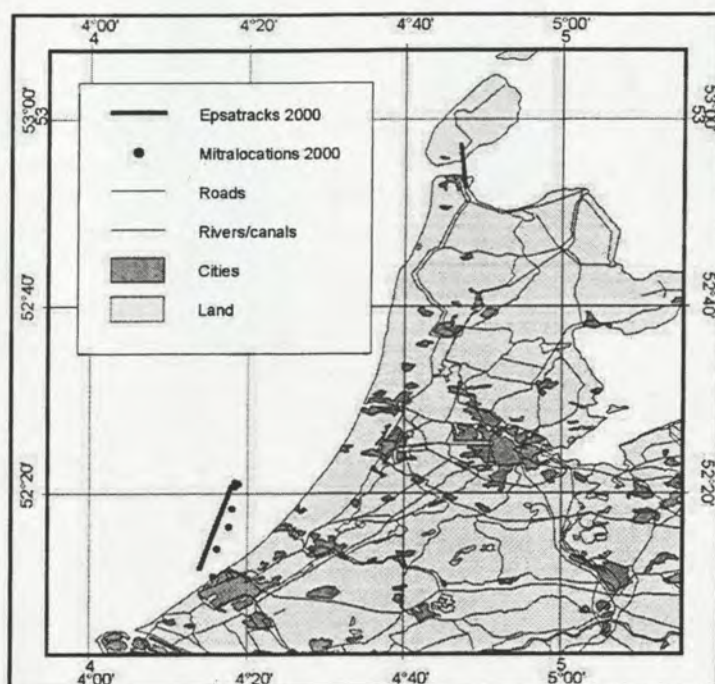


*Figure 5.9: Locations of the Mitra sampling stations and the EPS-A overflights*

The images of these two flights were analysed, but rejected for final processing because of uncorrectable patches of sun or sky glint and extreme haziness over the images.

### 5.2.2 Marsdiep flight

At 23 May 2000, 10:09 (UTC) data takes were made from the Marsdiep with the EPS-A. Coordinates of the flown track were 52 56 36N 04 47 08E to 53 01 12N 04 47 04E (See Figure 5.9). The following instrumental settings were used; water quality adapter block, 37 scans per second, normal grating. The flight altitude was 2000ft and the flight speed was 120 knots thus obtaining a pixels size of 1.7m in nadir. A higher flight altitude was preferred but sub-optimal weather conditions, scattered clouds, forced the plane to descend to 2000ft. Horizontal visibility was 25km. The raw image was corrected for rolling of the platform, dark current and the pixel sizes were recalculated such that all pixels of the images had the same size as the nadir pixel. The striping in the image, due to the mirrors of the Kennedy system, was removed by applying a moving average over the image of 4x4 pixels. Finally the calibrated radiance intensities as detected by the sensor were calculated. To get the subsurface reflectance an atmospheric correction procedure 'TOOLKIT' (De Haan et al., 19XX) was applied.

The Q-factor was obtained from the field measurements carried out from the R.V. Navicula. The obtained subsurface reflectance spectra (EPS-A) suffer from spectral noise (Figure 5.10). The origin of the noise is not clear but may be caused by the operation problems that occurred during the data takes. The instrument might have been not able to stabilise due to repeated crashes.



A subsurface reflectance spectrum was selected from the image near the Navicula. This spectrum was compared to ship based PR650 measurements (Gons method; L1) obtained at the same time (Figure 5.10). A reasonable match was obtained in the green part of the spectrum. In the blue part no match could be obtained. Variation of aerosol type and optical thickness did not result in a better fit. The reflectance obtained from the image in the blue is too low. In the near infrared part (700nm) the reflectance appears to be too high. Surrounding clouds may cause this tilt of the spectrum.

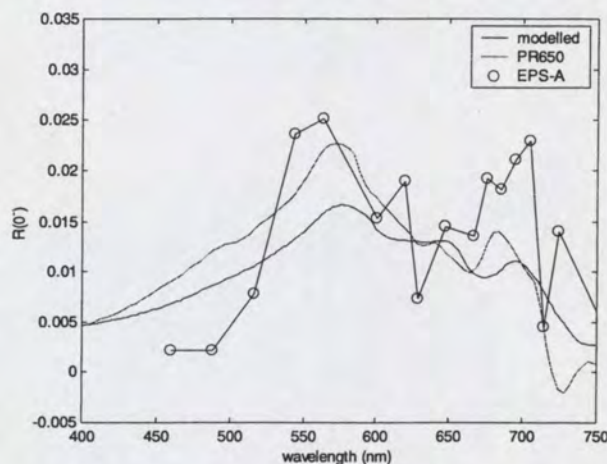


Figure 5.10 EPS-A  $R(0-)$  spectrum (after atmospheric correction) near the Navicula compared to a PR650 spectrum and a spectrum modelled with the Gordon model.

### 5.3 Comparison of Ferry borne Satlantics measurements to EPS-A and PR650

MERIS validation will require an insight in the quality of above water measured subsurface irradiance reflectance. The previous paragraphs already showed that there are strong similarities but also discrepancies between measured  $R(0-)$  spectra (PR650: PMNS and Gons method and EPS-A spectra). The third measurement set-up that was tested during the MERIMON project (by another NIOZ/RWS project) was the continuous registering set-up on board of the TESO ferry (see chapter 9.II.2.1). MERIMON received examples of those measurements in a late stage. Therefore this report only shows some preliminary results during the Navicula campaign (Figure 5.11). This figure shows a number of spectra:

1. Averaged L1 spectra for one day (day 144) PR650 method Gons
2. Averaged L2 spectra for one day (day 144) PR650 method Gons, offset corrected
3. Averaged L3 spectra (using Gordon model  $f=0.33$  and RMI-retrieved concentrations)
4. Averaged PR650 spectra (PMNS-method) for the same day.
5. The EPS-A spectrum
6. The average of all 3700 spectra from the Satlantics obtained during one crossing of the Marsdiep.



Figure 5.11 provides insight and question marks. If the modelled L3 spectrum is closest to the real spectrum then all measured spectra are too high (in amplitude or in offset). If the L1/L2 spectra are closest to the true value then the model results need rescaling. The

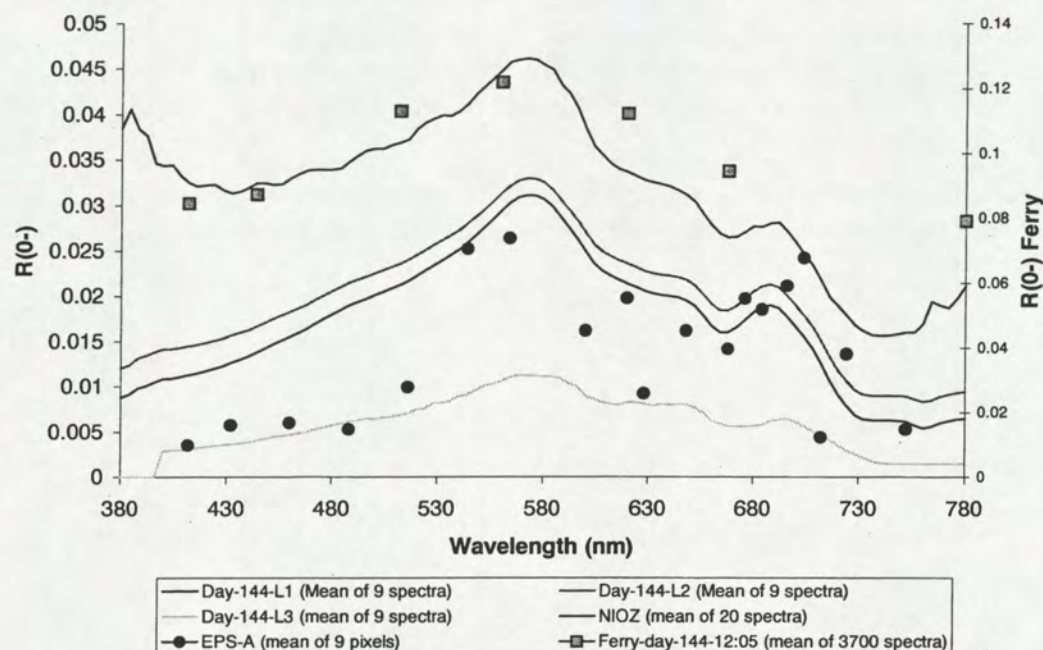


Figure 5.11  $R(0-)$  spectra measured by PR650, EPS-A and Satlantics instruments. (Note that the Ferry borne Satlantics measurements are plotted on the right Y-axis and are a factor two higher than the other spectra).

EPS-A values are calibrated (atmospheric correction) on the L1 spectra. Therefore the overall match in the red region is not too bad, but the spectrum clearly is degraded by noise. PR650 spectra from the PMNS method have their own peculiarities as explained in chapter 9.II.2. The ferry measurement is difficult to interpret. There is quite an offset in the spectrum (Note that it is plotted on the right hand y-axis!). The spectral shape seems to be flatter than the other measured spectra; especially the peak value at 550 nm is measured too low.

#### 5.4 Consequences for MERIS validation

In view of the results presented in the previous paragraph some conclusions can be formulated:

- PR650 Gons method: can be suitable for MERIS validation if the scaling problems (in the match with simulation models) are overcome



- PR650 PMNS method: is less suitable for MERIS validation because sky radiance disturbs the result
- EPS-A: Good spectra from EPS-A have been observed in images taken above the lake IJssel (Vos et al., 2000) and the Vechtplassen (Laanen and Peters, in preparation). Therefore this instrument should be re-tested under better conditions. Flight logistics should be adapted to minimise the risk of sun and cloud glint.
- Satlantics: In 2001 the instrument set-up will be improved (Wernand, pers. comm.) to accommodate independent simultaneous measurements in all channels in all three directions. It is expected that this will remedy spectral problems in the R(0-) measurement.
- Therefore it is recommended to set-up one other experiment during summer 2001 to test the improved Satlantics together with EPS-A and PR650 measurements.



## 6. Evaluation of combinations of algorithms and parameter sets

### 6.1 Introduction

This chapter describes a series of experiments whereby a number of algorithms are evaluated for (future) application with MERIS observations. The algorithms are, in first instance, applied to PR650 observations measured with the Gons method (see 9. Appendix II). Algorithm types have been discussed in chapter 3. In this chapter three types of algorithms will be tested:

- 1) Semi-empirical algorithms (e.g. PMNS-TSM, PMNS-CHL)
- 2) Semi-analytical algorithms (e.g. the POWERS-TSM algorithm)
- 3) Analytical algorithms (e.g. MIM, RMI)

Because all algorithms other than semi-empirical ones require SIOP input and, consequently are sensitive to SIOP variability, the issue of SIOP variability will be briefly recapitulated first.

### 6.2 SIOP Variability

#### *Mean concentrations*

This project had the opportunity to evaluate a number of SIOP datasets collected over the last years. A subset of these data sets was measured according to the same protocol. These will be discussed and used for algorithm testing in this chapter. Five data sets can be distinguished, of which 4 were gathered in 2000 and 1 in 1998.

Of importance to the understanding of SIOP-variability is the mean concentration of water quality parameters during the SIOP sampling. These values are given in Table 6.1.

*Table 6.1: Mean concentrations for five SIOP-datasets + mean estimated B value.*

	Belgica-98	Belgica-2000-I	Belgica-2000-II	Mitra-2000	Navicula-2000
<b>TCHL</b>	10.0	12.7	18.7	25.0	23.2
<b>TSM</b>	10.0	17.1	51.9	8.0	10.3
<b>CDOM</b>	0.46	0.27	0.39	0.31	0.80
<b>B</b>	0.040	0.016	0.016	0.025	0.020

Lowest concentrations were found during the Belgica-98 campaign. Extreme variations were found in the same waters during the Belgica-2000 campaign, which caused the



subdivision of the data set into a “high TSM” and a “low TSM” data set. Mitra-2000 concentrations are comparable to mean PMNS concentrations, except for TCHL, which is quite high. Navicula concentrations, representing Marsdiep water (probably coming from the Wadden Sea) features quite high CDOM concentrations and relatively high TCHL concentrations as well.

These values are also of importance because they can be used to either initialise analytical models or to parameterise semi-analytical models.

### 6.2.1 Variability of the normalized absorption of CDOM

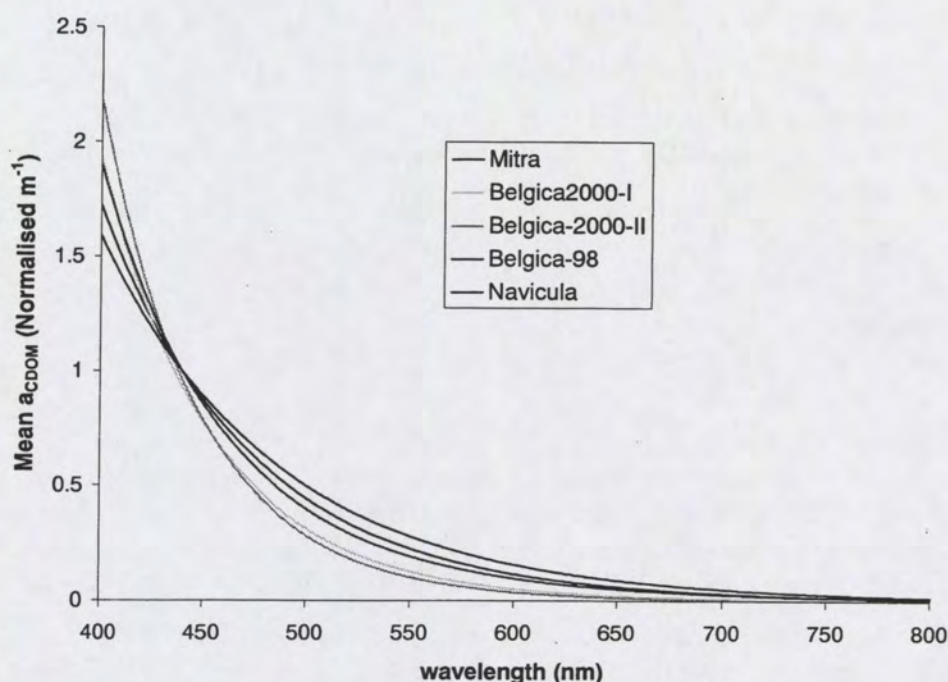


Figure 6.1 Mean normalized CDOM absorption for 5 North Sea SIOP data sets

The SIOP model for CDOM automatically causes water types to show inverse behaviour around the inflexion point at 440 nm. If absorption is high below 440 nm, it will be relatively low above 440 nm.

This is especially true for Marsdiep and Noordwijk waters. Both CDOM absorption curves show relatively high values from 500 to 600 nm. This is something to keep in mind while calibrating algorithms because it will cause substantial TSM errors if not accounted for.

It might be speculated that the distance to shore causes the differences between CDOM absorption in Belgian waters and the Dutch waters. This is because the colouring intensity of CDOM molecules depends primarily on the length of the molecule chain.



Waters farther from the coast generally have lower specific CDOM absorption because parts of the molecule chains have been broken down into smaller parts.

### 6.2.2 Variability in pigment absorption

Pigment absorption shows opposite characteristics if compared to CDOM absorption: the Dutch waters feature the lowest specific TCHL absorption, while the Belgian waters all have higher values over the entire absorption spectrum (Figure 6.2). The cause for this is not clear. It may be that Belgian waters with (in general) higher TSM concentrations, feature algae species that have more densely packed pigments to compensate for the lower light levels due to turbidity.

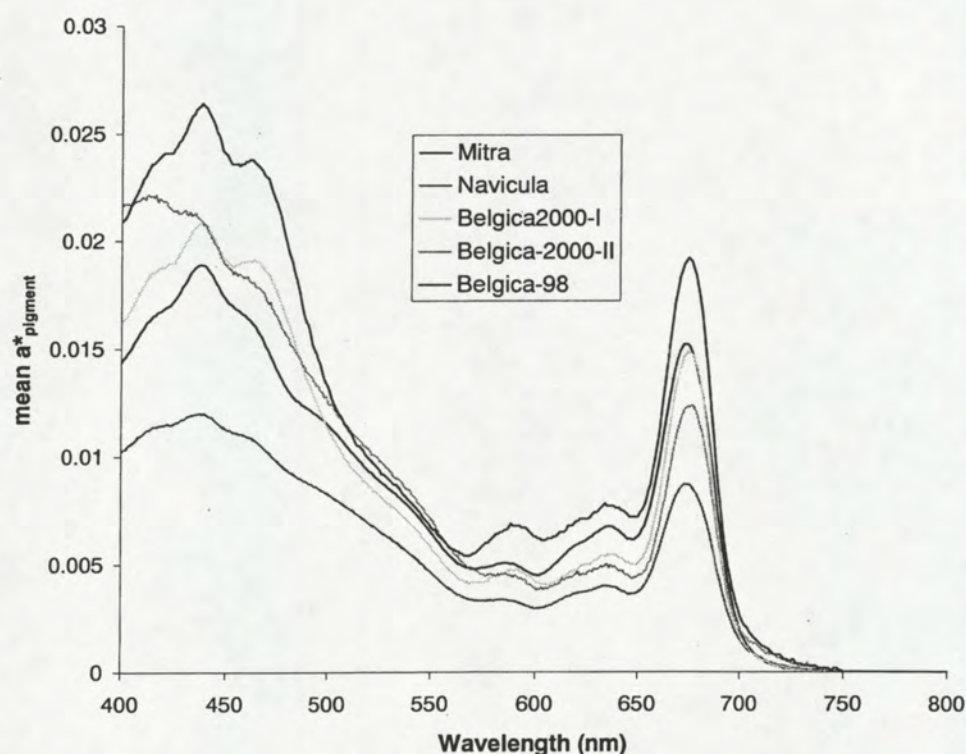


Figure 6.2 Mean specific pigment absorption for 5 North Sea SIOP data sets

It is important to note that the difference between the 667 nm absorption maximum and e.g. the 700 nm values is twice as large in some Belgian waters as compared to Dutch waters. This has as consequence that CHL algorithms (based on a ratio of the overall mean value of these two bands) may be up to 50% in error due to absorption variability!



### 6.2.3 Variability in tripton absorption

Tripton absorption is approximately of the same exponential decaying shape as CDOM absorption (because of a considerable organic component: detritus), though must lower in value. Still, the effect of tripton absorption can be influential because the concentration values of TSM can be quite high. Tripton absorption compensates the increase in reflectance due to scattering by suspended particles. It is of importance in algorithms that incorporate ratios of bands below the 600 nm. An example is the RMI-method.

Note that Marsdiep and Noordwijk water have the highest tripton absorption, which is similar to CDOM (Figure 6.3).

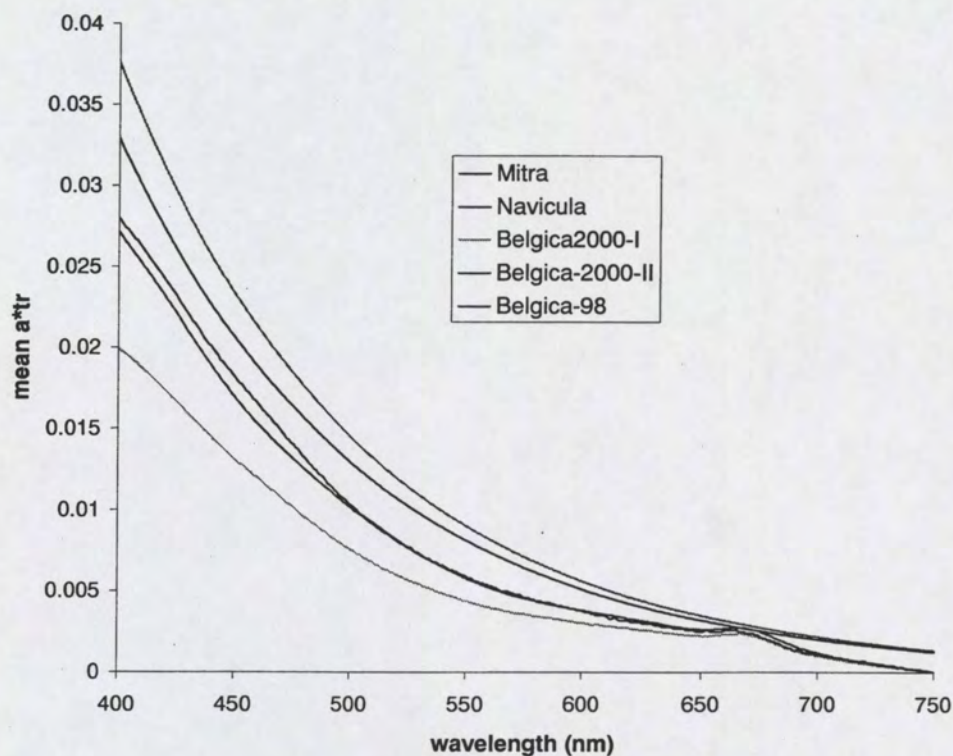


Figure 6.3 Mean specific tripton absorption for 5 North Sea SIOP data sets

### 6.2.4 Variability in seston scattering

Seston scattering was thoroughly discussed in Vos et al. (to be published) . Marsdiep water features a remarkably low seston scattering. Together with the relatively high tripton and CDOM specific absorption this causes the water to be perceived as very dark water.



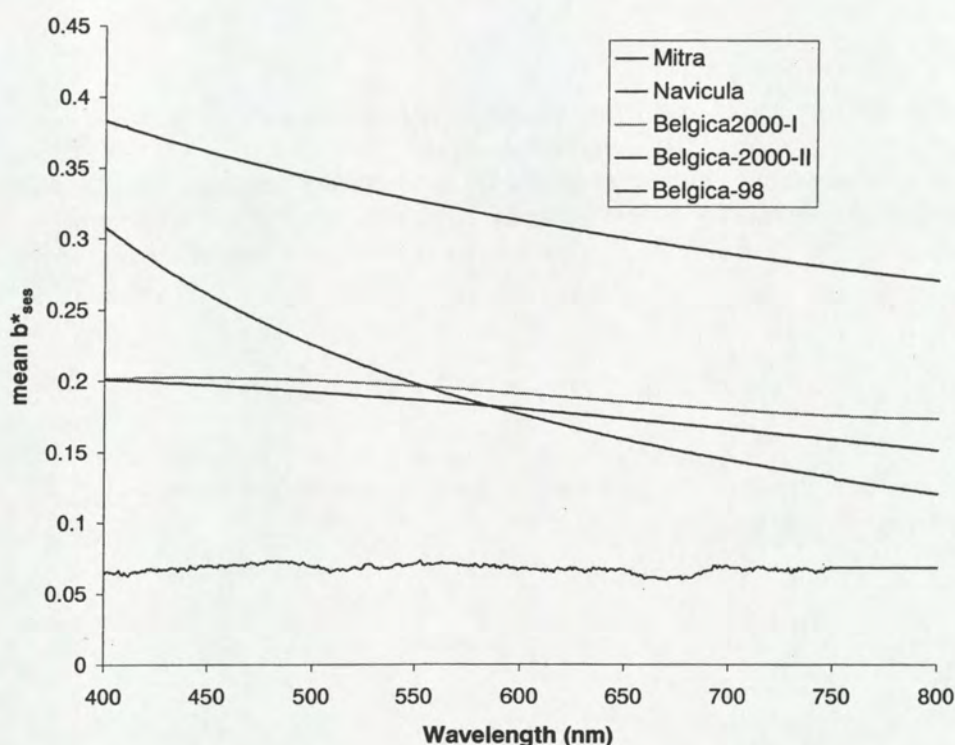


Figure 6.4 Mean specific seston scattering for 5 North Sea SIOP data sets

Figure 6.4 shows a historic evolution in seston scattering approximation. The Belgica-98 seston scattering was modelled using the exponential model. Belgica-2000 observations did not adhere to this model; therefore a polynomial was fitted to the observations. Mitra specific scattering was modelled using a linear equation, although there is quite some variability in the original data. Navicula scattering is not modelled at all; instead the mean original data is given. It was also recommended in Vos et al., (to be published) to use, for future studies, the original specific scattering measurements. As with most other parameters, Mitra seston scattering is the intermediate value between Marsdiep and Belgica values. The Noordwijk sample locations are also geographically in between the other sites but there is too little evidence to assume a gradient along the coastline. There probably is more to say for a distance to the coast hypothesis: Mitra locations are, qua distance to the coast also in the middle! Verification of this hypothesis would require analysis of SIOP profiles taken perpendicular to the coast at several locations, as was done in the PMNS study.



## 6.3 Evaluation of algorithms

### 6.3.1 Introduction

The purpose of the exercise of evaluating algorithm performance is to test the suitability of algorithms for application in the Dutch coastal waters using MERIS observations. Because MERIS observations are not available yet, the tests are performed on PR650 spectra, which are convoluted to MERIS spectral band settings. If SIOP are required, then these are also convoluted to MERIS band settings before the algorithm application.

### 6.3.2 Semi-empirical algorithms: PMNS-MERIS-TSM algorithm

The first test was performed on PR650-Gons-L1 spectra combined with the PMNS MERIS TSM algorithm (equations III.1 and III.2, See Figure 6.5).

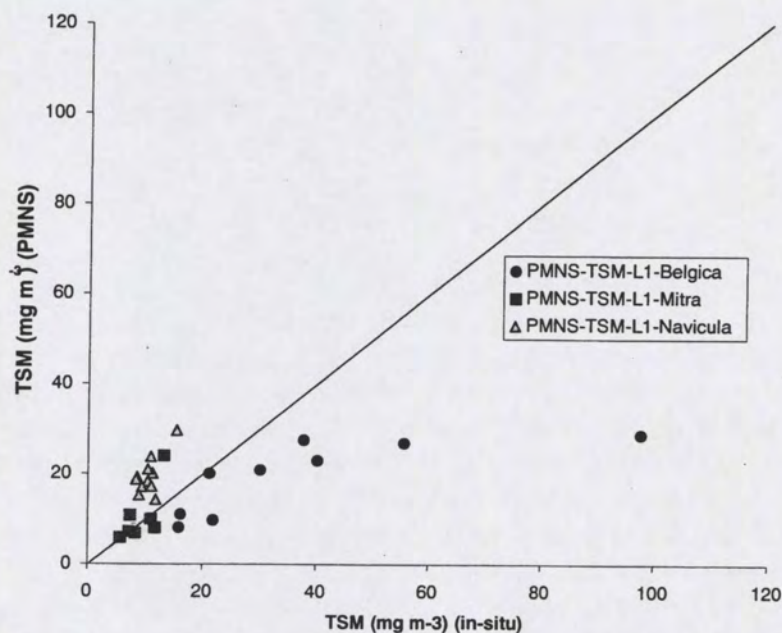


Figure 6.5 TSM retrieved from PR650-Gons-L1 spectra using the PMNS MERIS TSM algorithm.

The standard PMNS TSM algorithm for MERIS tends to overestimate TSM in the Marsdiep and to underestimate TSM in the Belgian waters. It was hypothesised that this may be due to several causes, namely:

1. Highly varying CDOM concentrations as compared to the PMNS database
2. Other ranges than the mean PMNS concentration ranges on which the algorithm was calibrated
3. Other method of reflectance measurement (Gons vs NIOZ method).



Applying the PMNS algorithm to 20 PR650/PR640 reflectance spectra measured using the NIOZ method eliminated the third cause (Figure 6.6).

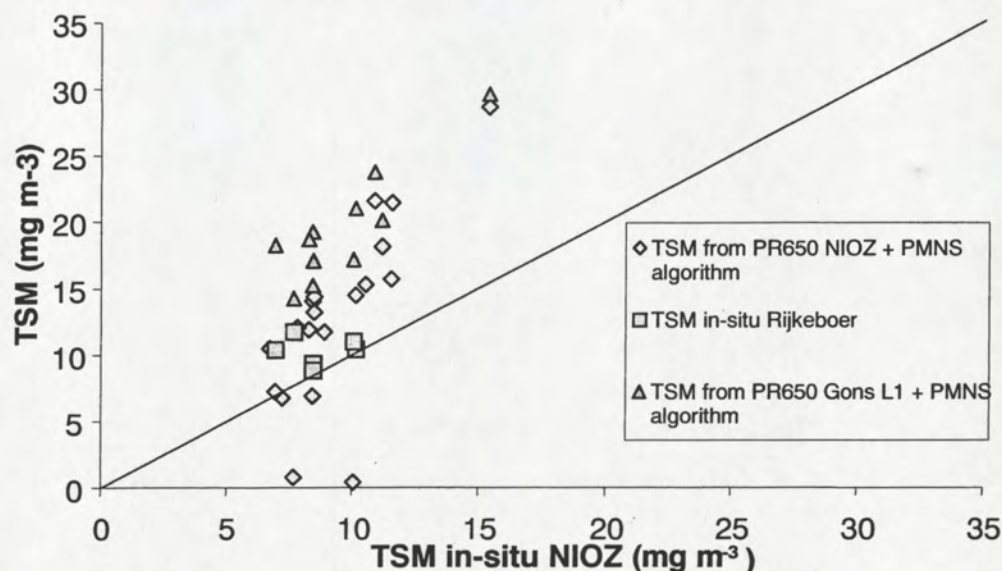


Figure 6.6 TSM retrieved from the MERIS PMNS algorithm using PR650/PR640 – NIOZ measurements.

Figure 6.6 shows that both the PR650/PR640 NIOZ spectra and the PR650-Gons-L1 spectra give rise to overestimation of TSM in the Marsdiep when applying the standard PMNS MERIS TSM algorithm.

In the same figure in-situ TSM sample values taken by IVM are plotted. It is interesting to see that there is general agreement but also a rather large spread in in-situ TSM measurements. There are however not enough samples to quantify this spread. MERIS validation should take into account this inter-method variability, which seems to amount to almost 20% in this case.

### 6.3.3 Semi-empirical algorithms: PMNS-MERIS-CHL algorithms

The PMNS study has proposed 2 CHL algorithms for MERIS. When both are applied to PR650-Gons-L1 observations results are good for the first algorithm (Figure 6.7; equation III.3) and bad for the second algorithm (Figure 6.8, equation III.4).



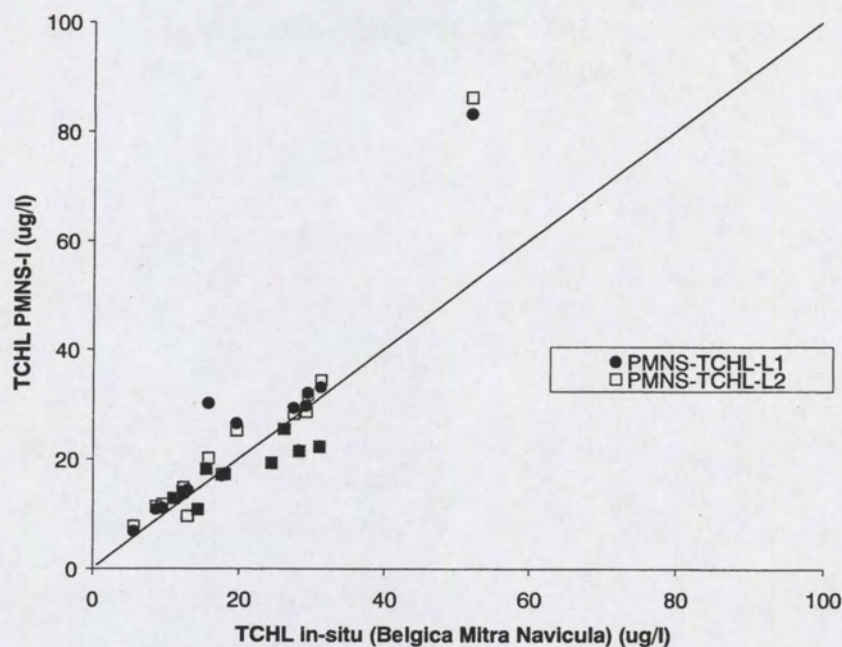


Figure 6.7 PMNS-CHL-I algorithm (equation III.3) applied to PR650-Gons-L1 and L2 spectra.

The difference in performance for L1 and L2 spectra is negligible. This is because an offset changes the value of a ratio very little. The PMNS-CHL-I algorithm performs quite well which is in line with the conclusions by Gons et al., 2000 for red-ratio algorithms.

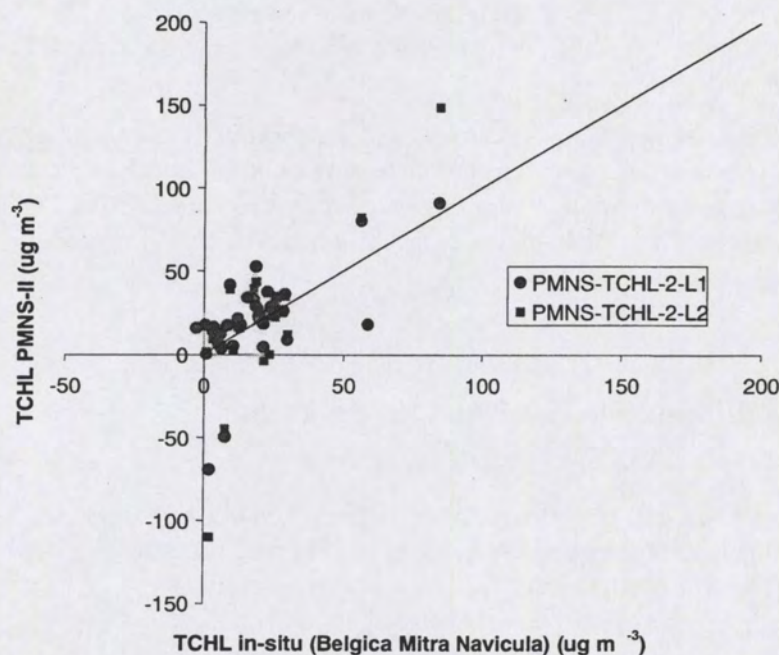


Figure 6.8 PMNS-CHL-II algorithm (equation III.4) applied to PR650-Gons-L1 and L2 spectra.



### 6.3.4 Semi-analytical algorithms: the DUP-POWERS TSM algorithm

This algorithm (equation III.7) was calibrated on the Belgica-98 SIOP data set (Van der Woerd, 2000). The results of the application of the algorithm to PR650-Gons-L1 and L2 data are illustrated in Figure 6.9.

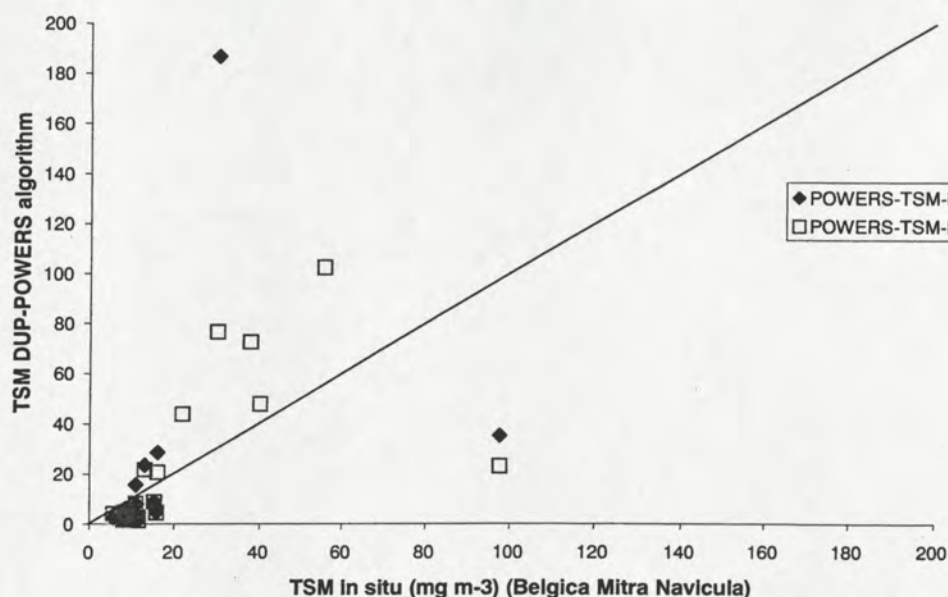


Figure 6.9 DUP-POWERS-TSM algorithm (equation III.7) applied to PR650-Gons-L1 and L2 spectra.

The POWERS algorithm seems to underestimate TSM at low concentrations (less than 20 mg/l) and to overestimate at higher concentrations (>20mg/l). This may be due to the fact that the SIOP for both ranges of concentrations differ from the Belgica-98 data set. In the operational practice of TSM mapping (using this algorithm), values higher than 30 mg/l are not taken into account because of the inaccuracy of the algorithm in this range. The underestimation at low concentration ranges is in accordance with the findings of Van der Woerd et al., 2000, who find the same phenomenon when comparing the algorithm results (applied to SeaWiFS) with MUMM long-term field observations. The conclusion of their report (atypical low TSM values observed by SeaWiFS in spring 1999) may be in error, in the sense that these low TSM values could be caused by an atypical calibration data set. Both the DUP POWERS and this study have collected relatively low volumes of SIOP data, which means that the dispute can only be resolved in future when the coverage of SIOP observations becomes complete.

### 6.3.5 TSM-Ratio Matrix Inversion

Ratio Matrix Inversion as described in chapter 9.III.2.3 allows to experiment with parameterisation sets. The results of such an experiment will be described here. In this



experiment Ratio Matrix Inversion was used to derive simultaneously TSM and TCHL from PR650-Gons-L2 spectra, while CDOM was kept constant at the value prescribed in the SIOP dataset (see Table 6.1).

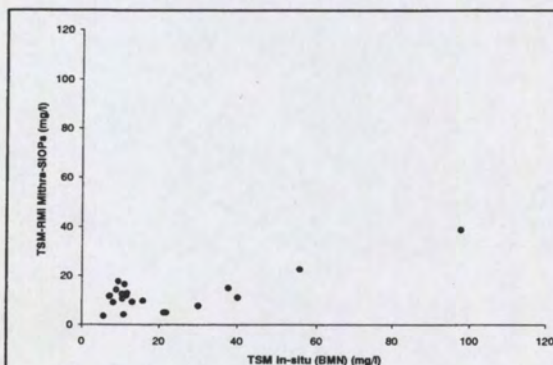


Figure 6.10.1

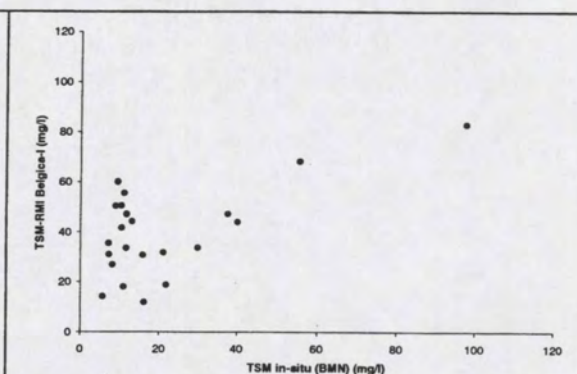


Figure 6.10.2

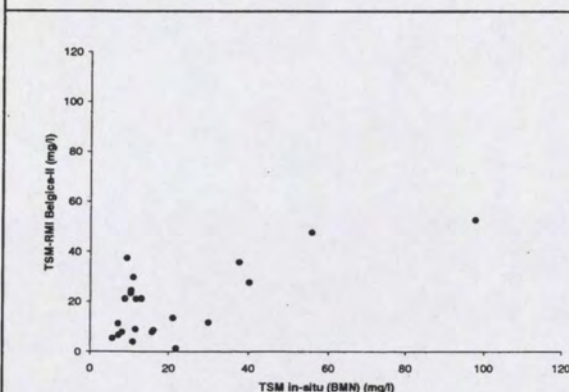


Figure 6.10.3

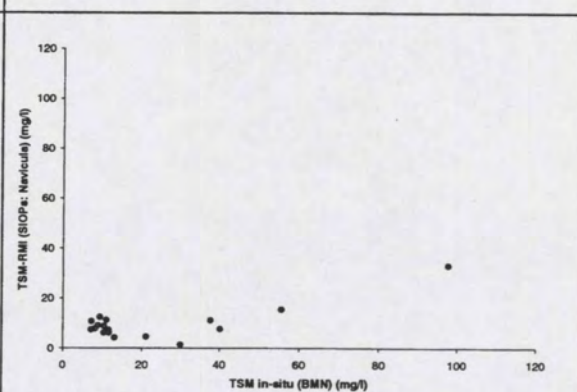


Figure 6.10.4

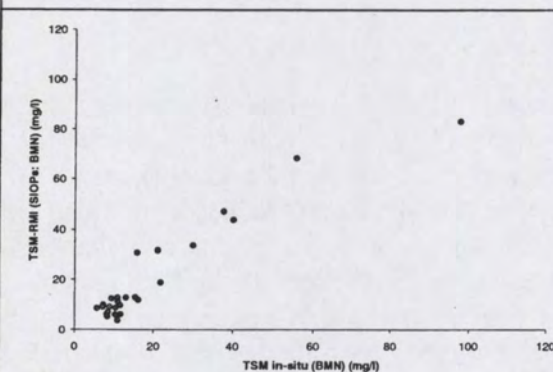


Figure 6.10.5

Figure 6.10 (Subfigures 1 to 4) Experiments with RMI: TSM retrieved for Belgica, Mitra and Navicula stations using single SIOP sets (respectively: Mitra, Belgica-I, Belgica-II and Navicula).

Figure 6.10.5: TSM retrieved from PR650-Gons-L2 spectra using MERIS band settings and site-specific SIOP sets.



Figure 6.10.1 to Figure 6.10.4 shows that only the Belgica-I SIOP-set does not lead to underestimation of TSM in Belgian waters. So, if accurate TSM values above  $30 \text{ mg m}^{-3}$  are required then a region specific SIOP set must be used. Both Belgica SIOP sets (I and II) lead to overestimation of TSM up to 100% in Dutch coastal waters. Accurate TSM determination therefore requires regional specific SIOP.

The explanation of the differences is somewhat difficult. The specific absorption of tripton is lower in Belgian waters while the scattering is higher as compared to Dutch waters. This could indicate a larger inorganic fraction in Belgian waters. Another explanation could be the differences in CDOM content and CDOM normalized absorption. Belgian waters feature lower normalized CDOM absorptions around 550 nm. If higher CDOM absorption is assumed then the spectrum from 400 to 600 nm is lowered which results in lower TSM estimations. This potential effect should be quantified in a subsequent (sensitivity) study.

Some other conclusions from this experiment:

- 1) The MERIS band settings are suitable to map TSM in North Sea coastal waters
- 2) RMI is a suitable technique to map TSM. The software is set-up to choose its own choices for ratio-band settings. From detailed analyses (not described here) it appears that ratios between bands in the green region and bands in the infrared have first preference. This means that atmospheric correction in the infrared must be adequate above turbid waters.
- 3) PR650-Gons-L2 spectra are suitable to test and calibrate analytical algorithms for TSM retrieval. Because of the use of multiple ratios, the sensitivity of the algorithm to scaling errors is relatively low, as compared to e.g. MIM. Still, the scaling differences between simulated spectra (using RMI retrieved concentrations) and measured spectra remains an issue of concern.

### 6.3.6 TCHL-Ratio Matrix Inversion

In this chapter the results of such an experiment with RMI for TCHL retrieval will be described. In this experiment Ratio Matrix Inversion was used to derive simultaneously TSM and TCHL from PR650-Gons-L2 spectra, while CDOM was kept constant at the value prescribed in the SIOP dataset (see Table 6.1).



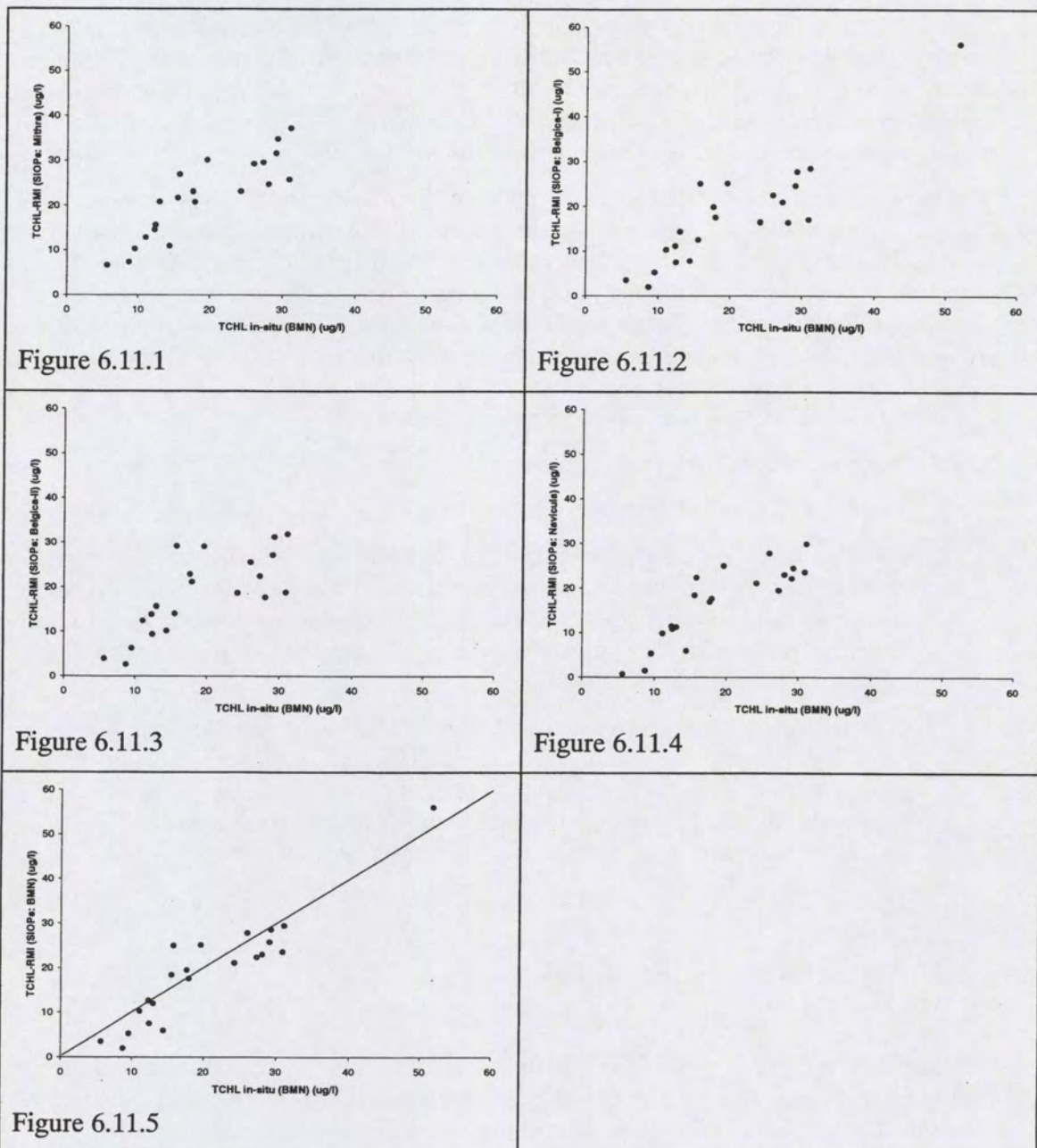


Figure 6.11 (Subfigures 1 to 4): Experiments with RMI: TCHL retrieved for Belgica, Mitra and Navicula stations using single SIOP sets (respectively: Mitra, Belgica-I, Belgica-II and Navicula).

Figure 6.11.5: TCHL retrieved from PR650-Gons-L2 spectra using MERIS band settings and site-specific SIOP sets.

Figure 6.11.1 to Figure 6.11.5 shows that the choice of SIOP set is (relatively) of little influence on the accuracy of the retrieved TCHL by RMI. This result is surprising because there are large differences in the absorption around 667 between the various SIOP data sets. Probably, the strong point of RMI is that not only ratios based on this wavelength are taken into consideration but also (in the same calculation) e.g. blue-green



ratios are taken into account as well. This amounts to a very stable TCHL algorithm with a high performance ( $r^2 = 0.86$  if site-specific SIOP are used; Figure 6.11.5).

Some general conclusions from this experiment:

- 1) The MERIS band settings are suitable for TCHL retrieval using RMI in the North Sea coastal waters.
- 2) The sensitivity of the RMI-TCHL results to variations in SIOP is low
- 3) If there is a scaling error in the PR650-Gons-L2 data then this error is of relatively little influence on the RMI-TCHL determination.



## 7. Options for MERIS validation

### 7.1 Introduction

In chapter 1

Figure 1.3 the various options for MERIS validation were illustrated. On the left side of the graph, validation was done on reflectance observations in points and transects. On the right side of the graph, validation was done on concentration products (also points and transects). MERIMON-2000 studies the potential of a number of methods to validate future MERIS products.

In chapters 2 to 7 a firm basis was laid for such a validation. In these chapters a further insight was gained in the variability of SIOP and the effect of this variability on MERIS algorithms. In view of the difficulties associated with field sampling for direct validation (more on this subject in this chapter) it is very important to do "validation" on relevant intermediate steps leading to the MERIS end-products. Which comes down to making sure that representative SIOP are used in an adequate (tested) algorithm, and that input (MERIS) spectra are of sufficient quality.

This chapter will treat mainly experiments to do validation of concentrations because there remain a number of uncertainties in the scaling and accuracy of above water measured reflectance. First some results from the TESO ferry will be discussed. Next a first image of the EPS-A and a TSM product will be evaluated. Finally the new Ratio Matrix Inversion will be adapted to be used with SeaWiFS to generate MERIS type of concentration products (TSM, TCHL and CDOM-index) with the purpose to demonstrate the robustness of the method.

### 7.2 Options for transect validation using the NIOZ Satlantics-TESO set-up

On the Ocean Optics conference (Monaco, 2000) two papers were published on the first preliminary results of this set-up (Hoogenboom et al., 2000 and Wernand et al., 2000).

Both authors published a TSM transect over the Marsdiep; Hoogenboom a transect at 23 May, 10:20 UTC and Wernand a transect for the same day at 10:00 UTC.

#### 7.2.1 Reflectance

Wernand used remote sensing reflectance as input (upwelling radiance divided by downwelling irradiance). Hoogenboom uses single scattering albedo as input. He arrives at this value by considering the  $R(0-)$  calculated similarly to the Gons method



(incorporating reflected sky light). As a refinement, Hoogenboom uses Hydrolight simulations (and measurements of windspeed) to come to an estimation of  $Q$ , the Fresnell coefficient, the refractive index and the albedo of the air water interface for light welling up. Next Hoogenboom uses the two-stream model of Aas to derive  $R(0^-)$  the single scattering albedo from  $R(0^-)$ .

### 7.2.2 Algorithms

Both authors (Wernand and Hoogenboom) differ in their algorithm approach. Hoogenboom solves a one band analytical model using the single scattering albedo and the SIOP of that band (555 and 715 nm). Wernand uses the semi-empirical PMNS-TSM model.

### 7.2.3 Results

The profile measured by Wernand is shown in Figure 7.1.

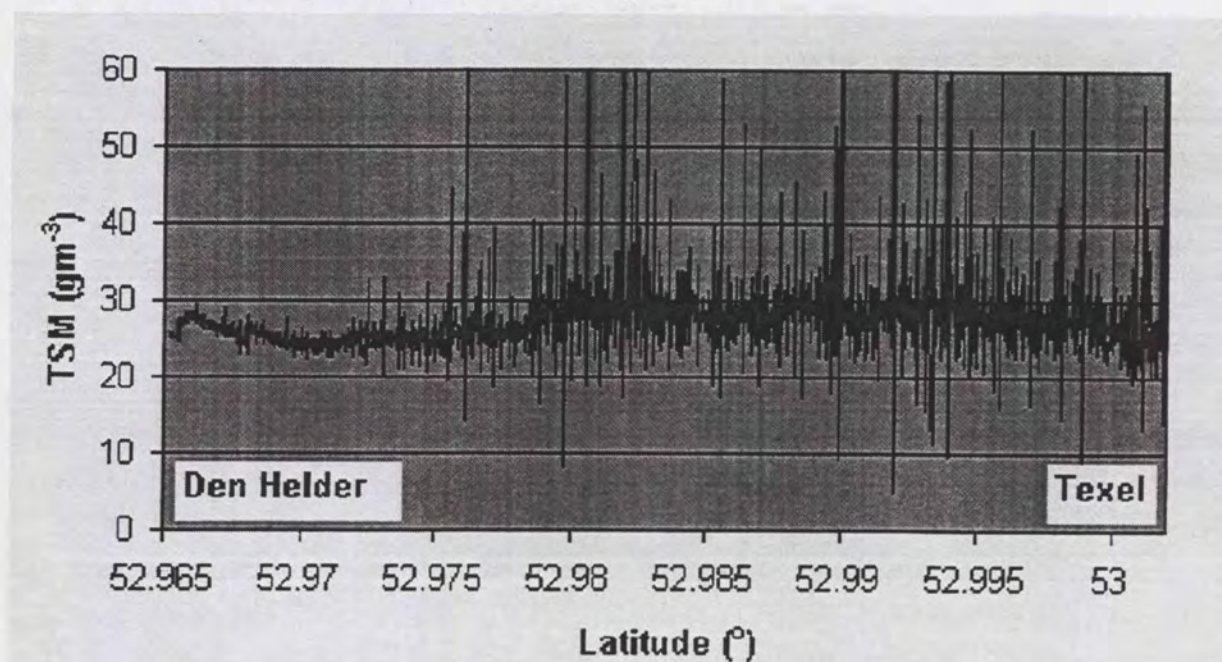


*Figure 7.1 A TSM transect from May 23 2000, 10.00 UTC. Black line indicates the TSM concentration (3 values/sec). The red line is the moving average of 6 TSM values.*

Figure 7.1 shows the enormous resolving power of the set-up. With 3 measurements per second a very detailed picture of TSM distribution over the Marsdiep can be made. The TSM transect of Wernand shows, however, some contradictory information when compared to the transect of Hoogenboom, that was taken 20 minutes later (Figure 7.2).



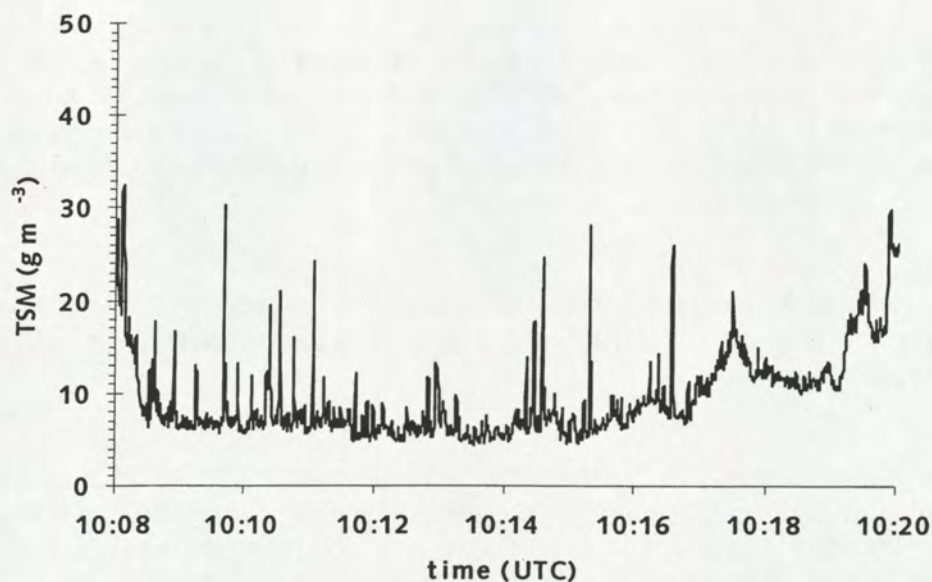


*Figure 7.2 A TSM transect from May 23 2000, 10.20 UTC.*

The Hoogenboom values are around 8 mg/l for the middle stretch of the Marsdiep. The concentrations increase to values higher than 20 mg/l in the vicinity of the harbours. Wernand's profile features higher values in the middle stretch (around 30 mg/l) with somewhat decreasing values towards the harbours. It was already shown in chapter 6.3.2 that the PMNS algorithm applied to Marsdiep spectra would lead to higher values than observed in the field. Hoogenbooms method is more advanced, in the sense that sky reflectance is accounted for. The analytical algorithm he uses is calibrated on SIOP observations of the same day, therefore it seems that his estimations of TSM are probably more realistic. Additional evidence for the selection of one of these two methods comes from the EPS-A image that is treated in the next paragraph. Note that both transects feature a number of spikes in the observations.

#### Conclusions for MERIS validation

- 1) It was already evident from chapter 4.4 that Marsdiep water is very atypical for Dutch coastal waters. This fact, combined with the relative short track distance between Den Helder and Texel, could make the TESO set-up at this location less suitable for actual MERIS validation. MERIS products will be based either on global or regional mean optical properties, which means that concentration retrieval in the Marsdiep will be based on (for the Marsdiep) non-representative SIOP.



- 2) The Ferry borne method is, however, very suitable for method and instrumentation development and testing.
- 3) If MERIS resolves the Marsdiep sufficiently (taking also e.g. the adjacency effect into account) the set-up, when validated using the proposed additional radiometers, could still function as an additional check on MERIS observations and products, especially because the CDOM values are relatively high for North Sea coastal waters.
- 4) A compensation for the sky light reflectance in the reflectance measurements combined with an analytical inverted model seems to provide the best TSM values for the selected day.
- 5) The analytical model was calibrated using synchronous SIOP, which makes the calibration less representative on other days. The PMNS model was calibrated on a multitemporal dataset. Therefore it is recommended to study the stability of both methods in time using a number of other transect observations.



### 7.3 Using EPS-A images for MERIS validation

#### 7.3.1 Introduction to the Marsdiep case study

At 23 May 2000, 10:09 (UTC) data takes were made from the Marsdiep with the EPS-A. Coordinates of the flown track were 52 56 36N 04 47 08E to 53 01 12N 04 47 04E. The following instrumental settings were used; water quality adapter block, 37 scans per second, normal grating. The flight altitude was 2000ft and the flight speed was 120 knots thus obtaining a pixels size of 1.7m in nadir. A higher flight altitude was preferred but sub-optimal weather conditions, scattered clouds, forced the plane to descend to 2000ft. Horizontal visibility was 25km. The raw image was corrected for rolling of the platform, dark current and the pixel sizes were recalculated such that all pixels of the images had the same size as the nadir pixel. The striping in the image, due to the mirrors of the Kennedy system, was removed by applying a moving average over the image of 4x4 pixels. Finally the calibrated radiance intensities as detected by the sensor were calculated. An image in RGB is given in Figure 7.3.



*Figure 7.3 RGB impression of the harbour of Den Helder as seen by the EPS-A. Turbidity patterns (plumes) and increasing turbidity towards the harbour can be observed.*

To get the subsurface reflectance an atmospheric correction procedure TOOLKIT (De Haan et al., 1996) was applied.



The parameters used for input into 'TOOLKIT' were:

Aerosol: maritime extinction (23km)	atmosphere profile: mid latitude summer
sun zenith: 37.05°	cloud model: no clouds or rain
view zenith: 180°	horizontal visibility: 25 km
sun Azimuth: 0°	Q factor: 3.15
view azimuth: 0°	refractive index: 1.84 (salt )
flight altitude: 0.66km	

The Q-factor was obtained from the field measurements carried out from the R.V. Navicula. The obtained subsurface reflectance spectra suffer from spectral noise. The origin of the noise is not clear but may be caused by the operation problems that occurred during the data takes. The instrument might have been not able to stabilise due to repeated crashes.

Subsurface reflectance spectra were selected from the image near the Navicula. These spectra were compared to ship based measurement obtained at the same time (Figure 5.10 and Figure 5.11). A reasonable match was obtained in the green part of the spectrum. In the blue part no match could be obtained. Variation of aerosol type and optical thickness did not result in a better fit. The reflectance obtained from the image in the blue is too low. In the near infrared part (700nm) the reflectance appears to be too high. Surrounding clouds may cause this tilt of the spectrum.

Matrix inversion technique applied on the subsurface reflectance image showed, as expected, poor results. Therefore an alternative algorithm was made using the green to red wavelength bands.

### 7.3.2 Reflectance model and algorithm

The Gordon model was calibrated using SIOP observations within the Marsdiep during the 23<sup>rd</sup> of May. Next a series of reflectances was simulated with the Gordon model using a fix values for absorption by dissolved organic matter and concentration of chlorophyll *a*, being 0.7m<sup>-1</sup> and 30μg l<sup>-1</sup> respectively. The concentration of total suspended matter was varied between 0 and 50 mg l<sup>-1</sup>. Reflectance was integrated to match the spectral bands of the EPS-A. The wavelength bands 563, 600, 619, and 629 were averaged to reduce spectral noise. To build the algorithm (a broad band, one band semi-analytical algorithm) a polynomial fit was used to calculate the relation between concentration of total suspended matter and reflectance:

$$TSM = 15013 \cdot R^2 + 594 \cdot R - 0.0436$$



### 7.3.3 Image processing results

Next the algorithm was applied to the spectrally averaged observations in bands 563, 600, 619, and 629. Concentration of Chlorophyll a could not be determined due to the poor quality of the EPS-A data.

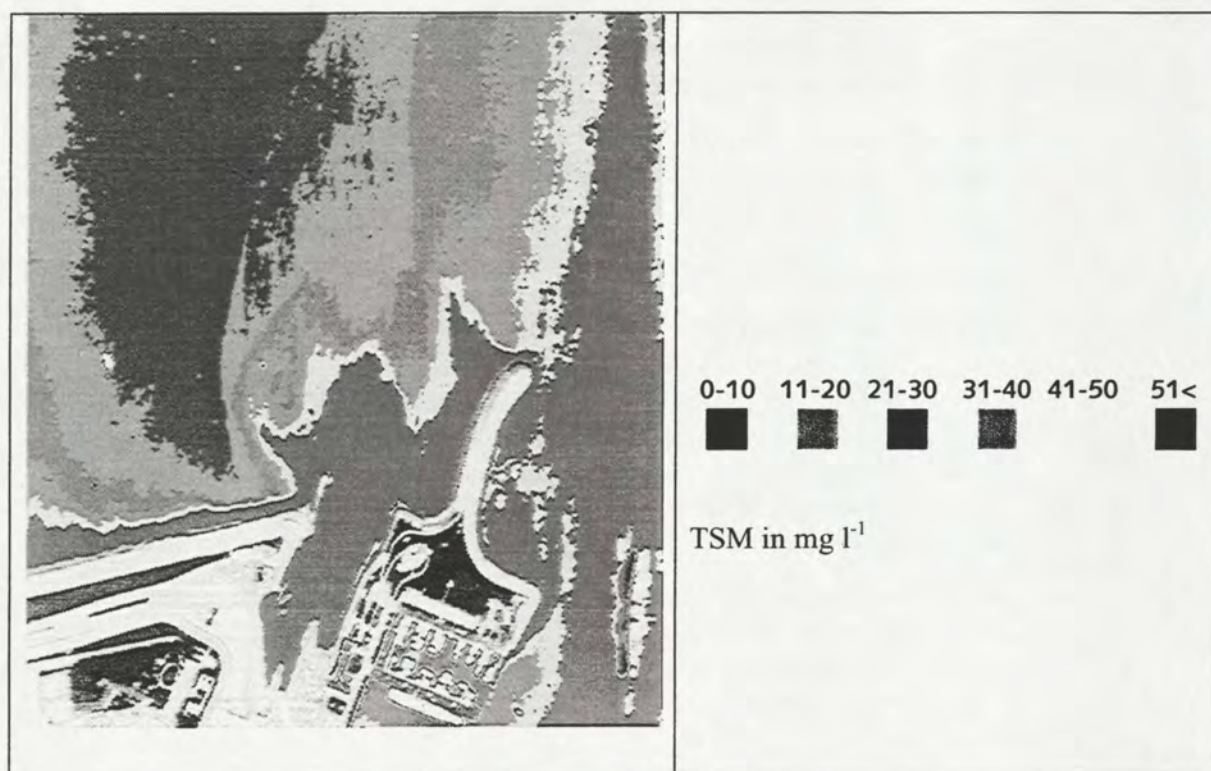


Figure 7.4 EPS-A observed TSM concentrations in the vicinity of the harbor of Den Helder (23 May 2000).

Figure 7.4 shows the image of TSM concentration: it clearly features patterns of high concentration near the harbour and lower concentration towards the North Sea. The zone of high TSM values in the right side of the image is however not related to turbidity but to increased reflectance caused by the angular configuration (increasing path length towards the side of the image) and also caused by sun/sky glint. Figure 7.4 essentially shows the same pattern as observed by Hoogenboom et al., using the Satlantics: low TSM values 10 mg/l or lower in the middle of the Marsdiep and higher values towards the harbour. The EPS-A values are a bit more extreme in the sense that they are lower than 10 mg/l in the middle of the Marsdiep and higher than 50 mg/l in the harbour. Field evidence (*Navicula* measurements) suggests that a mean value of approximately 10 mg/l for the middle of the Marsdiep is acceptable. TSM values near the harbours were not measured.



### 7.3.4 Conclusions for MERIS monitoring

- The EPS-A shows spatial structures in the TSM concentrations that are in same spatial domain as MERIS pixels. Therefore the EPS-A will be an important link between point measurements, transect measurements and MERIS observations.
- As all airborne instruments, the logistics of EPS-A flights remains complicated because the actual take of the image (in a validation setting) is determined by the logistics of the field campaign (organized months in advance). This means that flight time can be varied only in a small timeframe depending on weather conditions during the predetermined campaign days.
- The EPS-A takes over the North Sea have all suffered from small to large amounts of sun/cloud glint. This could partially be overcome by careful flight planning, whereby the flight direction should be adjusted to the flight time after the final decision to do the take. A second option would be to develop methods and software for glint removal.
- It is recommended to do a final rehearsal with the EPS-A in summer 2002, in which care is taken to avoid all disturbances to the take. This final rehearsal will then provide the definitive insight into the potential of EPS-A for the support of MERIS validation. A set-up must be sought (e.g. using a small hired vessel) to do supporting fieldwork during optimal weather, instead of allowing the fieldwork logistics to determine the flight day (without consideration for the weather).
- When accurate spectra are available from EPS-A both MIM and RMI should be tested to obtain concentration products. This is a result from the observation that the one-band semi-analytical algorithm used in this study does not compare well to Satlantics measurements (Hoogenboom) for the higher concentrations.

## 7.4 Validation of the MERIS-RMI algorithm using SeaWiFS images

### 7.4.1 Introduction

During this study Ratio Matrix Inversion has come forward as a serious candidate to use for mapping the North Sea water quality parameters with MERIS on the basis of regional optical properties. Unfortunately, the algorithm could not be tested on EPS-A images because the influence of cloud/sun/glitter and other disturbances proved to be too large (or at least not understood). Therefore an alternative was sought. MOS images are almost of the same spectral and spatial resolution as MERIS. Unfortunately, access to recent MOS images was difficult to obtain, therefore it was investigated whether SeaWiFS could serve as proxy sensor for MERIS. SeaWiFS has sufficient radiometric sensitivity to study coastal water concentrations since it was designed for the study of case 1 water. Unfortunately an essential spectral band is missing in the configuration, namely a spectral band around 700 nm. Tests by Gons (2000) and the present authors together with historical evidence (e.g. Dekker, 1993) indicates that TCHL can be determined with high accuracy using the red ratio (e.g. based on the 667 and 705 nm bands).



#### 7.4.2 Modelling the missing SeaWiFS band (MERIS 705 nm)

The PR650-L2-Gons spectra from the Belgica, Mitra and Navicula form a small but well documented database to do experiments with. Since the MERIS 705 band is missing in SeaWiFS an experiment was conducted to answer the following questions:

- 1) Is there a relationship between PR650 information in the MERIS 705 nm band and the PR650 information in the two surrounding SeaWiFS bands (667 and 765 nm)?
- 2) Can this relationship be used to simulate an extra "MERIS-705" band based on SeaWiFS information?
- 3) Can this band, together with the routine observations of SeaWiFS be used to estimate TCHL concentrations?

##### *Step 1) SeaWiFS – MERIS band settings correlations*

As a first step, the PR650-Gons-L2 R(0-) spectra (offset corrected) were convoluted to the MERIS and SeaWiFS band passes. Next a correlation analysis was done between MERIS band 705 nm and SeaWiFS 667 and 765 nm. It appeared that the correlation between MERIS 705 nm and SeaWiFS 765 was low, but the correlation between MERIS 705 nm and SeaWiFS 667 nm high ( $r^2=0.946$ : see Figure 7.5). Because the spectra represent a wide range of North Sea conditions (with respectively high and low TSM, high and low TCHL and even high and low CDOM conditions) this was taken as an indication that it should be possible to generate a synthetic MERIS 705 nm band from the SeaWiFS 667 band (alone or in combination with the 765 nm band for robustness).

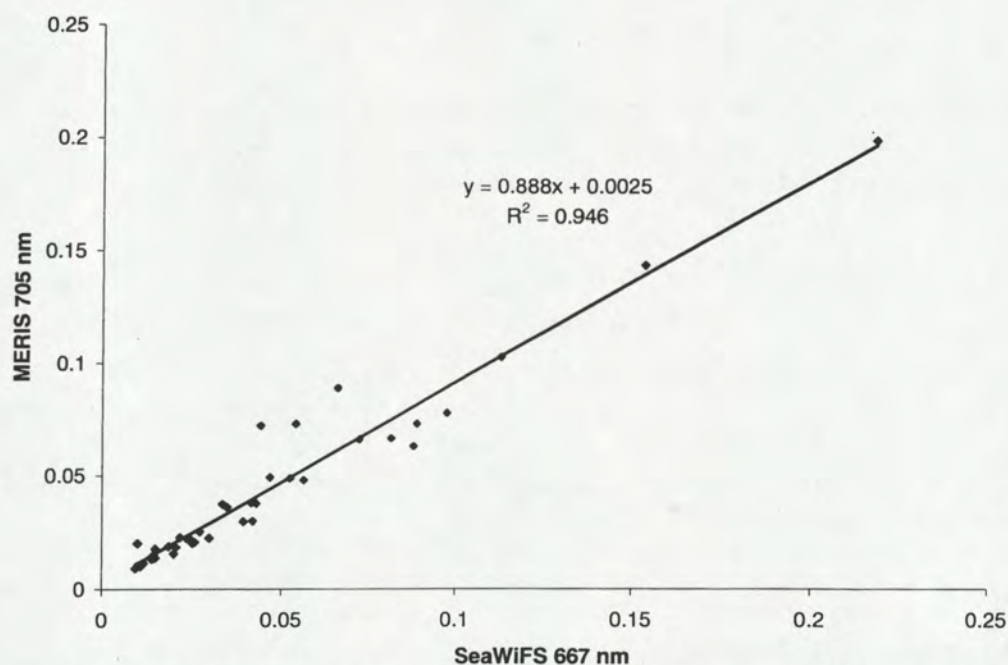
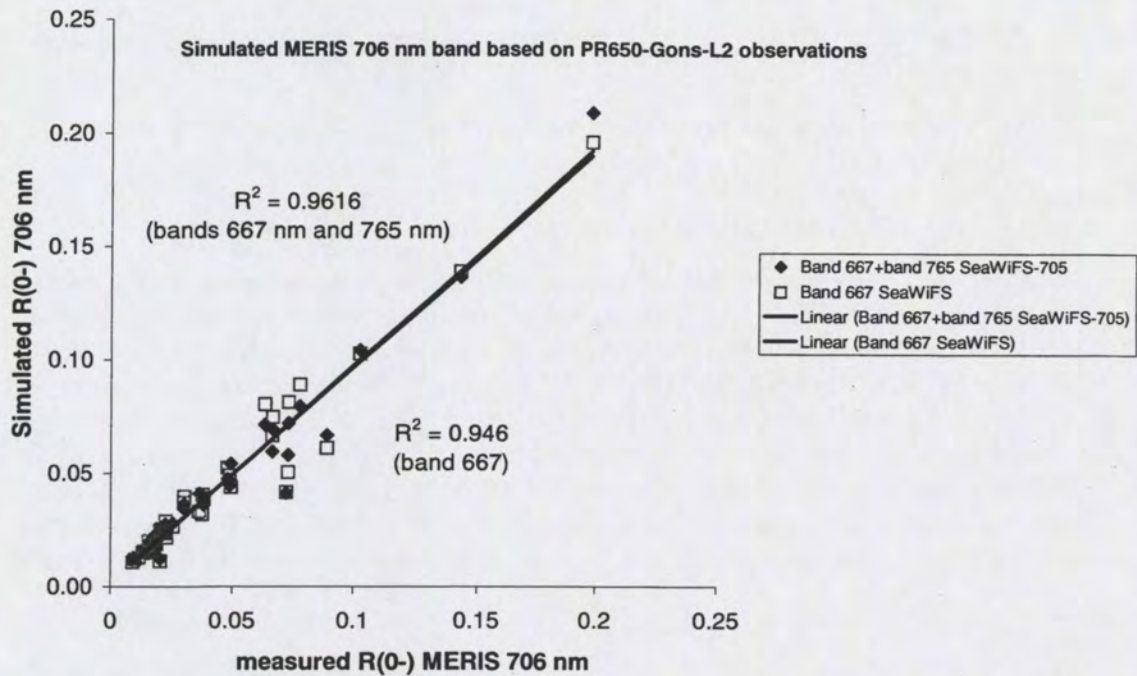


Figure 7.5 Correlation analysis between SeaWiFS 667 nm band pass values and MERIS 705 nm band pass values (both convoluted from PR650-Gons-L2 observations).



*Step 2): Making a synthetic "MERIS-705" band based on SeaWiFS information*

Next a linear model was used to try to generate the MERIS 705 nm band from SeaWiFS 667 nm observations. This proved to be quite successful. The SeaWiFS 667 band provided estimations of the MERIS 705 nm band with an explained variance ( $r^2$ ) of 0.946 (see Figure 7.6).



*Figure 7.6 The correlation between synthetic MERIS 705 nm bands derived from SeaWiFS band settings and PR650-Gons-L2 spectra and observed MERIS 705 nm band values derived from the same spectra*

It was furthermore found that adding the 765 nm band improved the correlation slightly to 0.96. Therefore this last combination was used giving the following equation:

$$R(0-)_705 = 0.7603 \cdot R(0-)_667 + 0.5035 \cdot R(0-)_765 + 0.0026 \quad (7.1)$$

This equation was used in the processing of approximately 10 SeaWiFS images to the three water quality parameters.

### 7.4.3 SeaWiFS processing sequence

The final processing of SeaWiFS images using the Ratio Matrix Inversion method was still quite cumbersome. First a selection must be made of bands that are inputted into the algorithm: these were the 511, 561, 621, 666 and 706 nm bands. In the blue and in the



765 nm bands irregularities in the atmospheric correction were found leading to zeros in these bands in ocean spectra. RMI cannot deal with zero (or very low) band values, therefore these bands had to be omitted.

Next a decision had to be made on the sequence of processing. RMI can be used to solve 3 parameters simultaneously but this works only for perfect and detailed spectra. It can also be used to derive two parameters simultaneously while holding one parameter constant or even to derive one parameter while holding the other two constant. Based on some considerations, a choice was made for the last option. These considerations are:

- 1) The estimation of TCHL is not very dependent on errors in SIOP and (to be proven in detail in a follow-up sensitivity study) also not very sensitive to errors in TSM and CDOM. At least TCHL is the least sensitive parameter with respect to errors in the other two parameters.
- 2) An initial estimate can be done of TSM using a scala of other algorithms, such as the POWERS one band algorithm: for best performance this algorithm should be recalibrated using the mean 2000 SIOP data set.
- 3) Initial CDOM estimations are very difficult but of large consequence to the estimation of TSM using RMI (also to be proven in a follow-up sensitivity study).

Therefore it seemed the best approach to make initial estimations of TSM using the POWERS algorithm and of CDOM using a mean North Sea value derived from in situ observations (See Table 6.1). Next TCHL was determined. TSM and the initial CDOM value were subsequently used to derive an improved estimate of TSM after which the new TSM and TCHL were used to derive CDOM from the spectra. The logical next step is to input the new CDOM and TSM into the algorithm and calculate an improved TCHL concentration after which TSM and CDOM can be determined again similarly to the earlier steps. It was tested if continuation of this iterative process would lead to stable TSM, TCHL and CDOM values and in some cases converging was found but in some cases the concentrations diverged. Therefore the procedure was stopped after the described sequence.

#### 7.4.4 Calibration of the algorithm using a selected SIOP data set

The final algorithm was calibrated using average SIOP. These were derived from the mean values of the Mitra, Navicula, Belgica-2000-I and II data sets. Based on the sensitivity studies in chapter 8 one may conclude that such a calibration data set will result in underestimation of TSM values in Belgian waters and overestimation of TSM in Dutch waters. Validation of the image concentration products could lead to an improved choice in mean SIOP data set in a subsequent project.

#### 7.4.5 Some conclusions on the set-up of the RMI-MERIS processor

- 1) Unless regional specific calibrations are performed, the RMI method (based on SeaWiFS bands; including the synthetic band) will inherently lead to



overestimation of TSM in Dutch coastal waters and underestimation in Belgian coastal waters.

- 2) In the blue and in the 765 nm bands irregularities in the SEADAS/MUMM atmospheric correction were found leading to zeros in these bands in ocean spectra. RMI cannot deal with zero (or very low) band values, therefore these bands had to be omitted.
- 3) An iterative one-parameter formulation of the RMI method was found to be very effective.
- 4) Initial estimations of TSM can be improved by reparameterizing the POWERS one band TSM algorithm for the actual mean SIOP set that was used.



## 7.4.6 Interpretation of the SeaWiFS image of 6 May 2000

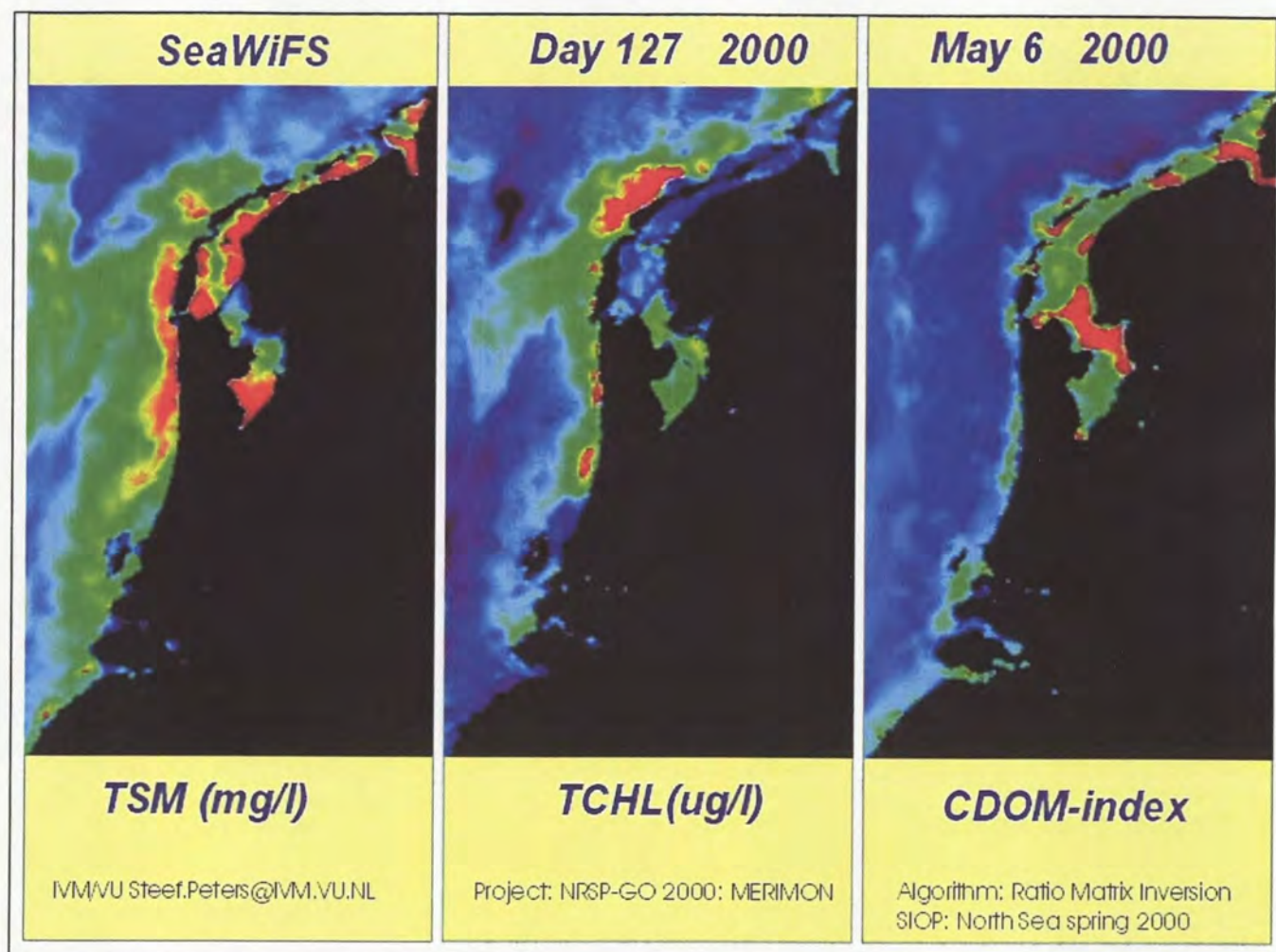


Figure 7.7 SeaWiFS water quality products for day 127: 6 May 2000

The maps in Figure 7.7 are based on RMI using a SeaWiFS image as input and the average value of the SIOP determined in 2000 in the Dutch part of the North Sea. Both the TSM and the TCHL map are quantitative with an absolute scale (Figure 7.8). The CDOM-index map is also quantitative but due to imperfections in atmospheric correction, SIOP or model formulation, the values are a bit off-scale, therefore it is presented as an index. Day 127 was an almost cloudless day with the exception of one cloud over the North Sea in the environment of Rotterdam. The TSM and TCHL map show different patterns. TSM is abundant on the “Vlakte van Raan” and the “Vlaamse Bank” and along the coast approximately from IJmuiden to Den Helder, with an intriguing plume extending from Terschelling. High concentrations of TCHL occur just along the coast with a probable bloom just above Terschelling. The CDOM index in general behaves as expected: higher concentrations along the coast and over the whole North Sea low values. The CDOM map reveals an intricate interplay between the North Sea and the Wadden Sea. An interesting phenomenon is the river Eems, that discharges water with high CDOM concentration



in the Wadden Sea, where it remains encapsulated. The scaling of the maps does not apply to the lake IJssel and lake Marken because SIOP are different. Still, the observed patterns will not change that much when correct SIOP are used. An interesting phenomenon in the lake IJssel is the large discharge of CDOM-rich water into the lake by the river IJssel. TSM patterns in the lake should be compared to field-data to study the validity: they are more detailed than patterns from earlier studies (Vos, 2000).

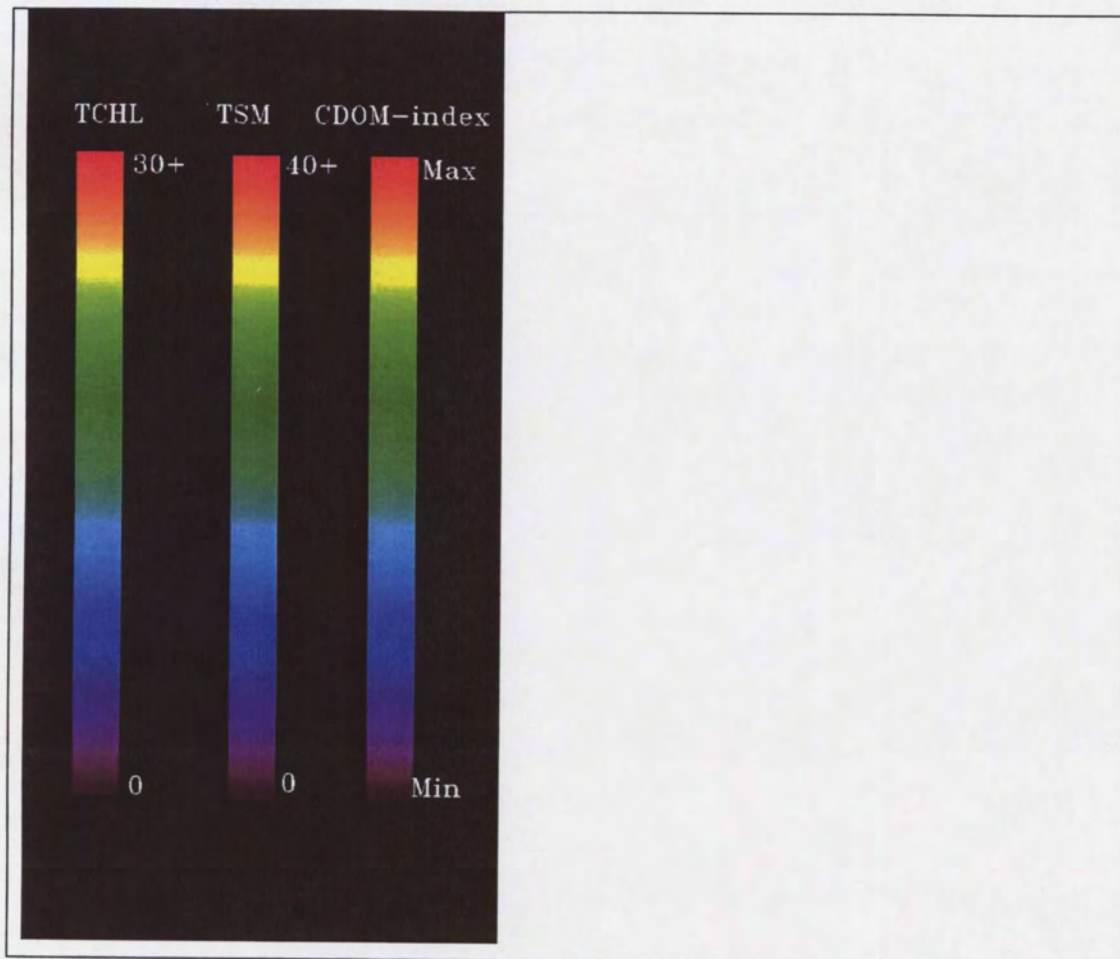
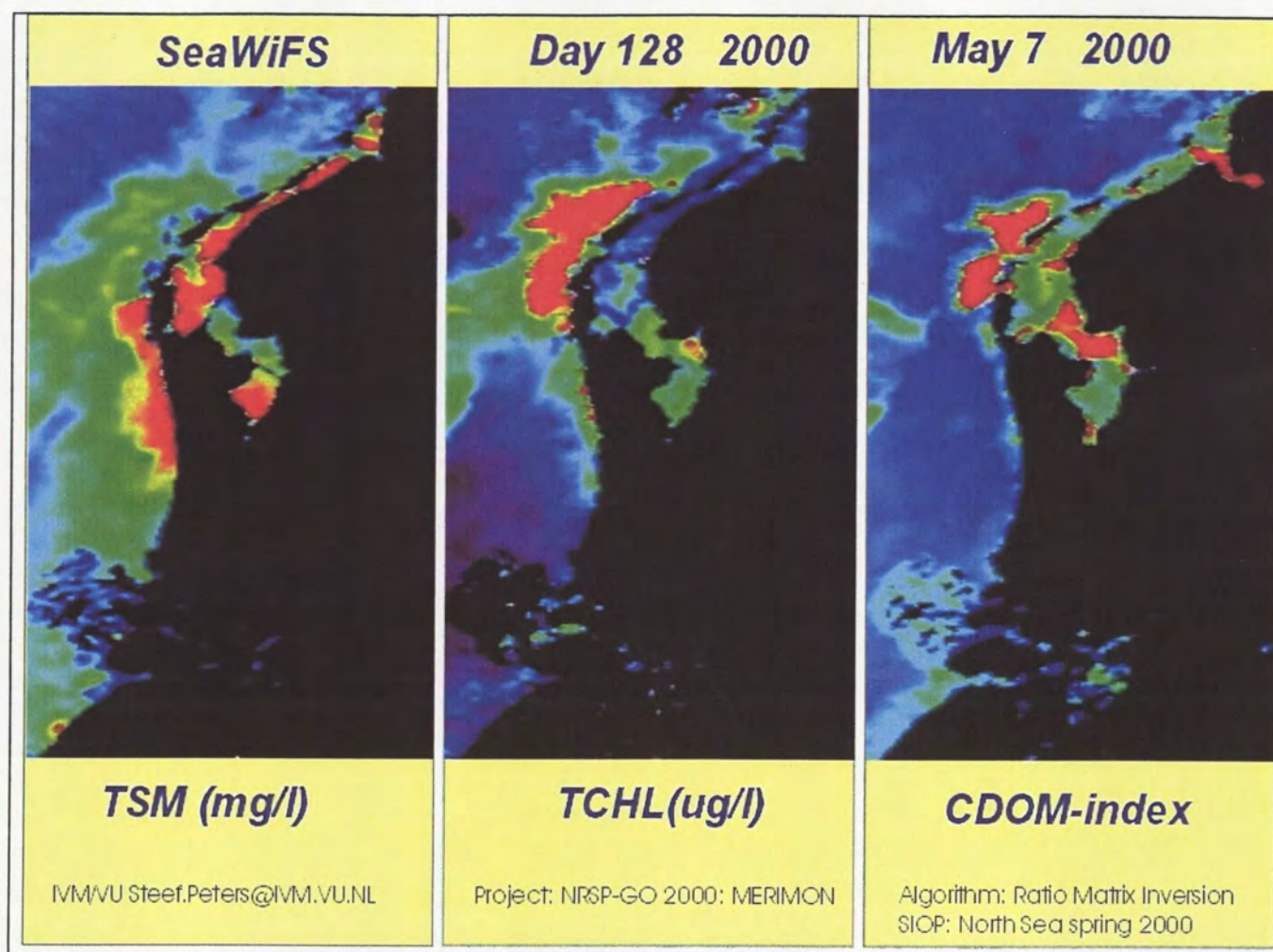


Figure 7.8 Legend for the SeaWiFS-RMI TCHL, TSM and CDOM-index maps



## 7.4.7 Interpretation of the SeaWiFS image of 7 May 2000



*Figure 7.9 SeaWiFS water quality products for day 128: 7 May 2000*

Figure 7.9 has cloudiness over the Southern part of the Dutch coast. TSM patterns along the Northern part of the coastline are similar to the day before. The TCHL bloom above Terschelling seems to have expanded. The CDOM patterns reveal that on this moment Wadden Sea water is discharged into the North Sea between the first three islands. The Eems plume is still distinctly visible. The river IJssel plume seems to have broken up.



## 7.4.8 Interpretation of the SeaWiFS image of 7 May 2000

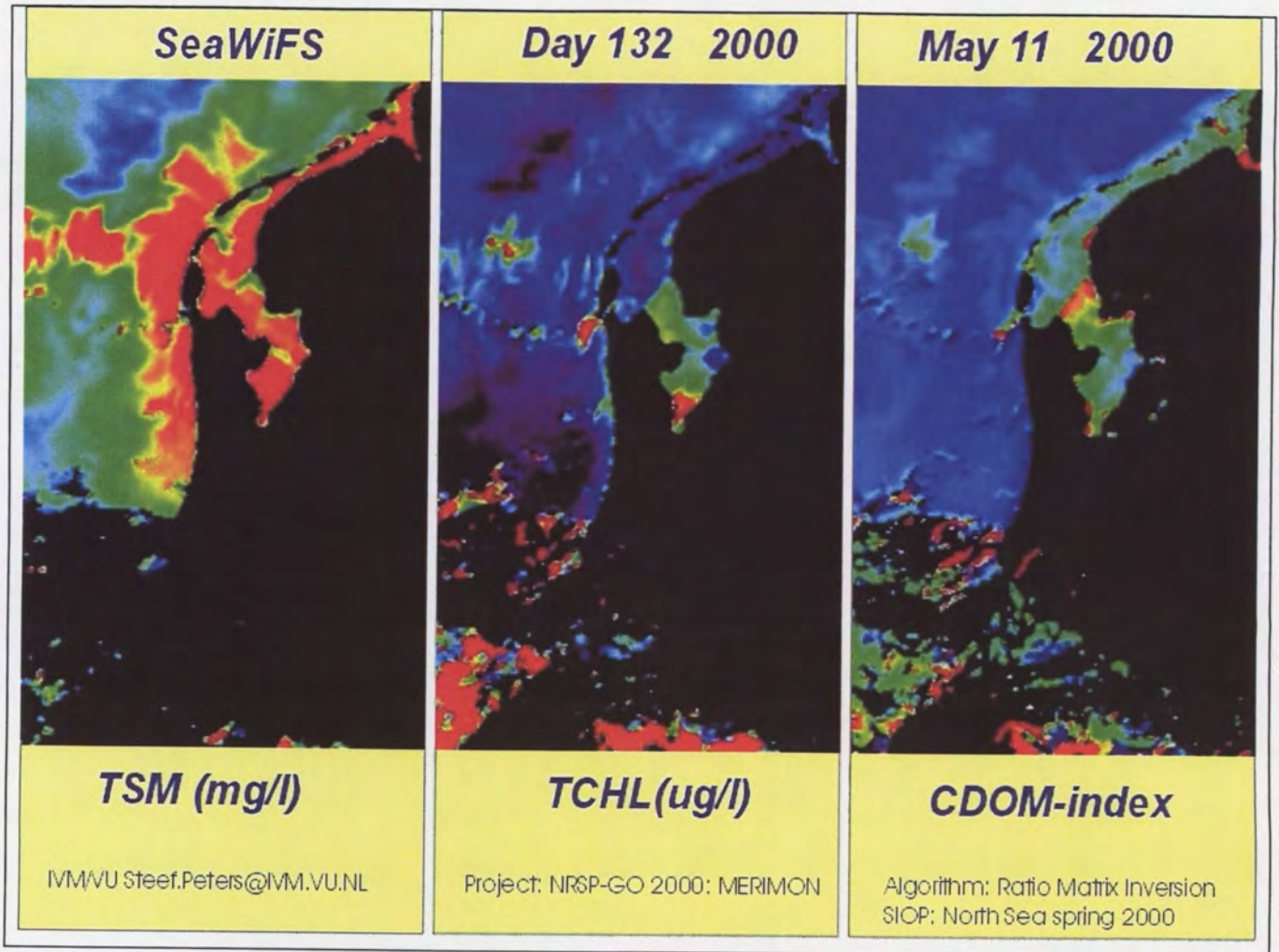


Figure 7.10 SeaWiFS water quality products for day 132: 11 May 2000

According to Figure 7.10, the situation in the North Sea has changed. TSM concentrations along the Northern part of the coast have increased, while TCHL concentrations have decreased substantially. There remains a possible TCHL plume at outlet of the Wadden Sea near the Marsdiep but this could also be a cloud relict. The TCHL map shows a number of other patterns that could also be related to clouds. Therefore it should be investigated if better cloud mapping can improve the TCHL product. Eems water seems to be pushed back into the river by upcoming tide. These phenomena could easily be groundtruthed in future studies. Lake IJssel patterns show a large spatial heterogeneity.



#### 7.4.9 Interpretation of the SeaWiFS image of 12 May 2000

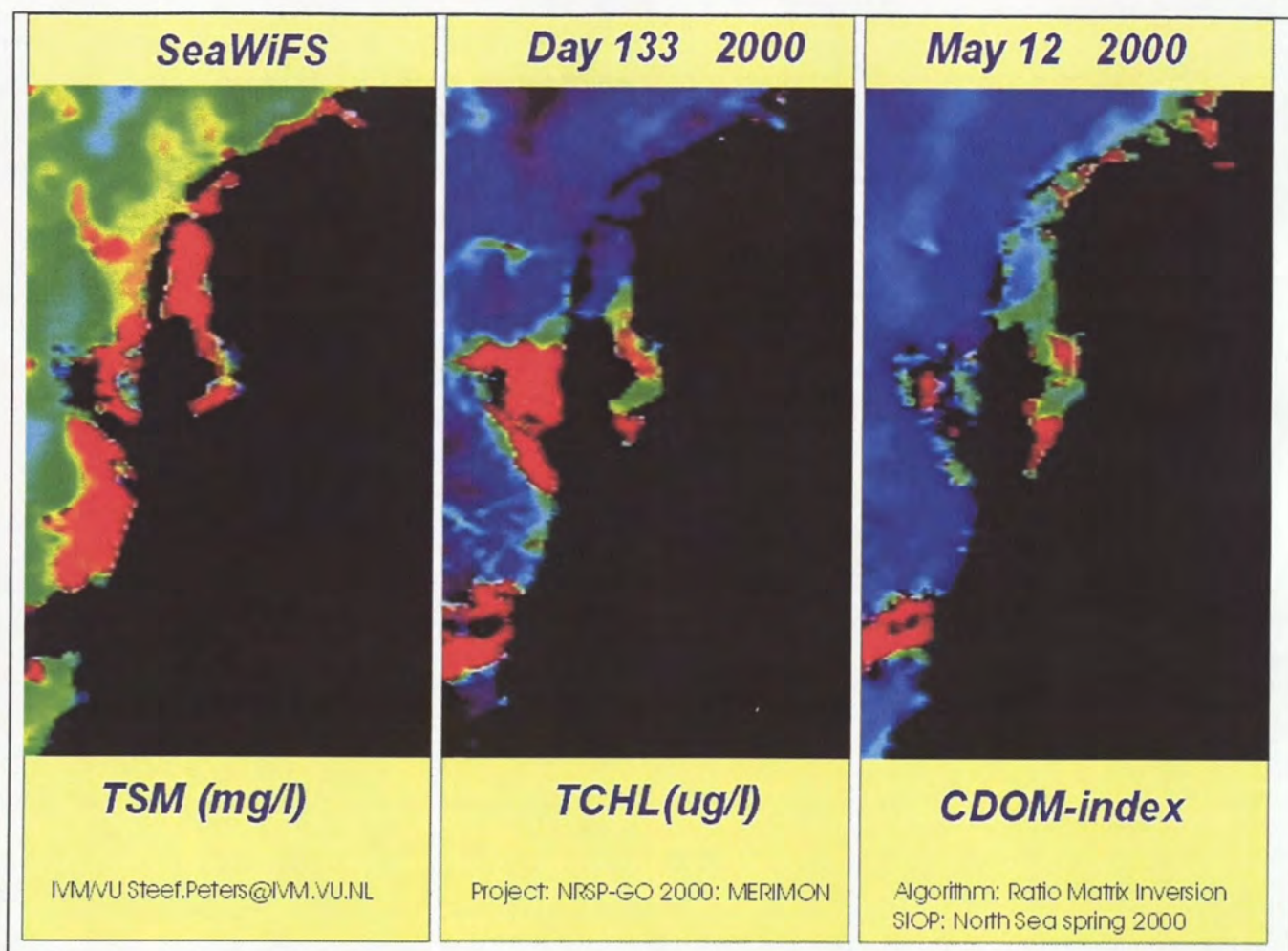


Figure 7.11 SeaWiFS water quality products for day 132: 11 May 2000

Figure 7.11 shows distinctly the errors in the TCHL map due to incomplete cloud flagging. The triangular shape extending from the coastline beneath Den Helder is either a cloud or an aerosol field. In the TSM maps and CDOM maps cloud structures are visible (masked as black) that are translated into high TCHL values. The same is true for the zone extending from Rotterdam into the North Sea.

#### 7.4.10 Other Images

A total of 10 SeaWiFS images of May 2000 were analysed with this method. Most images were affected by cloudiness to such an extent that interpretation became difficult. Therefore they are not shown here.



### 7.5 Comparison of SeaWiFS concentrations (TSM and TCHL) to field measurements

Field samples were taken during a Mitra cruise from the afternoon of May 8, 2000 until the afternoon of May 9, 2000. Sample locations are indicated in Figure 7.12.

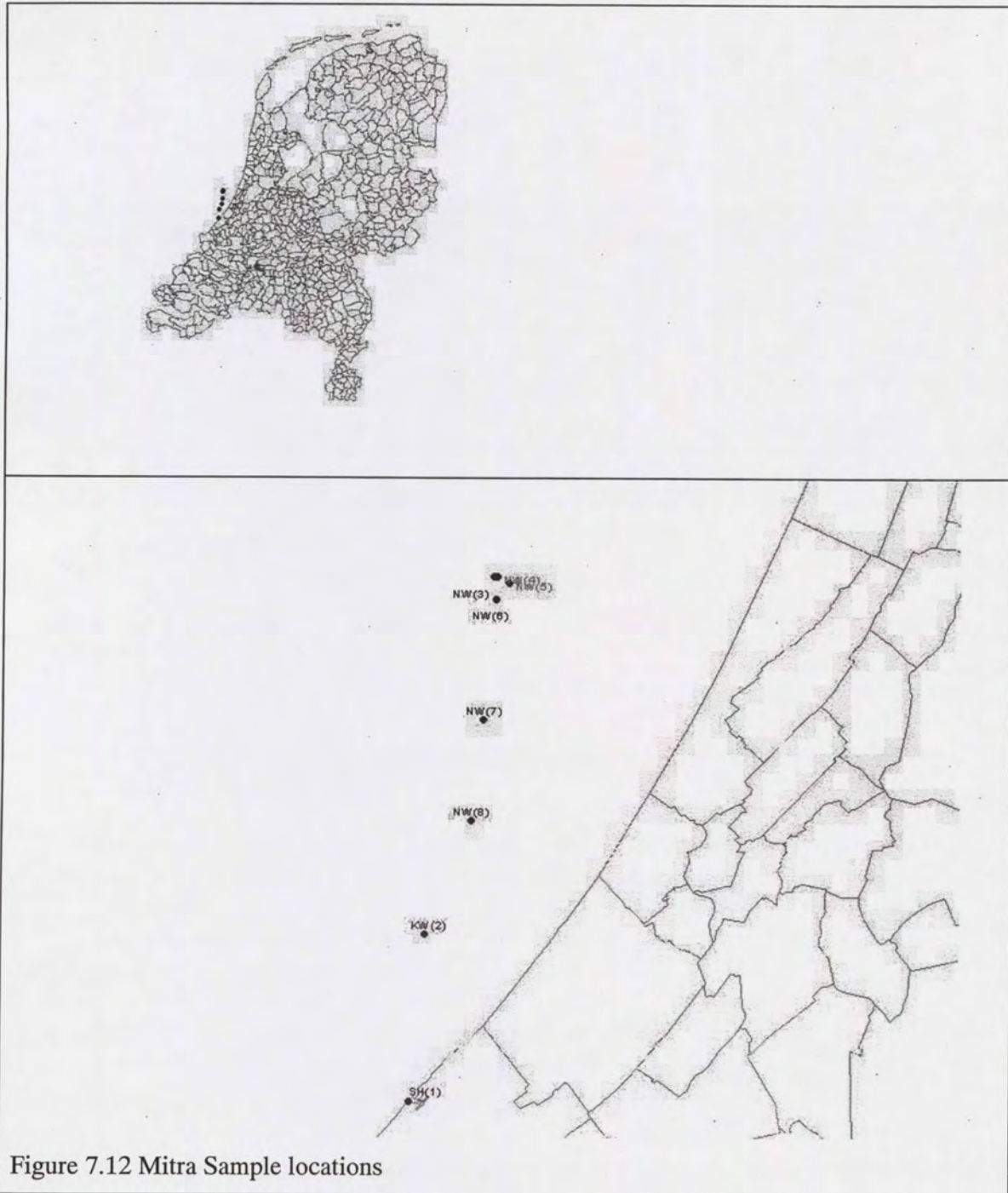


Figure 7.12 Mitra Sample locations



The measured transects of TSM and TCHL are shown in Figure 7.13 and Figure 7.14.

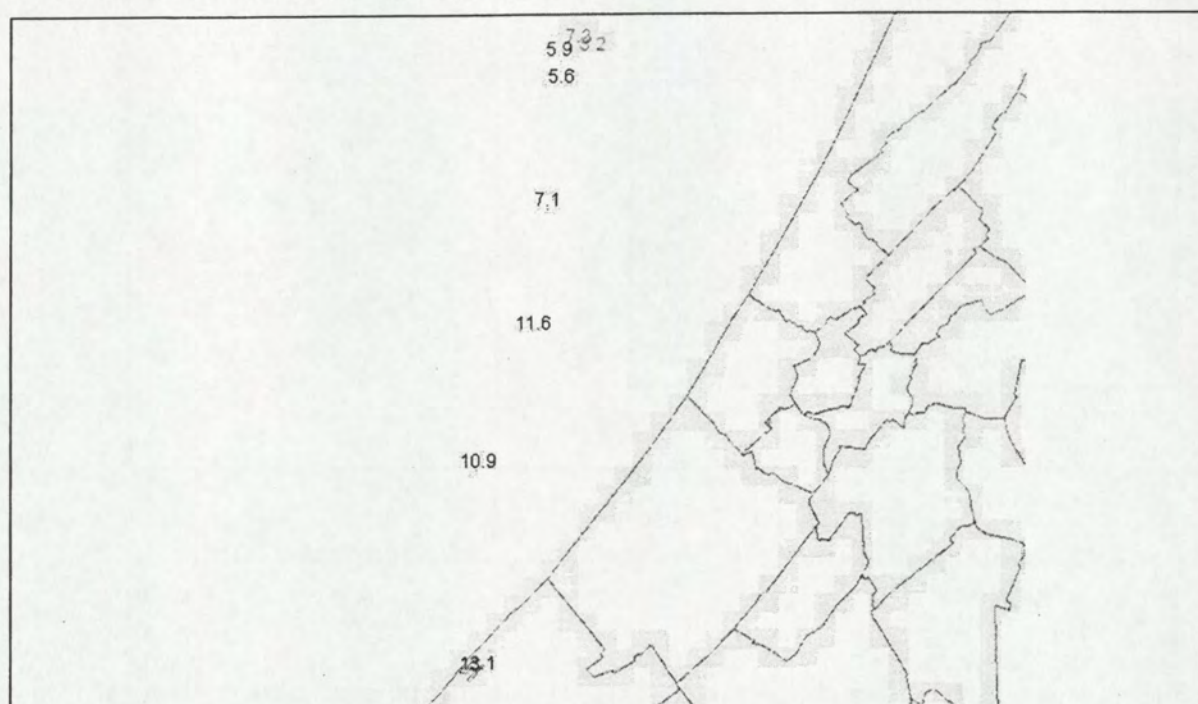


Figure 7.13 Mitra transect (8-9 May 2000): TSM concentrations ( $\text{g m}^{-3}$ )

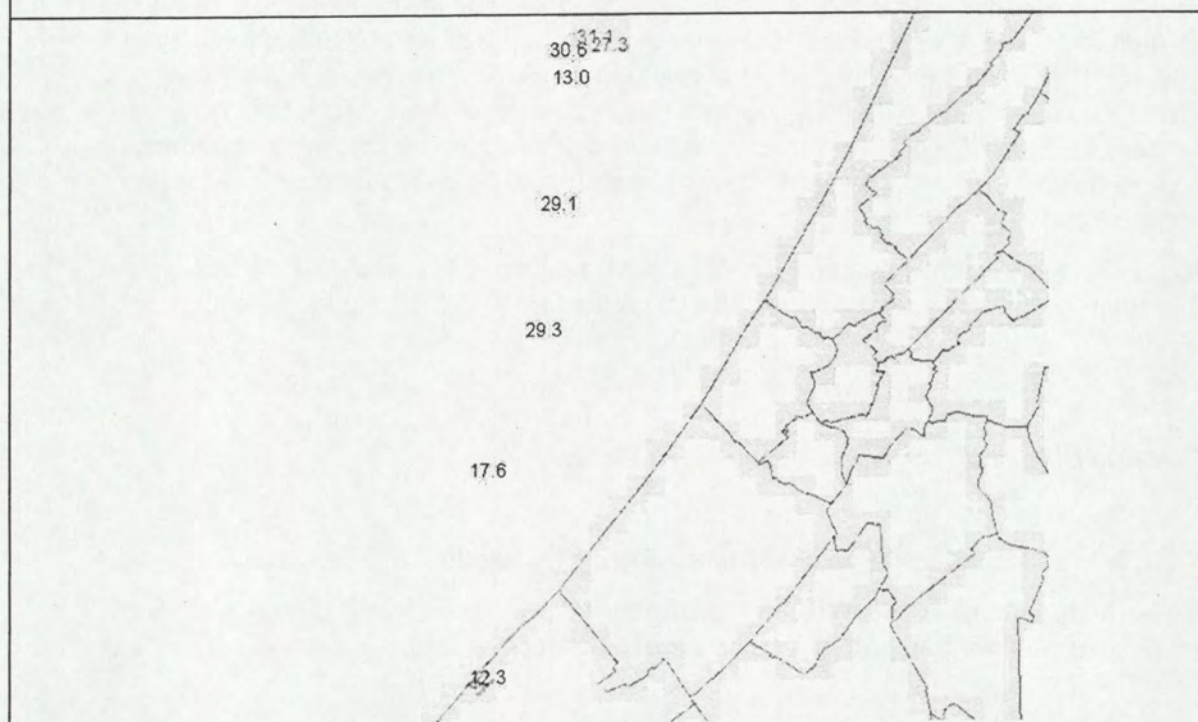


Figure 7.14 Mitra transect (8-9 May 2000): TCHL concentrations ( $\text{mg m}^{-3}$ )



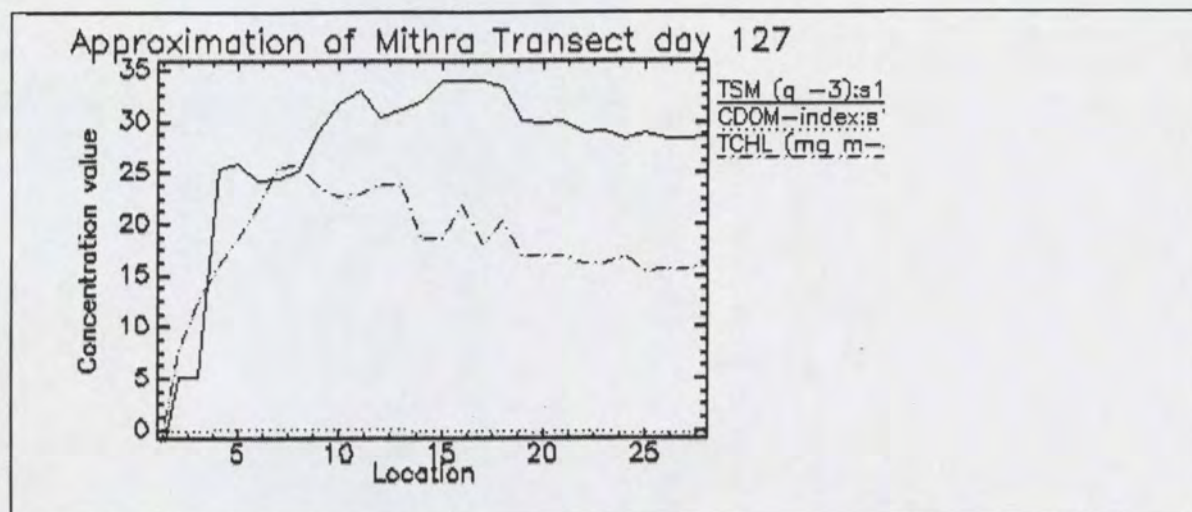


Figure 7.15 SeaWiFS transect along the Mitra cruise line extending further into the North Sea

In Figure 7.15 a transect is shown which was taken from the concentration maps derived from the 6 May image (best quality image in the series). The transect follows approximately the Mitra course (up till location index 10) and then continues in the same direction into the North Sea. Apparently TSM concentrations are a factor 3 higher than the values obtained during the Mitra cruise. This is in accordance with the observation that TSM values in the middle of the North Sea remain high ( $8-10 \text{ g m}^{-3}$ ) which is an indication that the overall range of TSM is too high. Furthermore, the TSM values increase (from the coast) in the SeaWiFS product, while they decrease (from the coast) in the Mitra observations. An evaluation of these differences is difficult because the SeaWiFS profile is instantaneous and of two days earlier, while the Mitra profile was obtained during two consecutive days. The scaling of SeaWiFS derived TSM values is probably in error.

The TCHL profile shows very nice similarity with the Mitra observed profile. Values increase (when going from the coast) up till a ceiling value of approximately  $25-30 \text{ mg m}^{-3}$  in both profiles.

#### *Conclusions from the preliminary transect validation*

- 1) TCHL is in good agreement with the values obtained along the Mitra transect.
- 2) TSM is in disagreement (SeaWiFS 6 May, Mitra 8-9 May) therefore it is recommended that the performance of the RMI method for TSM should be further evaluated.



*Conclusions for MERIS applications.*

- 1) General Conclusions: The Ratio Matrix Inversion method for SeaWiFS performs reasonably well for North Sea applications, judged from observed ranges and patterns. Validation along transects was difficult due to a lack of synchronous in-situ observations. Preliminary comparisons using the Mitra transect revealed good agreement for TCHL and disagreement for TSM. TSM patterns over the North Sea seem to be in agreement with earlier observed patterns (Van der Woerd, 2000). As a definite check on algorithm performance it is recommended to do a rehearsal exercise in 2001 using a EPS-A take without sunglint and other disturbances.
- 2) TCHL conclusions and recommendations: The synthetic 704 nm band provides a reasonable robust solution for the CHL mapping problem. However, there remain some question marks. It appears that TCHL products are sensitive to errors in cloud masking which should be checked. Implementation of the RMI method for North Sea CHL detection using MERIS should be straightforward.
- 3) TSM conclusions and recommendations: The RMI method should be recalibrated for TSM. This means that the initial estimation using the POWERS algorithm should be calibrated for the mean SIOP dataset for the North Sea (it is now calibrated on the Belgica-98 observations only).
- 4) CDOM conclusions and recommendations: In depth investigation could improve the quality of the CDOM map. Before doing this, the product should be discussed with experienced end-users to study whether it contains useful information and (when the product becomes a standard product) which form and accuracy it ultimately should have.



## 8. Conclusions and recommendations

MERIMON studied existing algorithms to select appropriate formulations for MERIS to produce regional correct estimations of TSM and CHL. In this the viewpoint of monitoring is taken, therefore the algorithms should be adaptable to temporal variations of optical water quality and relatively insensitive to small errors in instrument calibration and atmospheric correction.

Comparative algorithm evaluation was done to study the applicability and theoretical weaknesses of various types of algorithms for water quality parameters retrieval.

First semi-empirical algorithms were analysed. This type of algorithms is simple and robust: they relate directly the observed surface reflectance to concentrations. If  $R(0-)$  is used (customary for multi temporal studies) then the results of these algorithms can be linearly dependent on  $Q$ , depending on the type of algorithm formulation. This dependency on  $Q$  is also a factor of concern in one-band TSM algorithms based on semi-analytical inversion of the Gordon model and (semi-) analytical matrix inversion algorithms. Ratio algorithms assuming a spectrally neutral  $Q$  are dependent on the error in this assumption: the larger the spectral variability, the larger the error in the concentration. Therefore it was noted that comparison of various studies requires a rigid treatment of the  $Q$  and  $f$  factors and the  $B$  factor as well. This has implications for the standardization of ground truth  $R(0-)$  measurements as well as satellite  $R(0-)$  observations. At present different  $Q$  values are used for the Gons PR-650 method and the MUMM-Seadas software for  $R(0-)$  for the SeaWiFS sensor. This leads to scaling differences between the spectra. Standardization should also include the conversion of MERIS normalized water leaving radiances to level 2  $R(0-)$  end-products.

MERIS standard algorithms could not be studied by this project because the definitive parameterisation of the MERIS processor still had to be decided upon in October 2000. These algorithms were calibrated for average European case II water properties. It is questionable whether this parameterisation will be representative for the North Sea waters under consideration. Future validation should confirm the (in-) validity of MERIS algorithms. In the meanwhile, while MERIS standard products remain unavailable, this project has tested (and developed) other state of the art algorithms. Based on the outcome of this study and further sensitivity studies, in the next step, the best regional (algorithms calibrated on regional datasets) alternative for MERIS standard algorithms will be selected and calibrated.

### *Concentrations of TSM and TCHL in the North Sea*

A comparison with historical PMNS data indicates that the MERIMON field campaigns, as planned, occurred at locations (MARSDIEP, BELGIUM) and at time frames where relatively high concentrations of both suspended sediments and chlorophyll occur. The MERIMON results show that the ranges that were found are not consistent with the ranges in the PMNS-data set, therefore it was concluded that the variability of concentrations on the North Sea is still not well understood. It remains therefore important to keep monitoring concentration ranges during remote sensing studies. Care must be taken to apply algorithms based on the PMNS dataset (PMNS-TSM, PMNS-CHL and POWERS-TSM) to the MERIMON data. First the validity for the high-range values should be checked.



### *Above water measurements of R(0-) spectra*

In the Netherlands quite some progress has been achieved in the understanding and facilitation of above water measurements of R(0-). MERIMON found that various methods produce good results, especially if the reflected sky radiance term is taken into account. For MERIS validation it was concluded that the PR650 Gons method can be suitable for MERIS validation if the scaling problems (in the match with simulation models) are overcome. The PR650 PMNS method is less suitable for MERIS validation because sky radiance disturbs the result. The EPS-A is known to produce good spectra (observed in images taken above the lake IJssel (Vos et al., 2000) and the Vechtplassen (Laanen and Peters, in preparation)). Testing above the North Sea was hampered by aerosol gradients and cloud/sun glitter over the images. Therefore this instrument should be re-tested under better conditions. The Satlantics set up on the TESO ferry: In 2001 the instrument set-up will be improved (Wernand, pers. comm.) to accommodate independent simultaneous measurements in all channels in all three directions. It is expected that this will remedy spectral problems in the R(0-) measurement.

Therefore it is recommended to set-up one other experiment during summer 2001 to test the improved Satlantics together with EPS-A and PR650 measurements.

### *Testing selected algorithms using PR650 observations*

The standard PMNS TSM algorithm for MERIS tends to overestimate TSM in the Marsdiep and to underestimate TSM in the Belgian waters. The PMNS study has proposed 2 CHL algorithms for MERIS. When both are applied to PR650-Gons-L1 observations results are good for the simple band ratio algorithm and bad for the MRA-algorithm. The POWERS algorithm seems to underestimate TSM at low concentrations (less than 20 mg/l) and to overestimate at higher concentrations (>20mg/l).

Some experiments were conducted using the newly developed Ratio Matrix Inversion technique, with the following findings:

- Only the Belgica-I SIOP-set does not lead to underestimation of TSM in Belgian waters. So, if accurate TSM values above 30 mg m<sup>-3</sup> are required then a region specific SIOP set must be used
- The MERIS band settings are suitable to map TSM in North Sea coastal waters with RMI.
- RMI is a suitable technique to map TSM.
- PR650-Gons-L2 spectra are suitable to test and calibrate analytical algorithms for TSM retrieval. Because of the use of multiple ratios, the sensitivity of the algorithm to scaling errors is relatively low, as compared to e.g. MIM.
- The scaling differences between simulated spectra (using RMI retrieved concentrations) and measured spectra remains an issue of concern.



- The MERIS band settings are suitable for TCHL retrieval using RMI in the North Sea coastal waters.
- The sensitivity of the results to variations in SIOP is low.
- A scaling error in the PR650-Gons-L2 spectra is of relatively little influence on the RMI-TCHL determination.

For the Marsdiep study area and the TESO-Satlantics set up the following conclusions were drawn:

- Marsdiep water is very atypical for Dutch coastal waters.
- The Ferry borne method is very suitable for method and instrumentation development and testing.
- If MERIS resolves the Marsdiep sufficiently (taking also e.g. the adjacency effect into account) the TESO set-up, when validated using the proposed additional radiometers, could still function as an additional check on MERIS observations and products, especially because the CDOM values are relatively high for North Sea coastal waters.
- A compensation for the sky light reflectance in the reflectance measurements combined with an analytical inverted model seems to provide the best TSM values.

#### *Conclusions from the EPS-A applications*

- The EPS-A shows spatial structures in the TSM concentrations that are in same spatial domain as MERIS pixels. Therefore the EPS-A will be an important link between point measurements, transect measurements and MERIS observations.
- As all airborne instruments, the logistics of EPS-A flights remains complicated because the actual take of the image (in a validation setting) is determined by the logistics of the field campaign (organized months in advance).
- The EPS-A takes over the North Sea have all suffered from small to large amounts of sun/cloud glint. This could partially be overcome by developing methods and software for glint removal.

#### *Recommendations for continuation of the EPS-A and Satlantics evaluation*

It is recommended to do a final rehearsal with the EPS-A in summer 2002, in which care is taken to avoid all disturbances to the take. This final rehearsal will then provide the definitive insight into the potential of EPS-A for the support of MERIS validation. When accurate spectra are available from EPS-A both MIM and RMI should be tested to obtain concentration products. This is a result from the observation that the one-band semi-analytical algorithm used in this study does not compare well to Satlantics measurements (Hoogenboom) for the higher concentrations.



*A test case for satellite image processing*

As an illustration test case for the kind of products to be expected from MERIS RMI was used to process SeaWiFS images. The results were hopeful in the sense that independent TSM, TCHL and CDOM products seem to be feasible from satellite observations such as from MERIS. The results should however be seen as a rough approximation of MERIS results because of the coarse and sparse bandsettings of SeaWiFS. It was found that:

- A synthetic 705 SeaWiFS band could be estimated from SeaWiFS 667 nm and 765 nm bands.
- The mean North Sea SIOP that were used with RMI lead to overestimation of TSM in Dutch coastal waters and underestimation in Belgian coastal waters.
- Initial estimations of TSM can be improved by applying the updated set of SIOP to the POWERS one band TSM algorithm

*Conclusions of the validation along the Mitra transect*



- TCHL is in good agreement with the values obtained along the Mitra transect.
- TSM is in disagreement (SeaWiFS 6 May, Mitra 8-9 May) therefore it is recommended that the performance of the RMI method for TSM should be further evaluated.

*General RMI-SeaWiFS Conclusions:*

- The Ratio Matrix Inversion method for SeaWiFS performs reasonably well for North Sea applications, judged from observed ranges and patterns. Validation along transects was difficult due to a lack of synchronous in-situ observations. Preliminary comparisons using the Mitra transect revealed good agreement for TCHL and disagreement for TSM. TSM patterns over the North Sea seem to be in agreement with earlier observed patterns (Van der Woerd, 2000). As a definite check on algorithm performance it is recommended to do a rehearsal exercise in 2001 using EPS-A.
- TCHL conclusions and recommendations: The synthetic 704 nm band provides a reasonably robust solution for the CHL mapping problem. However, there remain some question marks. It appears that TCHL products are sensitive to errors in cloud masking which should be checked. Implementation of the RMI method for North Sea CHL detection using MERIS should be straightforward.
- TSM conclusions and recommendations: Initial estimations can be improved by recalibrating the POWERS algorithm using the mean North Sea SIOP set. The performance of the RMI method for TSM should be further evaluated by means of a sensitivity analysis. If necessary a combined approach using RMI for TCHL and e.g. MIM for TSM should be developed.
- CDOM conclusions and recommendations: In depth investigation could improve the quality of the CDOM map. Before doing this, the product should be discussed with experienced end-users to study whether it contains useful information and (when the product becomes a standard product) which form and accuracy it ultimately should have.



- From SIOP research it was concluded that scaling parameters such as B, Q and f are ill defined in various modelling approaches and observation formulations. Unification and quantification should lead to less confusion in this field.



## 9. Reference List

- Aas, E., (1987) Two-stream irradiance model for deep waters. *Appl. Opt.*, Vol. 26, p. 2095-2101.
- Aiken, J., G.F.T.C.C. Moore, S.B. Hooker, D.K. Clark, (1995) *The SeaWiFS CZCS type pigment algorithm*, Vol.29,
- Althuis, IJ.A., H. Buiteveld, (1996) Remote sensing toegepast voor waterbeheer. *H2O*, Vol. 29, No. 19, p. 586-588.
- Althuis, IJ.A., J. Vogelzang, M.R. Wernand, S.J. Shimwell, W.W.C. Gieskes, R.E. Warnock, J. Kromkamp, R. Wouts, W. Zevenboom, (1996) *On the colour of Case 2 waters: particulate matter North Sea: Part I-Results and conclusions*, BCRS 95-21A, BCRS, Delft, 161 p.
- Althuis, IJ.A., J. Vogelzang, M.R. Wernand, S.J. Shimwell, W.W.C. Gieskes, R.E. Warnock, J. Kromkamp, R. Wouts, W. Zevenboom, (1996) *On the colour of Case 2 waters: particulate matter North Sea: Part II-Instruments, methods and data base*, BCRS 95-21B, BCRS, Delft, 73 p.
- Babin, M., A. Morel, Fournier-Sicre V. et al. (2000) Scattering properties of case 2 water particles. Monaco,
- Bagheri, S. and A.G. Dekker. (1999) Remote Sensing of Nearshore Water Quality Using Bio-Optical Modeling and Retrieval Techniques. In: R.Green, editor. *9th JPL AVIRIS Workshop*, JPL/NASA, Pasadena, USA,
- Bricaud, A., M. Babin, A. Morel, H. Claustre, (1995) Variability in the chlorophyll-specific absorption coefficients of natural phytoplankton: Analysis and parameterization (Paper 95JC00463). *J. Geophys. Res.*, Vol. 100, No. Advances in Ocean Optics: Issues of Closure; C7, p. 13,321-13,332.
- Bricaud, A., A. Morel, L. Prieur, (1981) Absorption by dissolved organic matter of the sea (yellow substance) in the UV and visible domains. *Limnol. Oceanogr.*, Vol. 26, No. 1, p. 43-53.
- Carder, K.L., F.R. Chen, Z. Lee, S.K. Hawes, (1999) *MODIS Ocean Science Team Algorithm Theoretical Basis Document*, 19, 45 p.
- Cleveland, J.S. (2000) Inherent optical properties of coastal particles. *Ocean Optics XV, October 16-20*, Monaco.
- De Haan, J.F. and Kokke, J.M.M., (1996) *Remote sensing algorithm development Toolkit I: Operationalisation of atmospheric correction methods for tidal and inland waters*, NRSP-2 96-16, Netherlands Remote Sensing Board, Programme Bureau, Rijkswaterstaat Survey Department, Delft, The Netherlands, 91 p.
- Dekker, A.G., (1993) *Detection of optical water quality parameters for eutrophic waters by high resolution remote sensing*. PhD. Thesis, Vrije Universiteit, Amsterdam, The Netherlands; 240 p.
- Dekker, A.G., H.J. Hoogenboom, H. Volten, R. Schreurs, and J.F. De Haan. (1997) Angular scattering functions of algae and silt: an analysis of backscattering to scattering fraction. In: S.G. Ackleson and R. Frouin, editors. *Ocean Optics XIII*, SPIE, Bellingford, USA, p. 392-400.
- Doerffer, R. and H. Schiller. (1994) Inverse modelling for retrieval of ocean color parameters in Case II coastal waters: an analysis of the minimum error. In: J.S. Jaffe, editor. *Ocean Optics XII*, 6 -1994, SPIE, Bellingham, Washington, USA, p. 887-893.



- Doerffer, R., H. Schiller, (1997) *Pigment index, sediment and gelbstoff retrieval from directional water leaving radiance reflectances using inverse modelling technique. MERIS-Level 2 ATBD.*, PO-TN-MEL-GS-0005 12, 83 p.
- Gons, H.J., (1999) Optical teledetection of chlorophyll -a in turbid waters. *Environmental Science Technology*, Vol. 33, No. 7, p. 1127-1132.
- Gons, H.J., J. Ebert, J. Kromkamp, (1998) Optical teledetection of the vertical attenuation coefficient for downward quantum irradiance of photosynthetically available radiation in turbid waters. *Aquat. Ecol.*, Vol. 31, p. 299-311.
- Gordon, H.R., O.B. Brown, R. Evans, J. Brown, R.C. Smith, K.S. Baker, D.K. Clark, (1988) A semianalytical Radiance model of ocean colour. *J. Geophys. Res.*, Vol. 93(D9), p. 10,909-10,924.
- Gordon, H.R., O.B. Brown, M.M. Jacobs, (1975) Computed relationships between the inherent and apparent optical properties of a flat homogeneous ocean. *Appl. Opt.*, Vol. 14, No. 2, p. 417-427.
- Hakvoort, J.H.M., H. De Haan, R.W.L. Jordans, R.J. Vos, S.W.M. Peters, M. Rijkeboer, Towards airborne remote sensing of water quality in the Netherlands; validation and error analysis. [In Press] *Second EARSEL Workshop on Imaging Spectroscopy*, (2000)
- Hakvoort, J.H.M., (1994) *Absorption of light by surface water*. PhD. Thesis, Delft University Press;
- Hakvoort, J.H.M. and R. Doerffer. (1998) Optical closure for case II water. p. -8.
- Haltrin, V.I., G.W. Kattawar, (1991) *Light fields with raman Scattering and fluorescence in sea water*, Department of Physics, Texas A&M University, College Station, 74 p.
- Harkink, L., 1991, "Towards the operationalisation of NOAA/AVHRR products for the purpose of marine ecology research." BCRS report 91-09, PB-BCRS, Delft
- Hoogenboom, H.J., Roberti, J.R., Wernand, M. (2000), *An integral approach to retrieve total suspended matter in the Marsdiep (Netherlands)*, Proceedings of the Ocean Optics XV, October 16-20, 2000, Monaco
- Hoogenboom, H.J., (1999) *An analytical optical model for turbid waters*, RIKZ/IT99.119X, National Institute for Coastal and Marine Management/RIKZ, The Hague, The Netherlands, 31 p.
- Hoogenboom, H.J., A.G. Dekker, J.F. De Haan, (1997) *InveRSion: interpretation of reflectance spectra for water quality assessment*, W-97/05, IVM/VU, Amsterdam, The Netherlands, 83 p.
- Hoogenboom, H.J., A.G. Dekker, J.F. De Haan, (1998a) *InveRSion: assessment of water composition from spectral reflectance: a feasibility study to the use of the matrix inversion method*, NRSP-2 98-15, Netherlands Remote Sensing Board, Programme Bureau, Rijkswaterstaat Survey Department, Delft, The Netherlands, 48 p.
- Hoogenboom, H.J., A.G. Dekker, J.F. De Haan, (1998b) *MERIS data simulation for water quality applications in tidal and inland waters; a pilot study*, W98/12, Institute for Environmental Studies, Amsterdam, The Netherlands, 69 p.
- Joseph J., (1950) *Deutsche Hydrografische Zeitschrift*, Vol. 3, p. 324-335.
- Krawczyk, H., A. Neumann, Zimmerman G., and T. Walzel. (2000) 4 Years of MOS-IRS Mission: lessons learned for case-2 water with remote sensing from space. 16 -10 -2000, Monaco,
- Kromkamp, J., R. Wouts, (1998) *Particulate Matter North Sea Plus*, BCRS Report NRSP-98-04, BCRS, Delft, 62 p.



- Maffione, R.A. and D.R. Dana. (1997) Recent measurements of the spectral backward-scattering coefficient in coastal waters. *Ocean optics XIII*, SPIE, Bellingham, USA, p. 154-157.
- Marees, G., M.R. Wernand, (1991) *Interpretation of optical remote sensing data over coastal waters*, 91, BCRS, 105 p.
- Mobley, C.D., (1994) *Light and water; Radiative transfer in natural waters*, Academic Press, London,
- Mobley, C.D., (1995) *Hydrolight 3.0 Users' Guide - Final Report - March 1995*, SRI Project 5632, Contract N00014-94-C-0062, SRI International, 65 p.
- Mobley, C.D., (1999) Estimation of the remote-sensing reflectance from above-surface measurements. *Appl. Opt.*, Vol. 38, No. 36, p. 7442-7455.
- Morel, A., B. Gentili, (1991a) Diffuse reflectance of oceanic waters: its dependence on Sun angle as influenced by the molecular scattering contribution. *Appl. Opt.*, Vol. 30, No. 30, p. 4427-4438.
- Morel, A., B. Gentili, (1993b) Diffuse reflectance of oceanic waters. II. Bidirectional aspects. *Appl. Opt.*, Vol. 32, No. 33, p. 6864-6879.
- Morel, A., B. Gentili, (1996c) Diffuse reflectance of oceanic waters. III. Implication of bidirectionality for the remote-sensing problem. *Appl. Opt.*, Vol. 35, No. 24, p. 4850-4862.
- Nieuwenhuijzen, J.P., (1999) *Remote Sensing Optical Water Quality. Using neural networks for inversion of the bio-optical model.*, Vrije Universiteit Amsterdam, 101 p.
- Pasterkamp, R., S.W.M. Peters, M. Rijkeboer, A.G. Dekker, (1999) *RESTWES: Retrieval of total suspended matter concentrations from SPOT images*, W-99/33, IVM/VU, Amsterdam, The Netherlands, 45 p.
- Prieur, L., S. Sathyendranath, (1981) An optical classification of coastal and oceanic waters based on the spectral absorption curves of phytoplankton pigments, dissolved organic matter and other particulate materials. *Limnol. Oceanogr.*, Vol. 26, No. 4, p. 671-689.
- Rijkeboer, M., (1999) *Water Quality Parameters, inherent optical properties and reflectance spectra obtained in Lake Veluwemeer (26-5-1999)*, W-99/35, IVM, Amsterdam, 17 p.
- Rijkeboer, M., (2000a) *Water Quality parameters, inherent optical properties and reflectance spectra obtained in Marsdiep (22/23 may 2000)*, W-,
- Rijkeboer, M., (2000b) *Water quality parameters, inherent optical properties and reflectance spectra obtained in Belgica Campaign 2000/11*,
- Rijkeboer, M., (2000c) *Water Quality parameters, inherent optical properties and reflectance spectra obtained in coast zone North Sea (MITRA: 8/9 may 2000)*,
- Rijkeboer, M., A.G. Dekker, (1999) *Kleuranalyse van Nederlandse wateren ten behoeve van waterkwaliteitsonderzoek*, 99/12, ISBN 90 5773 044 8
- Rijkeboer, M., A.G. Dekker, H.J. Gons, Optical classification of Dutch inland waters. [In Press] *Verh. Internat. Verein. Limnol.*, (1999)
- Rijkeboer, M., A.G. Dekker, H.J. Hoogenboom, (1998) *Reflectance spectra with associated water quality parameters measured in Dutch waters (SpecLib-TK-database)*, E98/12, 18 p.
- Rijkeboer, M., H.J. Hoogenboom, A.G. Dekker, (1997) *Realisatie spectrale bibliotheek van Nederlandse wateren*, W-97/07, 48 p.



- Rijkeboer, M., R. Pasterkamp, S.W.M. Peters, (1999) *Voorbereidende studie voor de implementatie van een spectroradiometrische veldmeetmethode voor het monitoren van optische waterkwaliteitsparameters*, 0-99/09, IVM, Amsterdam, 51 p.
- Roesler, C.S., (1998) Theoretical and experimental approaches to improve the accuracy of particulate absorption coefficients derived from the quantitative filter technique. *Limn. & Oceanogr.*, Vol. 43, p. 1649-1660.
- Roesler, C.S., M.J. Perry, K.L. Carder, (1989) Modeling in situ phytoplankton absorption from total absorption spectra in productive inland marine waters. *Limnol. Oceanogr.*, Vol. 34, No. 8, p. 1510-1523.
- Roozekrans, J.N. and Prangma, G.J., 1992, "Observatie van het aard-atmosfeer-systeem door de NOAA-satellieten (ontvangst, productie, toepassing en gebruik van de NOAA-data).", BCRS-report 92-02, PB-BCRS, Delft
- Ruddick, K.G., F. Ovidio, M. Rijkeboer, (2000) Atmospheric Correction of SeaWiFS Imagery for Turbid Coastal and Inland Waters. *Appl. Opt.*, Vol. 39, No. 6, p. 897-912.
- Ruddick, K.G., F. Ovidio, A.P. Vasil'kov, C. Lancelot, V. Rousseau, and M. Rijkeboer. (1998) Optical remote sensing in support of eutrophication monitoring in Belgian waters. *Earsel conference on "Operational remote sensing for sustainable development"*, 98 A.D., Earsel, Enschede,
- Van der Woerd, H., J.H.M. Hakvoort, H.J. Hoogenboom, Omtzigt N., R. Pasterkamp, S.W.M. Peters, K.G. Ruddick, De valk C., R.J. Vos, (2000) *Towards an operational monitoring system for turbid waters*, 0-00/16, IVM\VU Amsterdam, 62 p.
- Vos, R.J., M. Schuttelaar, (1995) *RESTWAQ; Data assessment, data-model integration and application to the Southern North Sea*, NRSP-2 95-19, BCRS, Delft
- Vos, R.J., Villars, M., Roozekrans, J.N., Peters, S.W.M., and Van Raaphorst, W, (1998) *RESTWAQ 2, Part I. Integrated monitoring of total suspended matter in the Dutch coastal zone*, NRSP-2 98-08, BCRS, Delft
- Vos, R.J., (2000) *Monitoring of Algal Blooms in Lake IJssel with remote sensing*, 0-00/18, IVM, Amsterdam, 52 p.
- Vos, R.J., S.W.M. Peters, M. Rijkeboer, (1999) *Validation and error analysis of retrieval of water quality parameters from field spectra for inland waters*, W-99/48, IVM\VU Amsterdam, The Netherlands, 45 p.
- Vos, R.J., M. Villars, H. Roozekrans, S.W.M. Peters, W.v. Raaphorst, (1998) *RESTWAQ2, Part 1. Integrated monitoring of total suspended matter in the Dutch Coastal Zone*, NRSP-2 98-08, Netherlands Remote Sensing Board, Delft, 44 p.
- Walker, R.E., (1994) *Marine light field statistics*, Wiley, New York, 675 p.
- Weeks, A.R. and M. Darecki. (2000) *A semi-empirical model of optical properties for turbid coastal waters*. Proceedings of Ocean Optics XV, October 16-20, Monaco.
- Wernand, M.R., Hoogenboom, H.J. and Regeling, G.M., (2000) *Ferry-monitoring of suspended solids through coastal colour radiometry*, Proceedings of Ocean Optics XV, October 16-20, Monaco.
- Wernand, M.R., H.J. Hoogenboom, (1999) *Optische instrumentatie voor het meten van de kleur van water*, RIKZ/IT99.136X, Rijksinstituut voor Kust en Zee/RIKZ, 39 p.



Yentsch, C.S., (1994) Why is the measurement of fluorescence important to the study of biological oceanography? In: Spinrad, R.W., K.L. Carder, M. Perry (Eds.), *Ocean Optics*, New York, Oxford University Press,



## Appendix I. Contents of the MERIMON CD-Rom

The MERIMON-2000 CD-Rom was distributed amongst all project partners and can be requested at ivm: [steef.peters@ivm.vu.nl](mailto:steef.peters@ivm.vu.nl). It contains the following directories:

Data:	data files from the cruises Belgica, Mitra, Navicula and PMNS
Documents:	other documents
IOP_variability:	files on the variability of SIOP
Management:	files concerning project management
Merimon html:	html pages from the Mitra cruise
Mersops:	files concerning the Mersopsproject proposal
Ocean Optics XV:	files related to the Ocean Optics XV paper by Hoogenboom (RIKZ)
Pictures:	some photo's, (stored as .jpg files), mostly related to the Satlantic and TESO project
Presentations:	power point presentations of the project



## Appendix II. Instrumentation and techniques for close range and remote (above water) $R(0-)$ measurements

### II.1 The GONS PR650 method

#### II.1.1 Description of the system

Since a number of years experience has been gained with the above water measurement of subsurface irradiance reflectance (Gons, 1999, Rijkeboer et al., 1999 etc.). In all mentioned studies a single instrument was used to measure  $R(0-)$  spectra, namely the Photo Research (Chatworth, CA, USA) model PR-650 portable telephotometer/colorimeter. This instrument includes 1<sup>0</sup> measuring optics and holographic grating, 128-element diode-array spectrometer that acquired spectra from 380 to 780 nm. The full-width half-maximum bandwidth is 8 nm. The integration time was automatically selected. At each measurement cycle a dark current measurement of equal duration is automatically subtracted. The manufacturer calibrates the instrument regularly. See Gons (1999) for details on the method (See Figure II.1).



Figure II.1: Measurements with the Photo Research (Chatworth, CA, USA) model PR-650 portable telephotometer/colorimeter.



## II.1.2 Measurement sequence/protocol

The water-leaving radiance ( $L_{au}$ ) and the downward radiance of skylight ( $L_{sky}$ ) are scanned at a nadir and a zenith angle of  $42^\circ$ , respectively. The angle of  $42^\circ$  is used to avoid influence by reflection and shading from the boat. The measured water-leaving radiance includes reflected sky light. This can be corrected using the observation of the sky radiance ( $L_{sky}$ ). In order to calculate downward radiance ( $E_{ad}$ ) and discriminate between direct sunlight and the diffuse irradiance, radiance is measured from a calibrated reflectance panel before ( $L_{rp}$ ) and after shading ( $L_{rpd}$ ). For both practical and theoretical reasons the chosen direction of observation is  $90^\circ$  to the plane of the sun. Each scan involves 10 measurement cycles of which the average was filed. Usually three complete series of scans are done, which in general takes less than 3 minutes.

## II.1.3 The Gons PR650 method: theory

From the light measurements above the water surface, the subsurface irradiance reflectance  $R(0^-)$ , i.e. the ratio of upward ( $E_{wu}$ ) and downward irradiance ( $E_{wd}$ ) just beneath the water surface, can be computed (Gons, 1999). Calculation of the subsurface irradiance reflectance  $R(0^-)$  was carried out according to

$$R(0^-) = \frac{Q \cdot f \cdot (L_{au} - r_{sky} \cdot L_{sky})}{(E_{ad} - r_\Theta (1 - F) \cdot E_{ad} - r_{dif} \cdot F \cdot E_{ad}) + 0.5 \cdot E_{wu}} \quad (II.1)$$

The measured parameters are  $L_{au}$ ,  $L_{sky}$  and  $E_{ad}$ .

$Q$  = the conversion coefficient for  $L_{wu}$  to  $E_{wu}$ ,

$f$  = the conversion constant of  $L_{au}$  to  $L_{wu}$ ,

$L_{au}$  = the upward radiance above the water at nadir angle of  $42^\circ$ ,

$L_{wu}$  = the upward radiance just below the water surface,

$L_{sky}$  = the radiance of skylight at zenith angle of  $42^\circ$ ,

$r_{sky}$  = the Fresnel reflectance coefficient at zenith angle of  $42^\circ$ ,

$E_{ad}$  = the downward irradiance just above the water,

$E_{wu}$  = the downward irradiance just below the water surface,

$r_\Theta$  = the Fresnel reflectance coefficient for sunlight,

$r_{dif}$  = the Fresnel reflectance coefficient for diffuse light,

$F$  = the fraction diffuse light of  $E_{ad}$ .

Equation 2.14 essentially is a combination of equations 2.9, 2.10 and 2.11. In the standard processing (Rijkeboer et al., 2000) the value of the geometric parameter  $Q$  is calculated according to Gons (1999). Whereby  $Q$  is depending on solar angle and the ratio between total and diffuse downwelling light. For the value of  $r_{sky}$  the modelled



value of 0.0293 is used (Gons, 1999). Further the values  $f = 1.84$  for seawater (Austin, 1980), and  $r_{\text{dif}} = 0.06$  (Jerlov, 1976) are applied for North Sea measurements. The Fresnel reflectance coefficient for sunlight ( $r_{\theta}$ ) is calculated from Julian day, time and geographical position. The downward irradiance just above the water ( $E_{\text{ad}}$ ) was obtained by measuring the radiance from a calibrated reflectance panel. The fraction diffuse light ( $F$ ) was the ratio between  $E_{\text{ad}}$  measurements obtained from the reflectance panel before ( $Lr_p$ ) and after shading ( $Lr_{\text{pd}}$ ).

## II.2 The PMNS PR650/PR640 method

As documented in the PMNS-part II report (Althuis et al., 1996), the PR650 can also be used to measure upwelling radiance from a nadir measurement. The PMNS method further includes a second PR650 fitted with a cosine receptor, which is used to measure above water downwelling irradiance. Both terms can subsequently be used to calculate the remote sensing reflectance. PMNS suggests a Q factor of 5 to convert remote sensing reflectance to  $R(0-)$ . Note that most PMNS algorithms are defined as ratios of spectral bands. This means that algorithm performance is independent of the choice for Q.

### II.2.1 Measuring above water Transect $R(0-)$ using the Satlantics instrument on board of the TESO Ferry (adapted from Wernand et al., 2000)

#### *System set-up*

A Satlantic radiometer unit was experimentally mounted on the TESO-ferry between Texel and Den Helder by NIOZ in spring 2001. The objective was to study the possibilities to monitor mainly TSM over transects using above water measurements of the remote sensing reflectance. In 2001 an experimental set-up was installed consisting of amongst others the radiometer, a GSM hook up at the Ferry and a receiving station with processing software at NIOZ. The experiment was conducted within the framework of the NIOZ/RIKZ "TESO" project. The MERIMON project was allowed to study some of the data to analyze the possibilities for future use for MERIS validation.

The Satlantic radiometer (OCR/I 200) unit consists of an upwelling radiance sensor  $L_w$  (7 spectral bands), a downwelling irradiance sensor  $E_s$  (4 spectral bands) and a sky radiance sensor  $L_{\text{sky}}$  (5 spectral bands) (See Table 9.1)

Lup	Lsky	Es
412	412	412
442	442	442
620		
512		
561	561	
664	664	664
780	780	780



*Table 9.1 Year 2000 Spectral configuration of the TESO-Satlantic set-up.*

The availability of a maximum of 16 output AD-channels made that the sensors differ in the number of bands. As this system is still in a testing phase the missing bands at the moment are reconstructed. In 2001 the system will have the same number of bands per sensor. The 7 bands derive enough information on the specific spectral signature of the upwelling radiance and downwelling irradiance over coastal and oceanic waters.

The bands used are similar to the MERIS sensor bands but for  $L_w$  only. The upwelling radiance sensor is mounted at the South side of the ferry facing the East and pointed at an angle of 40 degrees towards the sea surface. The sky radiance sensor is mounted in the same direction looking towards the sky making an angle of 90 degrees with the upwelling sensor. The downwelling irradiance sensor measures the incoming solar irradiance through cosine collectors. All sensors are individually mounted in anti-shock mounts to avoid the constant vibrations. The best way to measure the above water radiance  $L_w$  is to point the radiometer to the sea surface at an angle of about 35° to 40° and away from the sun's azimuth by at least 90°. This is of course in the ideal situation. As the system is mounted in a steady position the morning azimuth angles are >90° and in the afternoon <90°. In this arrangement during a short period, when the sun is in the Southeast, the down looking sensor can detect direct surface glint. These data will be neglected.

#### *Data acquisition and telemetry*

A GPS system gives latitude and longitude information. After each North-South crossing the data is sent via GSM to NIOZ. Depending on the height of the sun the unit starts measuring at 07.05 UTC and is stopped at 15.30 UTC. Data are only collected during the Texel-Den Helder (North-South) track at the bow of the ferry to avoid any reflectance due to sea surface foam caused by the propellers of the ferry itself.

#### *Data processing*

Next the data is converted into radiometric units. From the ratio upwelling radiance  $L_w$  and downwelling irradiance  $E_s$  the remote sensing reflectance  $R_{rs}$  is calculated.

However the missing  $E_s$  bands (due to the max. availability of a total of AD-channels) at 512, 561 and 667nm have to be reconstructed first before the  $R_{rs}$  can be calculated for all existing  $L_w$  bands which is done via multiple regression analyses using historical datasets (Wernand, 2000).

After a sunglint correction, subtracting the  $R_{rs}$  at 752nm from all calculated reflectance data, the PMNS-TSM algorithm (which was applied successfully on different types of European coastal waters by Wernand *et al*, 1998 is applied for each crossing.

#### *Some recommendations by Wernand (2000):*

- 1) The number of bands for each type of sensor should be the same
- 2) A TSM validation has to be performed by in-situ sampling from the ferry.



- 3) Re-calibration of all sensors should be performed monthly to note any degradation
- 4)  $L_{sky}$  should be taken into account

### II.3 The EPS-A scanner on board of the on board of the RWS/NS airplane

#### *System set-up*

The EPS-A (Environmental Probe System-A) is an imaging scanner owned by the Directorate General of Public Works and Water Management. The instrument is mounted in the Remote Sensing airplane of the North Sea Directorate. This way exploitation costs are kept as low as possible, for example no stand by costs do occur.

The EPS-A is an imaging scanner of the Kennedy type. It measures radiance in a 2.3mrad instant field of view. The swath angle of the EPS-A is 80 degrees, (40 to -40), at right angle to the flight direction. By changing the scan speed of the EPS-A and the flight altitude a nadir pixel size between 1.5 and 8.5m can be obtained. All pixels are square. The smaller pixel size is limited by the maximal scan speed of the instrument, about 50 scans seconds. The size of a large pixel is limited by the maximum flight height, 10000ft.

#### *Spectral band settings*

The scanner detects radiance at 72 bands in the VIS/NIR region (400-1000nm), two bands in the IR (1600 and 2200nm) and one band in TIR (4500nm). Spectral band settings depend on the selected application (e.g. water quality or vegetation mapping; see Table 9.2).

*Table 9.2 Spectral bands of the EPS-A used for water quality applications. The instrument has two modes, normal resolution (about 11nm band width) and high resolution (7nm band width).*

Wavelength centre			
normal	High	normal	High
395.4	460.1	675.9	655.7
405.9	466.9	685.5	662.2
414.4	473.7	695	668.6
431.3	487	704.6	675.2
459.5	506.7	714.4	681.7
488.3	526.3	724	688.2
516.1	545.9	753.3	708.1
544.2	565.3	762.8	714.7
563	578.3	783	728



600.6	604.1	865	782.5
619.5	617.1	928.6	824.7
629	623.7	995.1	869.4
647.6	636.4	1700	1700
666.5	649.2	2200	2200

The noise equivalent radiance is used to recalculate the measured signal into absolute radiance. It determines the maximal possible discrimination in reflectance values. And, subsequently, also the number of classes in algae concentration, total suspended matter and dissolved organic matter. The signal to noise ratio per wavelength band depends on the scan speed of the EPS-A and the light intensity. At increasing scan speed the signal to noise ratio will decrease.

The signal detected by the EPS-A is stored in counts. To convert the counts into absolute radiance intensity a calibration equation is used requiring some system specific parameters such as the scan rate and count2rad, which is the calibration value.

The radiance at sensor is recalculated to reflectance above the surface, using MODTRAN4 imbedded in TOOLKIT (de Haan et al (1999)).

After conversion into R(0-) algorithms can be applied to calculate TSM, CHL and CDOM concentrations. The standard algorithm is of the Matrix Inversion type (Hakvoort et al., 2000).

#### *Use in MERIMON*

The MERIMON project was granted access to EPS-A flights to study the performance of the instrument over the North Sea for water quality analysis, to study the potential of the instrument for MERIS validation and to study the possibility to up-scale point measurements to the scale of MERIS.

## **II.4 The MERIS instrument (textual information mainly extracted from the MERIS website)**

### *General specifications*

MERIS is a programmable, medium-spectral resolution, imaging spectrometer operating in the solar reflective spectral range. Fifteen spectral bands can be selected by ground command, each of which has a programmable width and a programmable location in the 390 nm to 1040 nm spectral range.

The MERIS instrument has the following characteristics that meet many of the performance requirements for remote sensing of water quality parameters in coastal- and inland waters:

- In high-resolution mode a spatial resolution up to 300m x 300 m pixels; in low-resolution mode a spatial resolution of 1200m x 1200 m pixels.



- High radiometric accuracy and sensitivity required for water quality parameter assessment
- High spectral resolution: water with a complex composition of constituents requires flexible and precise spectral band positions for reliable estimations of water quality parameters.

#### *Spatial and temporal resolution*

The instrument's 68.5° field of view around nadir covers a swath width of 1150 km. The Earth is imaged with a spatial resolution of 300 m (at nadir). This resolution is reduced to 1200 m by the on board combination of four adjacent samples across track over four successive lines. The sensor will revisit the same area at approximately 3-day intervals. It is anticipated (based on experiences with SeaWiFS) that MERIS will deliver 18 to 30 good images of the Dutch coastal waters per year. Within one scene most of the Dutch inland and coastal waters can be covered. This means that MERIS constitutes monitoring potential for Lake IJsselmeer, Markermeer, Randmeren, the large Frisian lakes and the tidal waters in Zeeland and Waddenzee. In the North Sea, Waddenzee and IJsselmeer a reduced spatial resolution of 1200x1200 m (global mode) may suffice (Hoogenboom, 1999).

#### *Radiometric resolution*

MERIS has a dynamic range up to an albedo of 1 enabling monitoring of land surfaces that have relatively high reflectances compared to water surfaces. In the upper layer of the open ocean, the chlorophyll concentration varies from less than 0.03 mg m<sup>-3</sup>, in the oligotrophic waters, up to about 30 mg m<sup>-3</sup> in eutrophic situations. To this variation, which spans over 3 orders of magnitude, the watercolor responds in a non-linear way. The goal of MERIS is to discriminate 30 classes of pigment concentrations within the three orders of magnitude. The classes should be of equal logarithmic width. This requirement is translated into a radiometric sensitivity of  $2 \times 10^{-4}$  for NEAR (noise equivalent spectral reflectance at the sea level) set for MERIS.

#### *Spectral resolution*

MERIS is specifically designed for the assessment of marine phenomena. It has fifteen spectral bands for which, in principle, positions and widths can be programmed. However ESA has defined a pre-launch fixed bandset (Table 9.3), to which still small changes can be applied.



*Table 9.3 The MERIS bands as specified for ocean applications (ENVISAT website) were used in this study.*

<b>MDS Nr.</b>	<b>Band centre (nm)</b>	<b>Bandwidth (nm)</b>	<b>Potential Applications</b>
1	412.5	10	Yellow substance, turbidity
2	442.5	10	Chlorophyll absorption maximum
3	490	10	Chlorophyll, other pigments
4	510	10	Turbidity, suspended sediment, red tides
5	560	10	Chlorophyll reference, suspended sediment
6	620	10	Suspended sediment
7	665	10	Chlorophyll absorption
8	681.25	7.5	Chlorophyll fluorescence
9	705	10	Atmospheric correction, red edge
10	753.75	7.5	Oxygen absorption reference
11	760	2.5	Oxygen absorption R-branch
12	775	15	Aerosols, vegetation
13	865	20	Aerosols corrections over ocean
14	890	10	Water vapour absorption reference
15	900	10	Water vapour absorption, vegetation

The exact position of the MERIS spectral bands will be determined following a detailed spectral characterization of the instrument.

The spectral range is restricted to the visible near-infrared part of the spectrum between 390 and 1040 nm. The spectral bandwidth is variable between 1.25 and 30 nm depending on the width of a spectral feature to be observed and the amount of energy needed in a band to perform an adequate observation. Over open ocean an average bandwidth of 10 nm is required for the bands located in the visible part of the spectrum. Driven by the need to resolve spectral features of the Oxygen absorption band occurring at 760 nm a minimum spectral bandwidth of 2.5 nm is required.



*Standard concentration products (based on the MERIS ATBD: Doerffer et al, 1997)*

The new-generation ocean colour sensors such as the Medium Resolution Imaging Spectrometer (MERIS) are potentially capable of supplying end users with accurate water quality maps and derived products. The improved spectral, radiometric and spatial resolution of MERIS will enable retrieval of chlorophyll-a (CHL) and seston dry weight (DW) in coastal and inland waters. The accuracy with which CHL and DW can be determined from MERIS depends mainly on an accurate atmospheric correction and the appropriate water quality algorithm. Much research has been carried out on case I (ocean) waters but relatively little is known about the performance of MERIS in the optically complex case II waters.

The standard concentration products that are under development for MERIS are:

1. Phytoplankton pigment index expressed as chlorophyll-a concentration, unit:  $\mu\text{g/l}$
2. Non-absorbing suspended particle concentration (NSP), unit:  $\text{mg/l}$
3. *Gelbstoff* (yellow substance) absorption at 440 nm, unit:  $\text{m}^{-1}$

The spectral channels of MERIS enable that other variables may be retrieved in addition or as an alternative, but this extension has not yet been investigated:

- The organic fraction of suspended matter,
- Separation of two types of yellow substance, originating from rivers or produced in the ocean and differing in their spectral exponents,
- "Red Tides", which are plankton blooms which discolor the water by carotinoids
- Quantum efficiency of the sunlight stimulated fluorescence when including the fluorescence channel at 682 nm.

*Additional radiometric accuracy requirements for coastal waters (MERIS website)*

For a detection of several water substances, commonly used techniques like simple colour ratios, although successfully applied for open oceans, are not sufficient. The similarity of the spectral scattering and absorption coefficients for all optically active water substances poses problems for finding an adequate procedure for their detection. Here the sun-stimulated chlorophyll fluorescence at a wavelength of 681.25 nm can improve the detection of pigment concentration. The fluorescence signal is small, but detectable from satellite. The desired spectral resolution is about 5 nm and the radiometric resolution has to be better than  $0.03 \text{ Wm}^{-2}\text{sr}^{-1}\text{mm}^{-1}$  for a discrimination of  $1\text{mg/m}^3$  pigment concentration



## Appendix III. Some candidate algorithms for water quality detection using MERIS

### III.1 Semi-empirical algorithms

#### III.1.1 PMNS (Althuis et al., 1996)

##### *Introduction*

From the PMNS project several band-ratio algorithms and multi-regression algorithms (MRA) to bands and band-ratio's for SeaWiFS and MERIS were established by fitting  $R(0-)$  band-ratio's to collected field data. For each water quality parameter (TSM, TCHL and CDOM with TCHL including Chlorophyll-a,b,c and phaeopigments) such algorithms are given. In PMNS all  $R(0-)$  are first corrected for a possible bias by the atmosphere or the sea-water interface (sky and sun glint) by subtraction of the  $R(0-)$  at 752 nm (SeaWiFS) or 753.75 nm (MERIS).

Band-ratio's: algorithms were found to give a good performance in case one water quality parameter dominates the reflectance. However, performance is less good in typical Case 2 situations. Full subtraction of the 750 nm band is questionable for turbid waters (Vos et al., 1998), (Ruddick et al., 2000), but errors are probably compensated by the fit parameters.

Correlation coefficients for the fit using 'all PMNS data' are 0.8 for TSM, 0.5 for CHL and 0.6 for CDOM.

##### *PMNS - TSM*

The TSM algorithm uses 2 bands (560 and 620nm) and for MERIS this gives:

$$TSM (mg / l) = 53.14 R'(0-, \lambda_1, \lambda_2)^{-2.58} \quad (III.1)$$

With  $\lambda_1 = 560$  and  $\lambda_2 = 620$  and

$$R'(0-, \lambda_1, \lambda_2) = \frac{(R'(0-, \lambda_1) - R(0-, 754))}{(R'(0-, \lambda_2) - R(0-, 754))} \quad (III.2)$$

For the months June and July the TSM algorithm leads to poor fits and to concentrations that are out of the range. For months with good fits, there is rather a large spread in the power function, which makes that accuracy of the algorithm is questionable.

##### *PMNS - CHL*

CHL uses 665nm and 705 nm in correspondence with many semi-empirical CHL algorithms (Dekker, 1993b), (Gons, 1999):



$$CHL(\mu g / l) = 22.33R'(0-, 665, 705)^{-2.85} \quad (III.3)$$

Spread in fitted parameters for the various cruises makes that accuracy of this algorithm is questionable.

PMNS also gives results based on *multiple regression analysis* using  $R(0-\lambda)-R(0-, 754)$  at 2 to 4 wavelengths. Correlation coefficients are in the order of 0.8 for TSM, 0.7 for CHL and 0.5 for CDOM.

A better algorithm with MRA for CHL was obtained after normalisation of  $(R(0-\lambda) - R(754))$  with  $((R(0-\lambda) - R(520)))$ . In fact this is *MRA of band-ratio's* and the correlation coefficient increases to 0.8. This CHL algorithm (which was not further used in the Netherlands until now) performs remarkably better than the red-colour ratio CHL algorithm. It is given by:

$$CHL(\mu g / l) = 4.2 - (13.3R''(0-, 560)) + (86.6R''(0-, 620)) - (143.4R''(0-, 664) + (62R''(0-, 680))) \quad (III.4)$$

With:

$$R''(0-, \lambda) = \frac{(R(0-, \lambda) - R(0-, 754))}{(R(0-, 520) - R(0-, 754))} \quad (III.5)$$

For Chlorophyll retrieval it was proved that band-ratio's perform better than other algorithms (Dekker, 1993a). A similar algorithm is available for CDOM with correlation coefficient of 0.65.

Some of the PMNS algorithms (at least those shown here) are tested within the present project.

#### *POWERS TSM algorithm*

For the DUP-POWERS project an effort was made to choose an optimal SIOP model based on the concentration ranges found in the PMNS project. The reflectance in band 5 of SeaWiFS was calculated by forward modeling using different sets of SIOP, keeping  $f$  fixed at 0.38. Three SIOP sets were tested (see also appendix II)

1. The set of SIOP measured by H.Hakvoort and Doerffer (1998) for the Dutch North Sea (near shore). The backscattering at band 5:550 nm, which was not measured, is found by linear interpolation.



2. The average set of SIOP measured during the Belgica cruise in 1995. The scattering by phytoplankton pigments is assumed to be zero, the backscatter to scatter ratio of TSM is taken as 0.03.
3. The average set of SIOP found for the Western Scheldt estuary in the scope of the RESTWES project.

From simulations the following conclusions were drawn:

1. Using the SIOP set 1 will give good results for the month May, but will give seriously higher concentrations in February and September compared to the PMNS database. This might be due to a fast saturation in band 5.
2. Using the SIOP set 2 will give lower concentrations in May and higher concentrations for February and September compared to the PMNS database.
3. Using set 3 will give good results for the months February and September, but will give seriously lower concentrations in May compared to the PMNS database.

Following these considerations, the set obtained during the Belgica cruise in 1998 will give the best overall result.

Finally the TSM algorithm was defined as a one band semi-analytical algorithm (inversion of the Gordon model; fixed values for CDOM and CHL):

$$TSM = \frac{-(a_w + a_{pig}^* chl + a_g^* g_{440}) \frac{R}{f} + b_{bw} (1 - \frac{R}{f})}{a_{TSM}^* \frac{R}{f} - b_{TSM}^* (1 - \frac{R}{f})} \quad (III.6)$$

When substituting the Belgica '98 SIOP, a  $g_{440}$  of  $0.34m^{-1}$  an  $f$  of 0.38 and an average CHL concentration of  $5mg\ m^{-3}$  and using  $R(0-)$  from SeaWiFS band 5, TSM can be found from:

$$TSM = \frac{-0.530 \cdot R(0-)_{555} + 0.001}{0.0304 \cdot R(0-)_{555} - 0.0058} \quad (III.7)$$

The mean error introduced by the variability in CHL concentrations was found to be 16%. As a check the algorithm was applied to reflectances in band 5 of selected SeaWiFS images, to see how the TSM results compare to the values in the PMNS database. It was found that the log-average of the SeaWiFS TSM distribution is 4.38 mg/l, comparable to the log-average of the PMNS database of 4.66 mg/l.

The TSM algorithm was subsequently used in the DUP project POWERS (Van der Woerd et al., 2000) to process of one year of suitable SeaWiFS images. Resulting monthly mean concentrations were validated using twenty year mean monthly averaged data for the Belgian coast from one of the project partners (MUMM) and was found to



give accurate values in case TSM is not too high. For very turbid waters the algorithm might work well but this could not be concluded from the in-situ data since these showed a very large variability for such circumstances.

## III.2 Analytical algorithms

### III.2.1 Introduction

One of the opportunities that has led to the development of matrix inversion and other analytical algorithms is the fact that modern (hyper spectral) remote sensing provides a system where the number of observations can be much larger than the number of unknowns. In practice, the number of unknowns is 2 or 3 (TSM and TCHL and sometimes CDOM), whereas the number of *observations* for  $R(0-)$ , depending on the type of sensor may vary from 1 (POWERS TSM algorithm Van der Woerd, 2000), 9 or 10 (MERIS), 20 (EPS-a scanner) to 88 (PR 650 spectroradiometer).

Analytical models all use as input subsurface irradiance reflectance spectra:  $R(0-, \lambda)$  and the specific inherent optical properties (SIOP), and can be used for determination of the following water quality parameters:

1. TSM (Total Suspended Matter, also called Seston Dry Weight, in mg/l);
2. TCHL (Total Chlorophyll, in  $\mu\text{g/l}$ ) or CHL-a
3. CDOM (Coloured Dissolved Organic Matter), expressed in absorption ( $\text{m}^{-1}$ ) at 440nm.

It is expected that future applications of analytical models will include parameters such as: the blue algal pigment cyanophycocyanine, separation of the organic and inorganic component of suspended matter and e.g. the red tide algal pigments

#### *Analytical algorithm types*

The most common methods for retrieval of water quality parameters on basis of analytical algorithms are:

- Matrix inversion (Hoogenboom et al., 1998a); (Hakvoort et al., 2000);
- Principle component analysis (Krawczyk et al., 2000);
- Neural networks (Nieuwenhuijzen, 1999) ;
- Non-linear regression methods other than neural networks (Hoogenboom et al., 1998a), (Vos et al., 1999);
- Multiple linear regression.

A new analytical algorithm is the Ratio Matrix Inversion algorithm presented in this report.

Most of these methods use a statistical principle to reduce (by elimination and combination) the number of input spectral bands to the number of unknowns. This can e.g. be the '*maximum likelihood principle*' (leading to the minimization of least squares sum of differences between modelled and observed  $R(0-)$ 's) or principal components type of solutions.



### III.2.2 The standard Matrix Inversion Method (MIM) as used for EPS-A processing

$R(0^-)$  can be calculated by the simple reflectance model suggested by Gordon whereby the constant  $f$  is chosen to be 0.33 but may vary due to solar and viewing geometry (Walker formulation, eq 2.1). The model assumes an optically deep medium so that bottom effects can be ignored. Also stratification in the water column and inelastic scattering effects, such as Raman scattering and fluorescence are ignored. The absorption and backscattering coefficients are expressed as follows:

$$a = a_w + a_{CHL}^* \cdot CHL + a_{TSM}^* \cdot TSM + a_{CDOM}^* \cdot CDOM \quad (III.8)$$

$$b_b = b_{b,w} + b_{b,TSM}^* \cdot TSM \quad (III.9)$$

No scattering for CDOM and chlorophyll- $a$  is assumed. Substitution of equations (III.8) and (III.9) into equation 3 yields

$$R(0^-) = f \cdot \frac{b_{b,w} + b_{b,TSM}^* \cdot TSM}{a_w + b_{b,w} + a_{CHL}^* \cdot CHL + (a_{TSM}^* + b_{b,TSM}^*) \cdot TSM + a_{CDOM}^* \cdot CDOM} \quad (III.10)$$

This equation provides an explicit relationship between the SIOP, the concentrations of the water constituents and  $R(0^-)$ . To determine the concentrations from  $R(0^-)$  the equation is rewritten as a linear system of equations: with

$$Ax = y \quad (III.11)$$

Where A is defined by:

$$A = \left( \frac{R(0^-)}{f} \cdot a_{CHL}^* \right)_{\lambda=1..n} \quad \frac{R(0^-)}{f} \cdot [a_{TSM}^* + b_{b,TSM}^*] - b_{b,TSM}^* \quad \left( \frac{R(0^-)}{f} \cdot a_{CDOM}^* \right)_{\lambda=1..n} \quad (III.12)$$

and y is defined by:

$$y = \left( -\frac{R(0^-)}{f} [a_w + b_{b,w}] + b_{b,w} \right)_{\lambda=1..n} \quad (III.13)$$

and x is the concentration vector:

$$x = \begin{pmatrix} CHL \\ TSM \\ CDOM \end{pmatrix} \quad (III.14)$$

Thus, to estimate the unknown concentrations the linear equations can be solved with a least square approach using  $A^T \cdot A \cdot x = A^T \cdot b$  where  $A^T$  is the transpose of A. This can be done if observations of  $R(0^-)$  are available at minimal 3 wavelengths, the SIOP are known and a value for  $f$  is chosen.



### III.2.3 Ratio Matrix Inversion: Rationale

Matrix Inversion has shown to give good results for TSM (Vos et al., 1999). The weakness of this method is that  $f$  has to be accounted for fully. The method is sensitive to "white errors" where e.g. errors in the atmospheric correction give spectra that are either too high or too low over the entire range. For CHL the results have been disappointing. E.g. for the lake IJssel alternative approaches had to be developed where TSM was determined using MIM, after which CHL was determined using a one band analytical inversion of the Gordon model (two step approach, Vos, 2000).

On the other hand there is a long record of ratio-based algorithms that have proven to be very successful for the determination of pigment concentrations (Dekker, 1993; Gons 1999 and for the North Sea recently Gons, 2000).

Therefore a combination of both approaches was sought for in this project and found in the form of the Ratio Matrix Inversion method (RMI). This method may be used to derive TSM, CHL and CDOM concentrations from spectral observations of instruments such as (but not limited to) PR650, EPS-A, SeaWiFS and MERIS. RMI combines the advantages of ratio algorithms (stability, robustness etc) with the advantages of matrix inversion: all spectral bands can be used, the approach is fully analytical and easy to adapt for other water types and sensor types. The algorithm is parameterised using regional specific SIOP datasets.

#### Theory

Several authors have shown that the Gordon model can be written as a system of linear equations that can be solved by means of matrix inversion techniques (Hoogenboom et al., 1999, Hakvoort, 2000), see also chapter 3.2.2.

Based on the Gordon/Walker model, a more general formulation can be found for band ratios, which leads to a model formulation that can be solved by a form of matrix inversion. The ratio of two subsurface irradiance reflectances in different spectral bands  $R(0^-)^1$  and  $R(0^-)^2$  can be written as ( $f$  is assumed to be spectrally independent;  $^1$  and  $^2$  denote the spectral bands):

$$R = \frac{R(0^-)^1}{R(0^-)^2} = \frac{b_b^1 \cdot (a^2 + b_b^2)}{b_b^2 \cdot (a^1 + b_b^1)} \quad (\text{III.15})$$

In this equation,  $f$  (or the ratio ' $f/Q$ ' in the case of remote sensing reflectances) is eliminated. After rewriting this leads to:

$$\begin{aligned} & (R \cdot c_6 \cdot a_{CHL}^{*1} - c_5 \cdot a_{CHL}^{*2}) \cdot CHL \\ & + (R \cdot c_6 \cdot a_{TSM}^{*1} - c_5 \cdot a_{TSM}^{*2} + R \cdot c_2 - c_2) \cdot TSM \\ & + (R \cdot c_6 \cdot a_{CDOM}^{*1} - c_5 \cdot a_{CDOM}^{*2}) \cdot CDOM \\ & = (c^1 - Rc^1) + R \cdot c_6 \cdot a_w^{*1} + c_5 \cdot a_w^{*2} \end{aligned} \quad (\text{III.16})$$

With the following elaboration:



$$c_1 = 0.5 \cdot b_w^{*1} \cdot b_{TSM}^{*2} + 0.5 \cdot b_w^{*2} \cdot b_{TSM}^{*1} \quad (\text{III.17})$$

$$c_2 = B \cdot b_{TSM}^{*1} \cdot b_{TSM}^{*2} \quad (\text{III.18})$$

$$c_3 = \frac{0.5 \cdot b_w^{*1}}{B} \quad (\text{III.19})$$

$$c_4 = \frac{0.5 \cdot b_w^{*1}}{B} \quad (\text{III.20})$$

$$c_5 = \frac{c_3}{TSM} + b_{TSM}^{*1} \quad (\text{III.21})$$

$$c_6 = \frac{c_4}{TSM} + b_{TSM}^{*2} \quad (\text{III.22})$$

Note that no term or variable is omitted. Specifically, the specific scattering of seston is retained in the equation: each term that precedes a concentration contains the difference between the  $b_{TSM}^{*1}$  and  $b_{TSM}^{*2}$ . The influence of the seston scattering on the inversion efficiency will therefore primarily depend on the slope of the scattering function.

The only non-linearity in equation (III.16) is caused by the occurrence of TSM in  $c_5$  and  $c_6$ . There are two ways to solve this. The first solution to this problem is to assume that

$\frac{c_3}{TSM}$  and  $\frac{c_4}{TSM}$  can be neglected at higher TSM concentrations. This is a reasonable

assumption if TSM is larger than approximately 5-7 mg/l. The second option to solve equation (III.16) is by an iterative (predictor/corrector) approach. In the first step of the iteration scheme an initial estimate is made for TSM in  $c_5$  and  $c_6$ . In subsequent iterations the retrieved TSM concentration is fed into  $c_5$  and  $c_6$  until the difference between the initial and retrieved TSM value is smaller than a prescribed threshold. In general 3 to 4 iterations are necessary to obtain a TSM difference smaller than 0.01.

Thus, for any number of relevant band ratios a system of linear equations can be built that can be solved for TSM, TCHL and CDOM by matrix inversion techniques. Because the matrix is orthogonal, singular value decomposition (as implemented e.g. in MATLAB or from numerical recipes) is one of the feasible methods. The method requires  $R(0)$  to be available for at least 3 spectral bands and known SIOP. A reasonable estimate of  $B$  is required; the sensitivity of the algorithm to errors in  $B$  needs to be investigated.

### III.2.4 Inversion of radiative transfer models

Radiative transfer models are based on differential equations for light propagation (usually radiance) in the atmosphere, through the air-water interface and in the water column. The models make use of specific inherent optical properties (SIOP), but do not use any pre-factors or Q-factors since the light field is explicitly modelled. They do, however, require the volume scattering functions of particles. These models are more fundamental than analytical models. The direct inverse use of these models requires (at the current state of the art) still too much computation time. Alternatives are to use Look-Up Tables or to use neural networks (trained with radiative transfer models).



Two models are mentioned:

- Hydrolight;
- Monte Carlo radiative transfer approach and neural networks;

#### *Hydrolight*

Hydrolight (Mobley, 1994) solves the radiative transfer equations (RTE) using the invariant imbedding method. In this method standard operators are derived for an infinitesimally thin layer. These standard operators can be used to compute finally the radiances for the complete water column via the *imbed rules* and the *invariant imbedding relations*. In this way, no explicit integration of the RTE is required. Hydrolight is used in the Netherlands by RIKZ (Hoogenboom, to be presented at Ocean Optics XV, Monaco, 2000) for accurate simulation of experimental field conditions, and for generation of Look-up Tables. As input the method requires the SIOP for the water column.

A simplification of the RTE are the two-flow equations (solve RTE solely for upward and downward irradiance) which can be solved with the invariant imbedding method as well.

#### *Monte Carlo radiative transfer approach and neural networks*

Standard MERIS products will use neural networks (Doerffer and Schiller, 1997). The neural network is trained with simulated data from a Monte Carlo radiative transfer model including various atmospheric and sea-state conditions. These models use global SIOP for European waters based on average conditions for the North Sea and Mediterranean. Their applicability might therefore be limited for waters with SIOP that are non standard.

It is advised to compare the performance of the neural network with analytical models based on the local SIOP as soon as MERIS data become available.





The User Support Programme 1996-2005 (USP-2) is implemented under the responsibility of the Netherlands Remote Sensing Board (BCRS) and the Space Research Organization of The Netherlands (SRON).

The objectives of the USP-2 are: to support Dutch users of information from future European earth observation systems in the development of applications for operational and scientific use; to develop the required national infrastructure and to support users in developing countries with applications for the purpose of sustainable development, in connection with activities carried out by ESA and EUMETSAT.

The USP-2 is financed from the national space budget. During the period 1996-2000 the USP-2 element under the responsibility of the BCRS is executed in connection with the National Remote Sensing Programme 1996-2000.

Publication of:

**Netherlands Remote Sensing Board (BCRS)**  
**Programme Bureau**  
**Rijkswaterstaat Survey Department**

P.O. Box 5023  
2600 GA Delft  
The Netherlands  
Tel.: +31 (15) 269 11 11  
Fax: +31 (15) 261 89 62  
E-mail: [p.b.bcrs@mdi.rws.minvenw.nl](mailto:p.b.bcrs@mdi.rws.minvenw.nl)  
BCRS homepage: <http://www.minvenw.nl/rws/mdi/bcrs>